SHEAR BEHAVIOUR OF 0.6 % AND 0.7 % STEEL FIBRE REINFORCED CONCRETE BEAMS WITHOUT STIRRUPS

NG CHEAU WEN

A project report submitted in partial fulfilment of the requirements for the award of Bachelor of Engineering (Honours) Civil Engineering

Lee Kong Chian Faculty of Engineering and Science
Universiti Tunku Abdul Rahman

April 2019

DECLARATION

I hereby declare that this project report is based on my original work except for citations and quotations which have been duly acknowledged. I also declare that it has not been previously and concurrently submitted for any other degree or award at UTAR or other institutions.

Signature : _____

Name : Ng Cheau Wen

ID No. : 14UEB05381

Date : _____

APPROVAL FOR SUBMISSION

I certify that this project report entitled **"SHEAR BEHAVIOUR OF 0.6 % AND 0.7 % STEEL FIBRE REINFORCED CONCRETE BEAMS WITHOUT STIRRUPS"** was prepared by **NG CHEAU WEN** has met the required standard for submission in partial fulfilment of the requirements for the award of Bachelor of Engineering (Honours) Civil Engineering at Universiti Tunku Abdul Rahman.

Approved by,

Signature : _____

Supervisor : Ir Dr Lim Jee Hock

Date : _____

ACKNOWLEDGEMENTS

I wish to express my sincere gratitude to Universiti Tunku Abdul Rahman for providing an opportunity and funding to me to take this Final Year Project as partial fulfilment of the requirement for the degree of Bachelor of Engineering (Hons.) Civil Engineering.

I would like to convey my gratefulness to my research supervisor, Ir Dr Lim Jee Hock and other lecturers from the Department of Civil Engineering for their fruitful advice, guidance and their enormous patience throughout the development of the research.

In addition, I am thankful to receive countless blessing from my family members who always been there to support and give encouragement to me all the time. I also wish to convey my gratefulness to lab officers who have been so friendly and cooperative in rendering their guidance throughout the research period. Besides that, I would also like to express my deepest appreciation to all my fellow friends and seniors for their help and experiential sharing throughout the development of the research.

Lastly, I am immensely thankful to all the people for their contribution directly or indirectly all the time to the successful completion of this project.

ABSTRACT

Concrete is a brittle material and respectively weak in tensile strength and tensile strain. Concrete technology is applied at which concrete is reinforced with fibre or steel reinforcement to produce a versatile structural material to exhibit superior strength properties in terms of ductility, fracture energy, toughness, strength and durability. An example of a special type of concrete which required high technical specifications and possesses the properties above is known as steel fibre reinforced concrete (SFRC). The introduction of short, discontinuous and randomly oriented steel fibres into conventional concrete mixes improve various characteristics and performance of concrete which outstretch all over the depth of the structural element. Steel fibre has its dominance in possessing a strong bond with the concrete matrix with high elastic modulus. The goal of this study is to create a standard foresight in determining the potentiality of steel fibre as secondary shear reinforcement to partially or fully replace shear stirrups in conventional concrete. For this purpose, the series of SFRC beam specimens without stirrups which have the same concrete mixing ratios were produced with the inclusion of 0.6 % and 0.7 % steel fibre by volume fractions and compared with conventional normal weight reinforced concrete (NWRC) beam with stirrups. Hooked-end glued short steel fibres with an aspect ratio of 63.64 were used in this study due to its commerciality availability. The fresh properties of the produced SFRC specimens were determined by the slump test. The hardened properties were determined by compressive strength test, splitting tensile strength test and durability water absorption test. When the beam specimens had attained the target concrete characteristic strength of C25/30, four-point bending test was conducted to investigate the shear behaviour of SFRC beams as compared to conventional beams. The structural performance of shear beams was evaluated in the aspects of load-deflection, load-steel strain, crack patterns and failure modes. Analysis of experimental results was carried out and compared based on the variables in shear reinforcement and fibre volume content as parameters in this study. In conclusion, the ultimate shear strength of 0.6 % and 0.7 % SFRC beams had increased by 31.82 % and 36.36 % respectively as compared to the NWRC beam without stirrups. More than that, NWRC beam with stirrup increased 43.18 % in ultimate shear strength which possessed better performance in ductility.

TABLE OF CONTENTS

LIST OF TABLES

LIST OF FIGURES

LIST OF SYMBOLS / ABBREVIATIONS

A	Cross-sectional area of cube specimen at which uniform load applied
a	Shear span
a/d	Span-to-Depth ratio
b	Width of Beam
D	Average height/ length
d	Effective depth of beam
d_f.	Equivalent diameter of fibre
f_c	Compressive strength
f_{ck}	Characteristic strength of concrete
f_y	Yield strength of steel fibre, N/m^2
f_{yk}	Yield strength of steel
L	Length of beam
l_{an}	Anchorage Length
l_f	Length of fibre
$\frac{l_f}{d_f}$	Aspect ratio
M	Moment
N	Force
P	Peak load sustained by specimen
S_{cr}	Section where the critical shear crack initiated
T	Splitting tensile strength
V	Shear resistance
V_a	Inclined shear stress of aggregate interlocking
V_c	Shear force at compression zone
V_{cr}	First Crack Strength
V_d	Dowel action by flexural reinfrocement
V_f	Volume Fraction
V_u	Ultimate Shear Force
$v_{ULT,cal}$	Computed Ultimate Shear Strength
$v_{ULT,exp}$	Experimental ultimate shear strength
WA	Water absorption of hardened concrete specimen
W_{dry}	Weight of oven-dry of specimen

W_{sat}	Weight of saturated surface dry specimen
w/c	water-to-cement ratio
x	Depth of neutral axis
δ	Deflection
δ_{cr}	First crack deflection
ε	Longitudinal strain at the mid-span of the beam
θ	Inclination angle of concrete strut
ρ	Reinforcement ratio for longitudinal reinforcement
σ_{max}	Tensile stress in steel fibre, N/m^2
τ	Bond Stresses
Δ	Variation
2H8	2 reinforcement steel bar with diameter of 8 mm
2R8	2 reinforcement steel bar with diameter of 8.5 mm
ACI	American Concrete Institute
ASTM	Association Society for Testing and Materials
DOE	Department of Environment
EC2	Eurocode 2
EN	European Standards
LVDT	Linear Variable Displacement Transducer
MS	Malaysia Standard
NWRC-W/S	Normal Weight Reinforced Concrete beam with stirrup
NWRC-W/OS	Normal Weight Reinforced Concrete beam without stirrup
OPC	Ordinary Portland Cement
R8-100	Shear link or shear reinforcement with diameter of 8 mm, placed with 100 mm spacing in between each other
RC	Reinforced Concrete
SFRC-0.6	0.6 % Steel Fibre Reinforced Concrete
SFRC-0.7	0.7 % Steel Fibre Reinforced Concrete
SSD	Saturated Surface Dry

LIST OF APPENDICES

CHAPTER 1

INTRODUCTION

1.1 General Introduction

Concrete is the most accustomed synthetic material of construction throughout many years which has brought the about fast-paced and high magnitude of development in the construction industry today. In general, concrete as an artificial stone-like mass is formed by a coalition of cementing medium, water and aggregates (fine and coarse), and sometimes the addition of chemical admixtures or fibres in required proportions when it is placed in forms, allowed to cure and hardened with age. Hence, concrete is a type of composite made of different ingredients.

Nowadays, advanced concrete technology has been infused to cater and suit the need for desired properties in moving towards industrialized construction projects. Therefore, various researches on concrete technology have been developed as an alternative to conventional concrete, such as reinforced concrete (RC), to fulfil the demand for concrete strength in meeting the growth in structure size and complexity.

Concrete inherently brittle with high compressive strength, but has relatively low tensile and impact resistance, it has tensile strength which is practically 10 % of total compressive strength. Besides, external loads may be applied in any form of axial forces, shear bending moments, shear forces and torsion on concrete members in structural mechanics viewpoint. To cope with these external actions in practice, special concretes and concreting techniques have been introduced such as reinforced concrete to overcome the inherent weakness of the concrete. For instance, a continuous reinforcing steel, namely rebar is used as a tension medium in reinforced concrete to compensate for the lack of ductility and improve resistance to tensile stresses significantly. However, it requires labour skill in hand-tied rebar and placement of continuous reinforcement in concrete as compared to fibres in discrete form. Besides, fibre reinforcement is always cost-effective in comparison to the steel reinforcing bar.

Moreover, the concept of using fibre reinforcement to improve the engineering characteristics of construction materials was dated from the remote past. For instance, pottery was reinforced by asbestos in extensively, mud bricks with the incorporation of straw and horse hair were reinforced with plaster in the early applications. It is an indisputable fact that the introduction of discrete fibre into concrete mixes strengthen

the mechanical characteristics of concrete itself especially in tensile strength, flexural toughness strength, shear and energy absorption capacity, and ductility. Fibre reinforced concrete is very useful and applicative in numerous civil engineering applications. The use of fibre reinforced concrete in applications such as precast members, slabs, highway pavements, shotcrete, seismic structures, tunnelling, hydraulic structures, offshore structures, repairs and rehabilitation, and other fields of geotechnics is prevalent world over.

Reinforced concrete is contemporarily devoted with any fibre which is materially compatible with concrete, such as steel, glass, carbon, and polyethene, to improve tensile performance, shock resistance, fatigue resistance and crack resistance as well as to minimize the presence of microcracks at the mortar-aggregate interface. Generally, there is fibre bridging effect transition in transferring stresses at the internal microcrack which can improve shear resistance in minimizing diagonal crack width and spacing (Gambhir, 2013). Due to the enhancement of durability in controlling crack growth by fibres, fibre reinforcement could possibly minimize or even replace stirrup reinforcement by eliminating the shear size effect in beam depth. This can be explained as the increase in overall beam depth could decrease the shear strength (Wight and MacGregor, 2008).

An attempt is made in this experimental research to have a clear understanding on shear behaviour of different volume fractions of steel fibre reinforced concrete, abbreviated in SFRC, in determining its physical characteristics and mechanical strength as shear loading component. Short beams are investigated in this study as higher shear strength is exhibited by small scale beams than large beams. Two different volumetric percentage of commercially available deformed steel fibres are investigated in normal weight reinforced concrete with desired concrete strength class of C25/30 in comparison with conventional reinforced concrete. The structural beam design is mainly referred to British Standard, Eurocode 2 while the shear-flexure data are first analysed based on the routine of American Concrete Institute (ACI) methods and followed by unaccustomed analysis based on failure mode. The development of this research presented herein are to evaluate the mechanism of shear resistance in simply-supported SRFC beams as well as the potentiality of steel fibres in replacing minimum stirrup-type shear reinforcement.

1.2 Background of Study

Concrete is reinforced with fibre or meshes or steel bars to produce a versatile structural material which has improved strength in bending, shear, torsion, tension and compression, unlike plain concrete which is only strong in compression. Steel reinforcement is a flexible and versatile material suitable for limitless applications in a wide range of design fabrication. Use of steel materials is currently increasing in momentum due to its flexibility combined with its higher strength-to-weight ratio compared to other accessible building materials. The combination of concrete and steel works very well, figuratively cooperating with each other to play their own strengths while complementing each other in improving structural integrity. For example, fibres such as steel fibres possess a strong bond with the concrete matrix and very high elastic modulus in preventing the tensile cracking of concrete material as well as augmenting the tensile strength and composite stiffness properties.

Concrete with the inclusion of steel fibres is known as steel fibre reinforced concrete (SFRC). It is a material which promises fabulous working capacity when subjected to static or dynamic load as well as tensile strength and effective crack distribution. Due to the flexibility in deforming and indenting of steel fibres, improvement of their anchorage will definitely increase their bonding strength and toughening capabilities. The applications of steel fibre reinforcement to the composite especially the serviceability conditions by delaying the initiating of flexural cracking, enhancing the tensile strain capability, improving post-cracking ductility, controlling crack width at uncracked tension zones, increasing flexural stiffness in resisting deflections, as well as energy absorption capability (Mudgal, 2012).

SFRC is also popular in the construction of in-situ and precast concrete structures as auxiliary reinforcement to handle short-term load in controlling shrinkage cracks, which prevent cracking during transportation or installation of precast members; in combined reinforcement systems based on the partial replacement of the traditional reinforcement; and as complete substitution of traditional reinforcement in members such as tunnel linings, tilt-up construction, foundations, thin-shell structures and et cetera (Victor, et al., 2018).

1.3 Significance of Study

The brittle failure mode of structural elements is usually very sudden due to the brittle behaviour of tensioned concrete. A reinforced concrete beam with relatively low shear

reinforcement ratio or without shear stirrups can fail prematurely in shear when subjected to combined moment and shear force upon reaching its full flexural strength. In the year of 1955 and 1956, there were well-known structural failure cases of two Air Force Bases warehouse roofs in Ohio and Georgia respectively as shown in Figure 1.1 (Cuenca, 2014). The structure cracked and collapsed when subjected to a combined load, thermal effects and shrinkage.

(a) (b)

Figure 1.1: Shear Failure of Reinforced Concrete Beams: (a) Air Force Warehouse, Ohio, 1955 (Collins, et al., 2008 cited in Cuenca, 2014); (b) Air Force Warehouse, Georgia, 1956 (Cuenca, 2014)

Recognizing that shear failures tend to be more abrupt and brittle than tensile and bending failure, shear reinforcement is introduced to prevent shear failure and is constituted by diagonal tensile stresses in the tension zone (Altaan and Anay, 2015). However, an extension of general shear models encloses recent new materials such as steel fibre reinforced concrete. As steel fibres reinforcement possess aggregate interlocking by transmitting tensile stresses over diagonal cracks, the shear resistance has been greatly improved when the crack width and spacing has been minimized (Gambhir, 2013). Hence, the introduction of the steel fibres can possibly replace or minimize the installation of stirrups or shear links in a structural member. Although the reinforcement of steel reinforcing bar enhances the concrete physical strength significantly, it is also important to produce concrete with homogenous and isotropic properties in tensile by controlling the development of microcracks. The concept of using fibre reinforcement instead of shear links is to enhance the interfacial bonding of elements at the same time also increase the shear resistance.

Steel fibres which are mostly in discrete form; have become more popular in reinforcing concrete where tensile stress can be sufficiently distributed to avoid conspicuous cracking and higher durability. It is lately a form of binder which helps in bonding with concrete matrices. The incorporation of fibre into concrete often promises the engineering performance of the structure. Specifically, by the incorporation of a minor amount of short and arbitrarily oriented steel fibres throughout the concrete matrices, it can provide a frontline effect on the enhancement of serviceability behaviour, flexural strength, shear resistance and increases structural integrity. Hence, steel fibres can potentially replace the conventional and laborious shear stirrups, especially in shallow members by means of its properties in enhancing the resistance of shear friction, increasing the tensile strength of concrete, and suppressing and hindering cracks (Altaan and Anay, 2015).

Due to the shear behaviour enhancement effect possessed by steel fibres, lot of researchers work prominently over it and many studies have been carried out on the shear performance of SFRC members and have been applied abroad in construction, architecture and irrigation work. As mentioned in Vikrant and Kavita (2012), fibre has been focused in concrete reinforcement research for some time and up to 300 000 metric tons of fibres are used as reinforcement of concrete in the industry presently. Steel fibre remains the most used fibre of all, which occupies 50 % of total tonnage used; followed by polypropylene (20 %), glass (5 %) and other fibres (25 %) (Vikrant and Kavita, 2012).

1.4 Problem Statement

The problem statements are established correspondingly to the objectives of this research study as following:

i. The study of Babar, Joshi and Shinde (2015) presented that concrete samples had increased slightly in compressive strength from 2.6 % to 6.7 % and 12.7 % to 13.4 % for 0.5 % and 1 % of steel fibres addition in concrete respectively. Both variables were carried out for beam span-to-depth ratio of 1, 1.25 and 1.5. On the contrary, the study in Boulekbache, et al. (2014) showed that there was a reduction in compressive strength of around 7.9 % and 3.1 % for 0.5 % and 1 % fibre content by volume fraction respectively. Moreover, the previous studies reviewed by Dahake and Charkha (2016) which deal with the effect of steel fibres on concrete strength, showed that the incorporation of steel fibres improved particularly the concrete splitting tensile

strength. Besides, the experimental outcome of Velayutham and Cheah (2014) showed that the water absorption percentage decreased 18.5 % and 21.2 % for 0.5 % and 1 % steel fibre volume fraction respectively as compared to plain concrete whereas results carried out by Selvi and Thandavamoorthy (2013) showed an increment of 4.7 % by SFRC as compared to conventional concrete for 28 days of water absorption by immersion. Since most of the researchers mainly focused on the investigation of steel fibre content at the 0.5 % interval plus there were different output on the performance of hardened properties of SFRC with the same fibre content by different researchers, hence, this research aimed to further study the hardened properties of 0.6 % and 0.7 % SFRC which has not yet been focused or studied by other researchers.

ii. Tantary, Upadhyay and Prasad (2012) had done experimental research to study the influence of steel fibres on the concrete shear strength. It was found that at constant shear span-to-depth ratio, beam depth, fibres aspect ratio and mix proportions, by increasing steel fibres volume fraction from 0.5 % to 1 %, the ultimate shear strength of FRC is significantly increased as much as 30 % for the 1% addition of steel fibres, but the increase was less than 15 % in beam samples which showed failure in flexural. Hence, it can be attributed that steel fibres contribute more to shear than in flexure. Moreover, many pieces of researches explore the influence of moment in developing shear failure in RC beams caused by the reinforcements losing restrain within the supporting area (Vegera, Khmil and Blikharskyy, 2017). However, to allow better design and use of reinforcement, the major fracture that should be studied is the destruction of RC beam due to shear influence which destroys more abruptly and unpredictably and requires more effort than the failure said above. Even though additions of steel fibres are expected to increase the shear strength and deformation capacities significantly, the failure mechanisms of the structural element may still remain the same based on the volume fraction of steel fibres and shear span-to-depth ratio (Guray, Riza Secer, Semih, 2017). Besides, a concrete mix with a large steel fibres volume fraction may not be practical in workability even though steel fibres are used as shear reinforcement. Therefore, in this study, 0.6 % and 0.7 % of steel fibres content with an aspect ratio of 63.63, were incorporated to the beam specimens, which have span-to-depth ratio lower than 3 to study the influence of steel fibres volume fractions on the ultimate shear capacity of reinforced concrete beams.

iii: You, Ding and Niederegger (2010) had carried out two series of self-compacting concrete with the addition of hooked-end steel fibres by volume fraction of fibre content. The tests of simply supported rectangular beams with and without stirrups were carried out. The beams were tested with four-point concentrated loading. The results indicated that the stirrups worked in conjunction with steel fibres gave a complimentary hybrid effect on the mechanical properties. Hence, steel fibres can replace the stirrups partially. Besides, Zago, et al. (2013) also had done the study on replacement of conventional shear reinforcement in a steel fibre reinforced-ultra high-performance cement (SFR-UHPC) beams. The outcome of their experimental work proceeds the feasibility of SFR-UHPC beams by replacing conventional stirrups with fibre reinforced concrete, with or without a single additional diagonal shear link. Hence, this research aimed to study the shear behaviour of steel fibre reinforced concrete (SFRC) beams with the comparison of conventional normal weight reinforced concrete (NWRC) beam with stirrups.

1.5 Aim and Objectives of Study

The main aim of this study is to analyse the shear behaviour of fibre reinforced concrete short beam with the incorporation of steel fibre. The specific objectives of this study are listed as follows:

i. To study the hardened properties of 0.6 % and 0.7% steel fibres additions in concrete on compressive strength, splitting tensile strength and water absorption.
ii. To investigate experimentally the shear behaviour of 0.6 % and 0.7 % SFRC beams without shear stirrups.
iii. To study the shear behaviour of 0.6 % and 0.7 % SFRC beams as compared to conventional NWRC beam.

1.6 Scope and Limitation of Study

The primary focus brought into this study was to evaluate the structural response, mainly shear behaviour and strength properties of SFRC as to volume fraction of the steel fibre in determining its application as a shear loading component. This study was supported by means of experimental work and analysis of mechanical test results.

Moreover, this study was set with several limitations to narrow down the scope in dealing with such a huge topic. Herein, this study only concentrated on 0.6 % and

0.7 % volume fraction of hooked-end steel fibres due to its commercially available. Besides, incorporation of hooked-end steel fibres in reinforced concrete beam possessed higher resistance in deflection under loading (Holshemacher, et al., 2006). A target concrete characteristic strength of C25/30 of reinforced concrete beam was achieved as in industry practice. Besides, there is no international standard as a guideline in designing SFRC structure at present. Nonetheless, the European Standard (EN) is being prepared presently (Victor, et al., 2018).

The general British method developed by the Department of Environment, known as the DOE method is applied to conduct the mix proportion of concrete mix design. The mixes were taken by the mass of each material contained in a given fully compacted concrete volume. Besides, a pre-study on the mix proportion of SFRC and NWRC was carried out to achieve the required target strength of 30 MPa. The mix design ratio of cement, aggregates and water for NWRC was same as SFRC, except that 0.6 % and 0.7 % of steel fibres were added respectively by volume fraction in SFRC. Fresh concrete slump test and hardened concrete compressive strength test, splitting tensile strength test, shear strength test and water absorption test were conducted for both NWRC and SFRC beam specimens in evaluating the performance of concrete specifically.

Each set of different type of concrete testing consisted of three specimens to get the average results. Six concrete cube specimens with the side length of 150 mm were produced and water cured, where three of them were tested for compressive strength and water absorption at curing age of 7 days while the remaining three specimens were tested at curing age of 28 days. For the splitting tensile testing, an additional six concrete cylinder specimens with a dimension of 100 mm in diameter × 200 mm in length were produced and water cured for 7 days and 28 days as well.

In general, a total of six concrete cube and six cylinder specimens were produced for each different type of concrete, namely NWRC, 0.6 % steel fibre reinforced concrete (SFRC-0.6) and 0.7 % steel fibre reinforced concrete (SFRC-0.7) respectively. Furthermore, there were only three concrete beams with a dimension of 125 mm in width × 200 mm in depth × 800 mm in length were produced and cured with wet gunny bag for a period of 7 days for shear strength test at 28 days for each mix design of concrete. Hence, a total of twelve beams were produced, where each type of concrete had three concrete beams in quantity.

There were two types of NWRC beams, one with shear stirrups and the other without shear stirrups, namely NWRC-W/S and NWRC-W/OS respectively. NWRC-W/S beam was treated as a control beam whereas NWRC-W/OS was referred to the conventional beam. However, both SFRC-0.6 and SFRC-0.7 beams were produced without shear stirrups. Preparation of concrete formwork and reinforcement cage were performed to produce RC beam specimens. By justification, the steel reinforcements used for the top and bottom rebar were 2R8 and 2H8 respectively; R8 was used for shear stirrups with a spacing of 100 mm. However, shear stirrups do not apply to the full span of beams but only located at shear span to avoid the delay of concrete crack at the flexure zone.

All the beams were treated as simply-supported beams in this study by applying four-point loading using Structural Magnus Frame in conservative mean to utilize the shear strength results. It was applicable to beams having the ratio of effective span-to-overall depth less than two.

1.7 Contribution of Study

Despite the fact that concrete dominant with its desirable properties, it has its weak point with relatively low tensile strength and deformation properties which prompted numerous researchers to involve in the investigation in improving these properties (Vasudev and Vishnuram, 2013). Therefore, the supplementing of steel fibre into a concrete matrix can improve and modifies the brittle characteristic of concrete. Incorporation of steel fibres in concrete has found to improve in tensile strength, shear strength, cracking and impact resistance, as well as ductility (Behbahani, Nematollahi and Farasatpour, 2011). These properties proved to have a broad range of applications in practical and reliable construction material in possessing better structural performance than conventional concrete.

SFRC has its advantages in time effective, labour effective and cost effective. Since the steel fibre has its potentiality as secondary shear reinforcement to partially or fully replace shear stirrups in conventional concrete, the time consumed in assembling and placing the traditional shear reinforcement cage is minimized as well as saving time spent for reinforcement position checking and taking the final approval for placing and pouring. Construction of SFRC saves the manpower in fabricating structural reinforcement especially in tying reinforcement bar at the same time increases the production rate by using the dispersed reinforcement. Labour cost is

saved for reinforcement installation. Moreover, the minimization or eliminating of traditional steel reinforcement saves the material costs. Besides, SFRC able to eliminate voids during casting of concrete especially when there are closely spaced stirrups. Concrete and placement costs can be saved when there is a reduction of slab thickness and the possibility of wider spacing of joint. Simpler joints are formed with minimum errors in positioning of steel fabric and hence save the maintenance costs.

From the prospect of the structural solutions, the minimization in using stirrups can increase the concrete strength and so lightly elements can be obtained. Besides, by the implementation of fibres to replace conventional stirrups, a sufficient reinforcement can be met when web-openings are needed where utility ducts can be placed through beams. This economical solution is achieved because utility ducts can minimize the height of the free building as they need to be hidden. Hence, the production of beam can be simplified whenever the web-openings are needed as there is more free space without stirrups. More than that, steel fibres also solve the problem of void and poor bonding between concrete and reinforcing bar for concrete casting in elements with closely-spaced stirrups. Therefore, it is imperative to develop more experimental database to study the shear failure problem and customary solutions in minimizing shear failure in addition to investigate the viability of utilizing steel fibres as minimum shear reinforcement in NWRC beams.

1.8 Layout of the Report

This report comprises of five chapters. Chapter 1 outlines the general introduction of study, background of study, significance of study, problem statement, main aim and specific objectives of study, scope and limitation of study, contribution of study and organization of report.

Chapter 2 commences with a review of constituent concrete materials, including fibrous properties in steel fibre. The bonding relationship between steel fibres and concrete matrix in SFRC have been discussed in terms of their characteristics and stress-strain behaviour, followed by mechanical properties and shear failure behaviour of SFRC. The remainder of this chapter is dedicated to further discuss the literature reviews and the investigations of previous researchers' work related to SFRC.

Chapter 3 outlines the methodologies applied in the experimental program of this study. The studied parameters, mix proportion, materials preparation, design,

production, instrumentation and testing method to obtain the properties and performance of SFRC specimens adhering to standards are discussed in this chapter.

Chapter 4 consists of all the data and discussion of the experimental test outcome. The shear behaviour of the tested SFRC beams is analysed and interpreted throughout the tests with respects to the strength and failure mode of tested beam specimens as compared to NWRC-W/S and NWRC-W/OS.

Chapter 5 concludes and summarises the entire research along with major findings based on the discussion in Chapter 4 in accordance with respective objectives. The recommendations are provided for further studies and improvement purposes in this chapter.

CHAPTER 2

LITERATURE REVIEW

2.1 Introduction

The concept of incorporating fibres to compensate concrete brittle nature and improve its tensile strength, fracture toughness, post cracking response and strain capacity had been applied since ancient civilizations. Fibre Reinforced Concrete (FRC) is a compound material made of traditional concrete reinforced by discrete strips of short, thin and arbitrary distributed fibre of specific shape. This chapter reviews the material properties of concrete, FRC, and fibrous material particularly steel fibre. Besides, the bonding relationship between steel fibres and concrete matrix in SFRC has been discussed in terms of their characteristics and stress-strain behaviour, followed by mechanical properties and shear failure behaviour of SFRC beam. The remainder of this chapter consists of the study of previous researchers' work related to SFRC.

2.2 Concrete

Concrete is a composite artificial stone which essentially made of a binding medium, hydration of cement-water mixture with an embedded combination of fine and coarse aggregates particle within. All the materials are mixed in a required proportion and bind themselves into a hardened mass. Oven-dried normal weight concrete has a density greater than 2000 kg/m^3 and not more than 2600 kg/m^3 (British Standards Institute, 2013). Concrete shows a very strong compressive strength property and has unlimited applications when combined with steel reinforcement, which is known as reinforced concrete. Concrete is, therefore, the most versatile and economical construction material than other building materials as it can be engineered to fulfil performance specifications in a wide range. However, concrete also possesses a poor tensile strength and is relatively brittle which can cracks easily under service condition. These microcracks are induced by the concentration of stress and strain, plastic shrinkage, thermal contraction and bleeding. Due to the movement of thermal and drying shrinkage, there is an initiation of potential stable localized crack at a microscopic level before any loading is applied. Hence, macrocracks will be produced when these potential microcracks propagate and align themselves under the introduction of loading. The crack width has a significant impact on the corrosion

process as localized corrosion at the cracked area will reduce the stiffness and strength of the structure due to further surface cracking followed by delamination and debonding within concrete (Migashi and Leite, 2004). Hence, concrete can be reinforced with short, randomly distributed fibres to increase the concrete tensile strength by mitigating the cracks formation and suppressing their growth and propagation.

2.2.1 Ordinary Portland Cement (OPC)

Portland Cement is defined as hydraulic cement made from pulverizing clinkers which contains essential hydraulic calcium silicates, and normally consists of one of several forms of calcium sulphate as an interground addition (ASTM C150-07, 2007). The standard specification for OPC is Type I cement which is general-purpose used in the construction industry without the need of special characteristic. Basically, OPC is a combination of calcareous, argillaceous and silica materials which contribute the calcium silicate hydrate gel formation during the hydration process. As stated in Neville (2010), an ordinary chemical makeup of OPC is ranged and tabulated in Table 2.1.

Table 2.1: Oxide Composition of OPC (Neville, 2011)

Oxide	Chemical formula	Amount (%)
Calcium Oxide	CaO	60-67
Silicon Dioxide	SiO_2	17-25
Aluminium Oxide	Al_2O_3	3-8
Iron(III) Oxide	Fe_2O_3	0.5-6.0
Magnesium Oxide	MgO	0.5-4.0
Sodium Oxide	Na_2O	0.3-1.2
Sulphur Trioxide	SO_3	2.0-3.5

The cement acts as a binding medium among discrete raw ingredients. It is being grounded by burning in a rotary kiln under high temperature to a partial fusion, and hence chemical compounds take place when there are reactions. Table 2.2 shows the typical percentage amount of chemical compound compositions for OPC.

Ordinary Portland Cement (OPC) is the most important type of cement found in the industry by far. There are three grades of Portland cement in India which they

are Grade 33 (IS: 269-1989), Grade 43 (IS: 8112-1989) and Grade 53 (IS: 12269-1987) and having mean compressive strength exceeding 33 MPa, 43 MPa and 53 MPa respectively at 28 days.

Table 2.2: Typical Ranges of Chemical Compound Compositions in OPC (Neville, 2011)

Compound name	Chemical formula	Abbreviation	Amount (%)
Tricalcium Silicate	$3CaO.SiO_2$	C_3S	42-67
Dicalcium Silicate	$2CaO.SiO_2$	C_2S	8-31
Tricalcium Aluminate	$3CaO.Al_2O_3$	C_3A	5-14
Tetracalcium Aluminoferrite	$4CaO.Al_2O_3.Fe_2O_3$	C_4AF	6-12

2.2.2 Aggregates

In the production of concrete or mortar and the constitution of concrete skeleton, aggregates are basically used as a filler material. They form the body of concrete by occupying 70 % to 80 % of the volume (Duggal, 2008). Some of the aggregates are active by forming a chemical bond between the cement paste and interface of aggregates due to physical, thermal and maybe chemical properties.

On the basis of size, aggregates are subdivided into coarse aggregate and fine aggregate to increase the bulk density of concrete. In accordance with ASTM C33-06, coarse aggregates are those aggregates retained on a No. 4 sieve (4.75 mm opening) predominately, and generally has a size ranges from 5 to 150 mm. Maximum coarse aggregate size is about 25 mm for mixing of normal concrete used for structural members (Zongjin, 2008). Figure 2.1 depicts the coarse aggregates in a different range of sizes.

On the other hand, the fine aggregates are aggregates which able to pass through a No. 4 sieve (4.75 mm opening) and retained on a No. 200 sieve (75 μm opening) predominately. The commonly used fine aggregates are natural sand which normally deposited by crushed stone sand and rivers (Duggal, 2011). Fine aggregate has the smallest size of 60 μm.

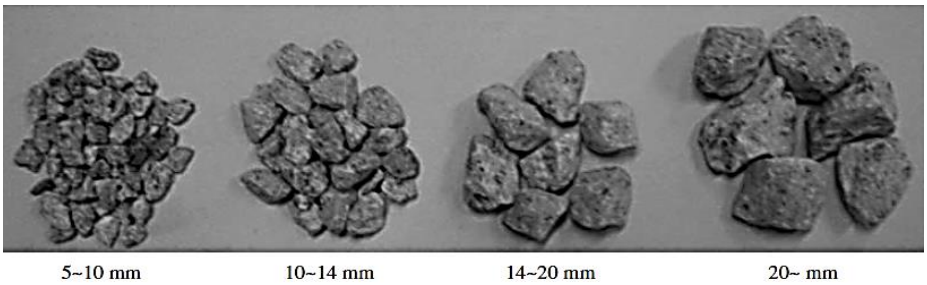

Figure 2.1: Coarse Aggregates in Different Sizes (Zongjin, 2008)

Aggregates are also subdivided into rounded, irregular and angular on the basis of shape. Rounded aggregates can produce minimum voids, about 32 % in the concrete (Duggal, 2008). Minimum cement paste is required as they have a minimum surface area ratio to the volume. However, it is unsuitable to use rounded aggregates in high strength concrete and pavements because of its poor interlocking bond. However, aggregates in irregular shape can develop a good bond and suitable to be used in ordinary concrete due to its angular shape and roughness. Angular aggregates provide a very good bond among the three due to its sharp, angular and rough surface. However, it has relatively high requirement of cement paste to maintain water-to-cement (*w/c*) ratio and 40 % of voids in maximum.

With compliance to ASTM 33, only 3 % of natural sand material containing clay is allowed to pass through the No. 200 sieve and 1 % of natural coarse aggregate. This is due to the fineness of clay which highly increases the required demand for mixing water and leads to strength reduction and increases bleeding. Besides, moisture content of mixing materials with saturated surface dry (SSD) are considered as it is an equilibrium condition used in concrete mix design which allows neither water absorption nor water desorption during the concrete mixing process.

2.2.3 Water

Water occupies 15 % to 25 % in total volume and has its significant effects on a designed concrete mixture. Part of the water functions to hydrate the cement to form a binding matrix or hydration products when the concrete is hardened. Another part of the water acts as a lubricating medium between aggregates and possess the desired workability for fresh concrete. In fact, excessive water can reduce concrete strength where concrete becomes porous due to evaporation, whereas too little water makes the

concrete unworkable due to nonuniformity and resulting in weaker concrete strength. Hence, the amount of water should be controlled to produce good quality concrete.

The raw water supply used in mixing and curing of concrete should be free from detrimental materials or restricted impurities and water samples should be tested for its suitability. The setting time, concrete strength, durability, corrosion of steel will be affected due to excessive impurities. Table 2.3 shows the limit of permissible impurities in mixing water.

Table 2.3: Tolerance Concentration of Impurities in Mixing Water (Duggal, 2008)

S.No.	*Impurity*	*Tolerable concentration*
1.	Silt and suspended particles	2,000 ppm
2. i)	Carbonates and bicarbonates of Na or K	1,000 ppm
ii)	Bicarbonates of Mg	400 ppm
3.	Chlorides	10,000 ppm
4.	Sulphates	20,000 ppm
5.	Sulphuric anhydride	3,000 ppm
6.	Calcium chloride	2 per cent by weight of cement
7.	Sodium sulphide	< 100 ppm
8.	Sodium hydroxide	0.5 per cent by weight of cement provided quick set is not induced
9.	Dissolved salts	15,000 ppm
10.	Organic matter	3,000 ppm
11.	pH	6-8
12.	Iron salts	40,000 ppm
13.	Acids (HCl, H_2SO_4)	10,000 ppm
14.	Sugar	500 ppm

2.2.3.1 Water to cement (*w/c* ratio)

Besides, *w/c* ratio is influenced by the concrete grade, aggregates nature and types, workability and durability (Gambhir, 2013). A *w/c* ratio should be controlled between 0.4 and 0.6 to coat the large surface area of the fibre with paste. The higher initial water content will result in further spacing between the cement grains. As a result, concrete has a lower strength, lower durability and higher penetrability with higher initial water/cement ratio, due to the interconnectivity of resulting pore structure within the hydrates (Nyiutsa and Aondowase, 2013).

2.3 Fibre Reinforced Concrete

Referring to American Concrete Institute (ACI) Committee 544's terminology, fibre reinforced concrete is categorized into 4 types, namely steel fibre reinforced concrete (SFRC), glass fibre reinforced concrete (GFRC), natural fibre reinforced concrete

(NFRC) and synthetic fibre reinforced concrete (SFRC). Fibres are discrete, thin, short and randomly orientated throughout the concrete member.

2.3.1 Fibrous Materials

Fibre reinforced concrete can be varied with different concretes, fibre materials, configurations, densities, orientation, and distribution. Fibres have a significant effect on controlling cracking as they tend to be more closely spaced in discrete form than conventional rebar. Fibres can be subdivided with their elasticity modulus or their origin. Fibre is known as hard intrusion when it possesses higher elastic modulus than concrete mixes, such as carbon, steel, glass and so on; whereas fibre is referred to soft intrusion when it has lower modulus in elasticity than concrete mixes, such as vegetable fibres and polypropylene (Behbahani, Nematollahi and Farasatpour, 2011). Fibres with high elasticity in modulus can enhance both flexural and impact resistance. However, fibres with low elastic modulus contribute less to its flexural strength but still improve the impact resistance.

Figure 2.2 shows the classification of fibres on the basis of their origin and further subdivided into natural sources from animal, plant or mineral fibres, and man-made sources such as natural polymer and synthetic fibres.

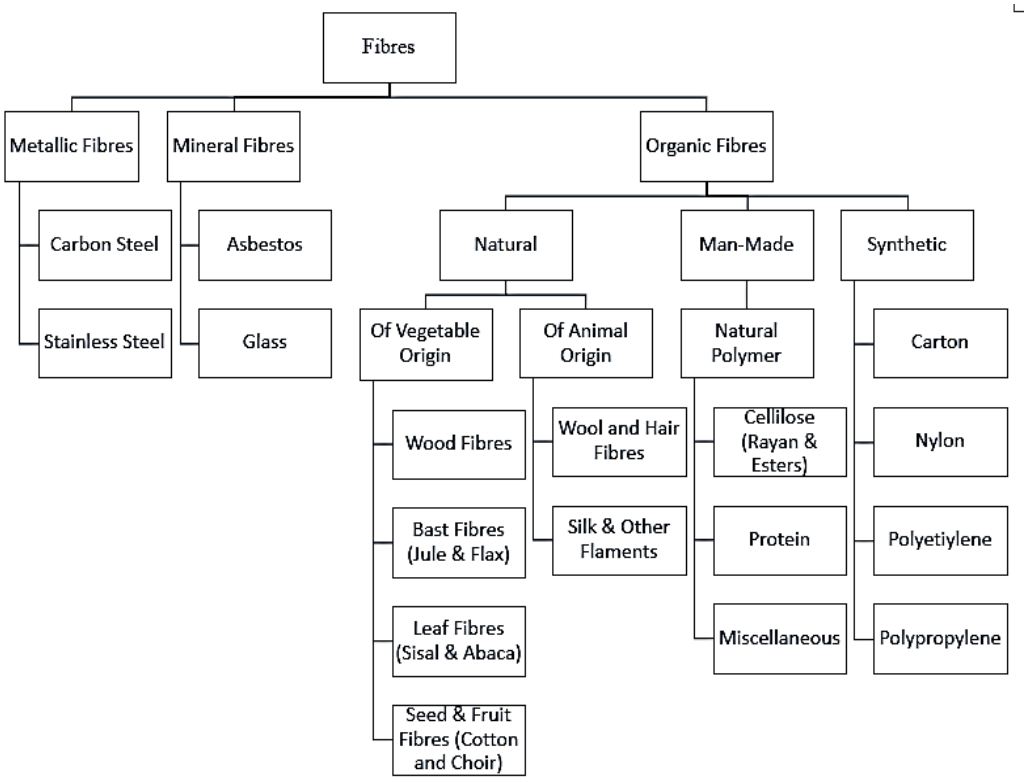

Figure 2.2: Classification of Fibres (Behbahani, Nematollahi and Farasatpour, 2011)

2.3.2 Effects of Fibres in Concrete

Fibre reinforcement in concrete possesses crack controlling property by delaying the initial shear and flexural crack as well as transforming unstable propagation of tensile cracking to a gradual and stable crack growth (Siva Kishore and Mallika Chowdary, 2016). As a result, the traits of ductility capacity in absorbing the energy of the composite can be enhanced when the extensive post-cracking behaviour is transfused throughout the matrices.

Fibres are more closely spaced than conventional rebars. The usage of fibres in concrete can control crack as well as plastic and drying shrinkage due to its random distribution throughout the concrete. It manages to reduce the permeability of concrete and bleeding of water and; at the same time also consolidates the structural integrity of the concrete. As discussed previously, fibres also improve both flexural and impact resistance in concrete.

The inclusive of fibres in concrete can improve its tensile strength if the particular fibres have higher elastic modulus than the concrete mix. However, the capacity of water absorption in fibres can cause low workability and potentially corrosion stains whenever the fibres are exposed at the surface.

2.3.3 Durability of Fibres Reinforced Concrete

The resistance of concrete toward the aggressive ions ingression can be one of the major factors the affects its durability. The volume of permeable pore and connectivity between the pores in concrete can be presumed as the characteristic of concrete absorption indirectly reflects its porosity. According to the study of Rahmani, et al. (2011), SFRC had lower water absorption than plain concrete due to its low permeability characteristic. However, irrespective of the amount of fibre and fibre length, it was found that inclusive of steel fibres to concrete increased gas and water permeability (Miloud, 2005). Hoseini, Bindiganavile and Banthia (2009) gave a statement that fibre reinforcement resulted in a reduction in the concrete permeability when subjected to mechanical stress. The explanation was given that there was changeability in crack profile due to the addition of fibres whereby a lot of closely spaced microcracks formed and mitigate the occurrence of large cracks. Hence, the addition of fibres can enhance crack control through crack bridging which reduces the permeability of concrete at the same time.

2.4 Steel Fibre Reinforced Concrete (SFRC)

SFRC which under uncracked state has similar elastic mechanical properties as conventional concrete with the same mix proportions. Steel fibres pledge excellent crack resistance due to its performance in increasing toughness and energy absorption capacity of the composite. The technology of reinforced concrete with steel fibres actually transforms to be a more ductile material than a brittle plain concrete by suppressing and bridging the cracks in the concrete matrix, hence prevent total loss of the bearing capacity after the first crack, which happens in brittle fracture failure.

Steel fibres can contribute up to 5 % to 50 % to the total shear strength of SFRC depend on their amount. The fibre reinforcement contributes to the composite flexural toughness significantly than strength improvement. Besides, steel fibres reinforced concrete manages to withstand external impact and hence enhances the toughness characteristic of hardened concrete. The major aspects which need to take into consideration in evaluating the shear performance of fibre reinforced concrete include volume fraction of fibre, aspect ratio and anchorage conditions of steel fibres. Higher efficiency of fibre reinforcement can also be achieved with a uniform dispersion of the fibres in the composite and bonding between fibre and cement matrix.

Crack density in fibre reinforced concrete is increased, but the crack size is minimized. Moreover, Amit Rai and Joshi (2014) justified that SFRC manages to sustain considerable loads continuously even at substantial deflections beyond the fracture deflection of the plain concrete. As compared to plain concrete, there will be unforeseen failure upon transcending the deflection corresponding to the ultimate flexural strength.

2.4.1 Steel Fibre

The type and volume percentage of fibre has significant influences on the physical characteristics of concrete. For example, fibres with circular sections may have different tensile strengths due to varying diameters. Steel fibre dosages added to a concrete mix depend on application objectives in structural improvement, shear reinforcement, crack control, durability, joint spacing increment or cost savings.

2.4.1.1 Type, material and size of steel fibre

The plain steel fibres are produced by straight cutting of smooth galvanized steel wires whereas the hooked steel fibres are glued together into bundles with water-soluble adhesive. The plain traditional straight steel fibres however are unable to utilize full-range strength of steel due to its anchorage deficient in the concrete matrix. Presently, shaped fibres occupy over 90 % of all produced fibres. Fibres with anchorage at ending and high aspect ratio can possess higher effectiveness. It was proven that crimped-end fibres with 40 per cent less volume can achieve the properties as straight fibres for the same length and diameter (Faisal, 1990). Anchorage of fibres or shape is taken into concern when considering the influence of roughness of the fibre surface on their adhesiveness to the matrix.

According to BS EN-14889-1 standard, steel fibres can be categorized with respect to the production process as shown in Figure 2.3(a), whereas EN 16120-2 and EN 10088-5 proposes the specification on cold-drawn carbon-steel and stainless-steel for groups I, III and IV as shown in Figure 2.3(b). The cold-drawn wire which has a deformed geometry with end hook is commonly used the most in hardiness investigations of SFRC. The researchers include Nguyen Duc and Nguyen Viet (2018), Jin-Ha, et al. (2013), Bernard (2014), O' Neil and Devlin (1999), Balouch (2010), Christina, et al. (2015) and more. Besides, there is a limitation of scope in interpreting result with respect to other fibres, including cut-sheet fibres which are only investigated in few pieces of researches as can be seen in Mangat and Gurusamy (1987) and Batson (1977).

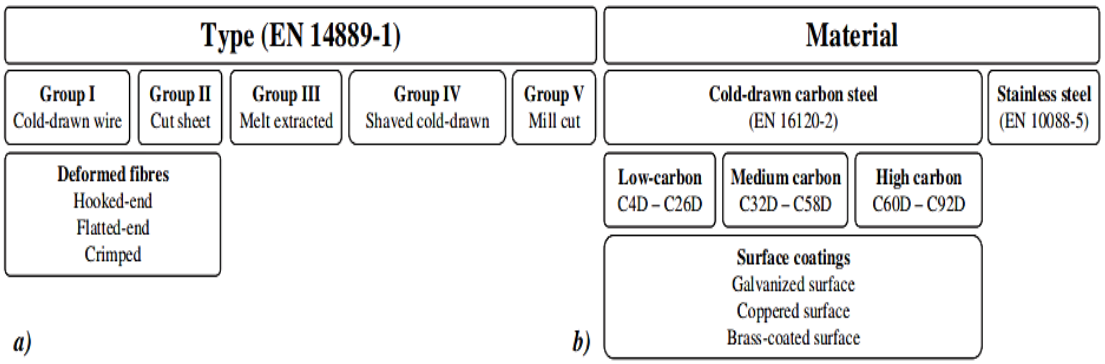

Figure 2.3: Classification of Steel Fibres for Concrete: a) Type of Steel Fibre According to EN 14889-1; b) Type of Steel Fibre According to EN 10016-2 and EN 10088-5 (Victor, et al., 2018)

The common efficiency of produced fibre can be described in terms of its effectiveness in the concrete matrix and the ease to manufacture (Katzer, 2006). Five steel fibre types which are most popular in the market are straight, hooked, crimped, stranded and twisted in the market. Figure 2.4 shows the geometries of various types of steel fibres. There are also odd types of fibres which are rarely encountered unless they are ordered specifically by clients, such as ringed or mechanical deformed fibres.

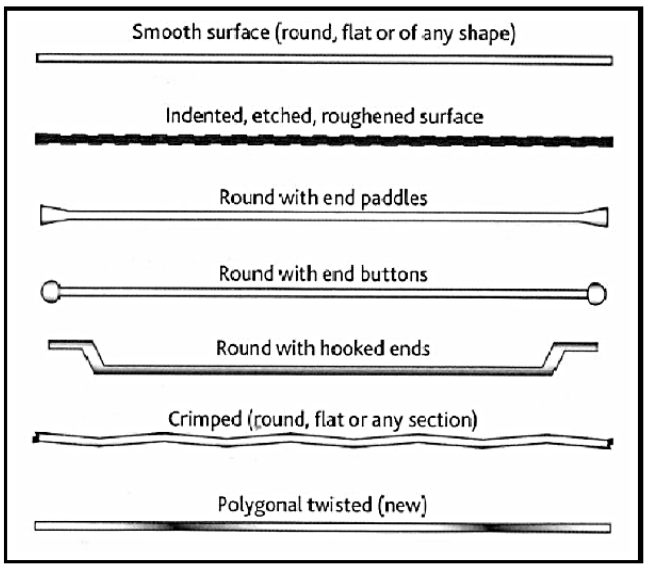

Figure 2.4: Variety Types of Fibre Profiles

Katzer (2006) had addressed the assortment production of steel fibres in the world based on statistical analysis and tabulated in Table 2.4.

Table 2.4: Statistical Analysis of Steel Fibre Global Production by Type (Katzer, 2006)

Type of steel fibres	Percentage accounted for world production (%)
Hooked	67.1
Plain straight	9.1
Twisted	9.1
Crimped	7.9
Other fibres with different endings	6.6

Aspect ratio, $\frac{l_f}{d_f}$ is a parameter used to describe a fibre in term of ratio of its length, l_f to its equivalent diameter, d_f. Aspect ratio of fibres is a major factor with great influence in efficiency of dispersed reinforcement as well as workability and

distance between fibres in a fresh concrete mix. As a result, Katzer (2006) suggested that the aspect ratio of steel fibres need to remain lower than 150 to sustain practicable workability. Statistical analysis was performed in a frame chart with respect to aspect ratio of manufactured fibres as depicted in Figure 2.5. Typical aspect ratios of fibres are commercially available from 30 to 150 for the length of 6 mm to 75mm. However, the interquartile distance is narrowed and embraced the aspect ratio from 45 to 63.5 from the frame presented in Figure 2.5. Hence, it shows that fibres in this range of aspect ratio comprise half of the all types offered by manufacture of steel fibre used for reinforcing concrete. In general, the strength of SFRC increases marginally with increasing aspect ratio.

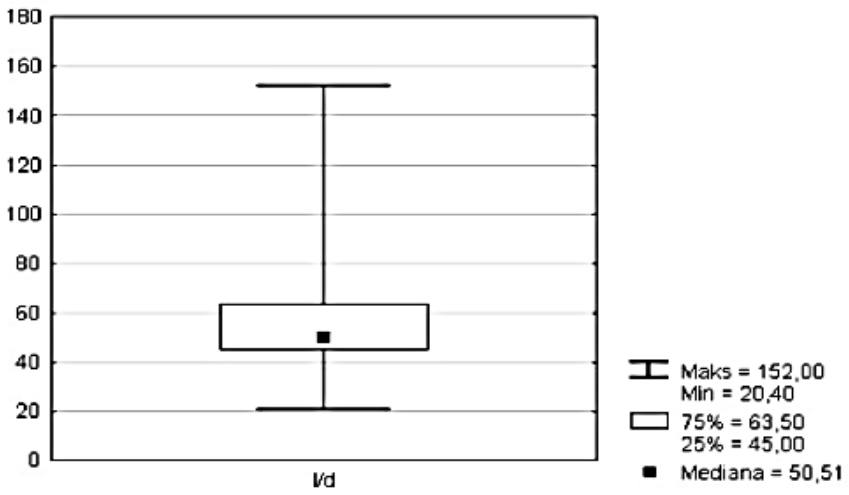

Figure 2.5: Statistical Analysis of Steel Fibres Production by Aspect Ratio (Katzer, 2006)

2.4.1.2 Properties of steel fibre

The properties of steel fibres which can be found in the market are listed in Table 2.5. The coefficient of linear thermal expansion of steel is approximately equal to that of modern concrete which is in the range of 11×10^6 - 13×10^6 /°C (Taylor, 1998). This can indirectly reduce the additional perpendicular and longitudinal stresses when there is difference in temperature from the setting and concrete has versatile structural applications in combination with steel reinforcement.

Table 2.5: Properties of Commercial Steel Fibres (Karim, Abas and Mydin, 2014)

Characteristics	Descriptions
Diameter	0.3 mm–0.7 mm (max 1mm)
Length	25 mm–35 mm
Aspect ratio	45, 55, 65, 80
Density	7840 kg/m^3
Specific gravity	7.84
Young's Modulus	2.1 × 10^5 N/mm^2
Tensile Strength	500 N/mm^2–2000 N/mm^2
Resistance to Alkalis	Good
Resistance to Acids	Poor
Heat resistivity	Good
Elongation at break	5 % - 35 %
Dosage for 1 m^3 of concrete	10 kg/m^3

2.4.2 Relationship Between Steel Fibre and Concrete-based Matrix

This subsection discussed the response of steel fibre and concrete-based matrix with respect to bonding behaviour, bond-slip mechanisms and stress-strain relationship to explain the compatibility between fibres and concrete matrix.

2.4.2.1 Bonding behaviour between steel fibres and concrete-based matrix

It had been extensively conceded that delamination was the major physical detriment in concrete laminates which need to be accounted seriously in the design of composite structural (Liaojun, et al., 2017). Laminates here are referred to composition in layers of different materials in concrete which are bound together viscidly. Delamination resistance, namely interlaminar fracture toughness is also distinguished as the releasing rate of critical strain energy and sliding shear (Anyfantis and Tsouvalis, 2010). When fibres are adequately bonded with hardened concrete, there will be an interaction between fibre and the matrix at the micro-cracks level. Fibres act as a stress transfer medium to bridge these cracks effectively which tend to delay the coalescence and unstable growth of cracks (Vikrant and Kavita, 2012). Once the microcracks transform into macro-cracks when the tensile capacity is reached, the crack opening and crack growth will still be restrained by the fibre by bridging across the macro-cracks effectively. The primary reinforcement mechanisms are referred to this post-

peak macrocrack bridging in most of the commercial fibre reinforced concrete composites (Vikrant and Kavita, 2012).

As the crack propagates and conduced to meet the increase of applied load, fibre bridging effect is developed. Followed by the crack tip, a large fracture process zone (FPZ) is formed and can be addressed with traction-separation laws (Anyfantis and Tsouvalis, 2010). Generally, fibre bridging effect developed when there is an interaction between delamination cracks in composites and misaligned or randomly oriented fibres (Spearing and Evans, 1992). Fibre bridging is favourable as it increases fracture resistance when the crack grows. The growth of delamination will be curbed when this effect is utilized especially when the cracks extend. Besides, consequential specimen geometry effects are taken into consideration at the same time. As discussed in Liaojun, et al. (2017), initial crack growth behaviour may not depend on nonobjectivity alignment, whereas interface geometry had significant influences on the propagation of cracks. This is due to the presence of fibre bridging in multidirectional delamination of composite in large-scale (Liaojun, et al., 2017).

As a result, steel fibres which act as shear reinforcement increases the composite aggregate interlock by transmitting tensile stresses through diagonal cracks as well as reducing crack width. The shear failure modes of fibre reinforced concrete can be referred to as material failure or bond failure between fibre and matrix.

2.4.2.2 Bond-slip mechanisms of concrete reinforced with steel fibres

Investigations done by Jean-Francois and Nemkumar (1994) concluded that the bond-slip characteristic of fibres parallel to the loading direction was significantly superior to inclined fibres. This can be explained as inclined fibres absorbed less pull-out energy with smaller peak pull-out bearing load. Hence, decrease in the energy absorption capability can be caused by brittle fibre and matrix failures. Bridging fibres which possess bond-slip characteristics play a pivotal role in delaying further crack openings and also resisting complete fibre pull-out to fibre fracture across a crack. The mechanisms of fibre reinforcement can be understood through a single fibre pull-out test to evaluate the effectiveness of a given fibre in transferring stress. Those mechanically deformed fibres with positive anchorage ends in concrete can retain its pull-out resistance when bonded in cementitious matrixes.

In actual, fibre and matrix properties including strength, strain capacity and modulus of elasticity are more significant in dealing with deformed fibres than plain

straight fibres as stress field in the vicinity of the fibres can become more complex due to the inclination of fibre to the loading direction. This is because stresses are transferred through the elastic or frictional interfacial bond as well as through anchorage. Three deformed steel fibres namely hooked-end, crimped and twin-cone were chosen to investigate the bond-slip characteristics in Jean-Francois and Nemkumar (1994).

An overall pre-peak bond-slip curves for the three fibres which indicated as F1 (hooked-end), F2 (crimped) and F3 (twin-cone) are shown in Figure 2.6 for normal and high-strength matrixes. A bend over point (BOP) at which nonlinear behaviour began is where a distinct linear initial portion terminating in the pull-out curves (Jean-Francois and Nemkumar, 1994). By assuming that the load at the BOP indicated to the breaking of the elastic fibre-matrix bond, the higher average interfacial bond strength values corresponded to higher pull-out of deformed fibres from high-strength matrixes (Jean-Francois and Nemkumar, 1994). Even though the curves corresponded to the fibre bridging behaviour only after the cracking of matrix, however, some minor matrix cracking may be expected to occur before the appearance of a micromechanical crack in the composite. It can be said that the fibre bridging effect may happen before the first perceived micromechanical crack occurs in the composite.

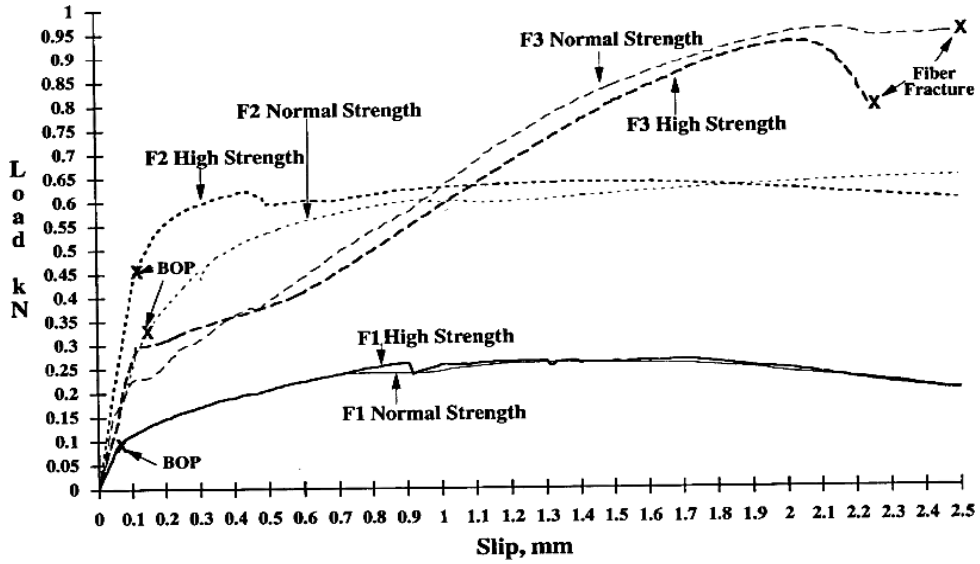

Figure 2.6: Prepeak Bond-slip Curves for Aligned Fibres F1, F2 and F3 in Normal and High Strength Matrices (Jean-Francois and Nemkumar, 1994)

The maximum resistance to crack-widening offered by fibres can by represented by the ultimate load supported by the fibre throughout the pull-out process. The outcomes of peak loads supported by the three fibres in the matrixes are shown in Figure 2.7 as a function of the fibre inclination angle. As can be seen in Jean-Francois and Nemkumar (1994), the peak loads decreased whenever the inclination angle increased, however, there was an exception in the case of hooked-end steel fibre, where the loads remained nearly unchanged. However, Naaman, Antoine and Shah Surendra (1976) addressed that the peak pull-out load at an angle is at least as high as an aligned angle for a straight fibre, which can explain that hooked-end fibre likely behaves a straight fibre. In general, the energy absorbed for a given slip decrease when there was an increase in fibre inclination angle with respect to the loading direction.

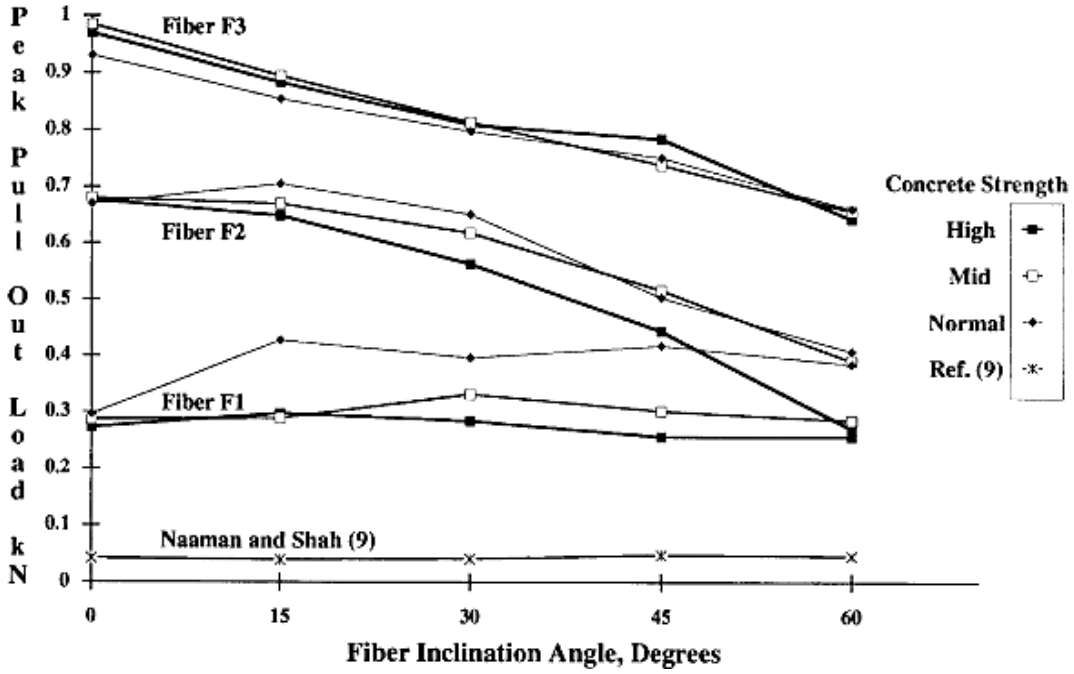

Figure 2.7: Peak Pull-out Loads Supported by Different Fibres as A Function of Inclination Angle (Jean-Francois and Nemkumar, 1994)

From the investigations of Jean-Francois and Nemkumar (1994), there is additional shear stresses imposed on the inclined fibres once the fibres enter the matrix. This process can be explained with inter-crystal slippage where yield is substantively aided by the presence of accompanying shear stresses on the material. Therefore, fibres will gain the ultimate conditions earlier at lower values of the externally applied load, where lower peak pull-out loads for the inclined fibres. However, since hooked-end

fibres occur remote from the hook where yielding really occurs, these additional shear stresses do not influence them. Hence, the peak pull-out load is independent of fibre inclination. From an energy absorption point of view, fibre which is aligned with respect to the loading direction has greater energy absorption capacity at a certain slip compared to the one that is inclined. Hence, an optimal inclination can be referred to zero-degree inclination with respect to the loading direction.

Figure 2.8 shows the demonstration of fibre pullout test where the steel fibres were embedded in small dog bone-shaped concrete specimen. The effects of steel fibre type and inclination angle on the steel fibres pullout behaviour was to be evaluated. Besides, Table 2.6 summarized the pullout test results for four different types of steel fibres at inclination angle of 0^o, 30^o, 45^o and 60^o.

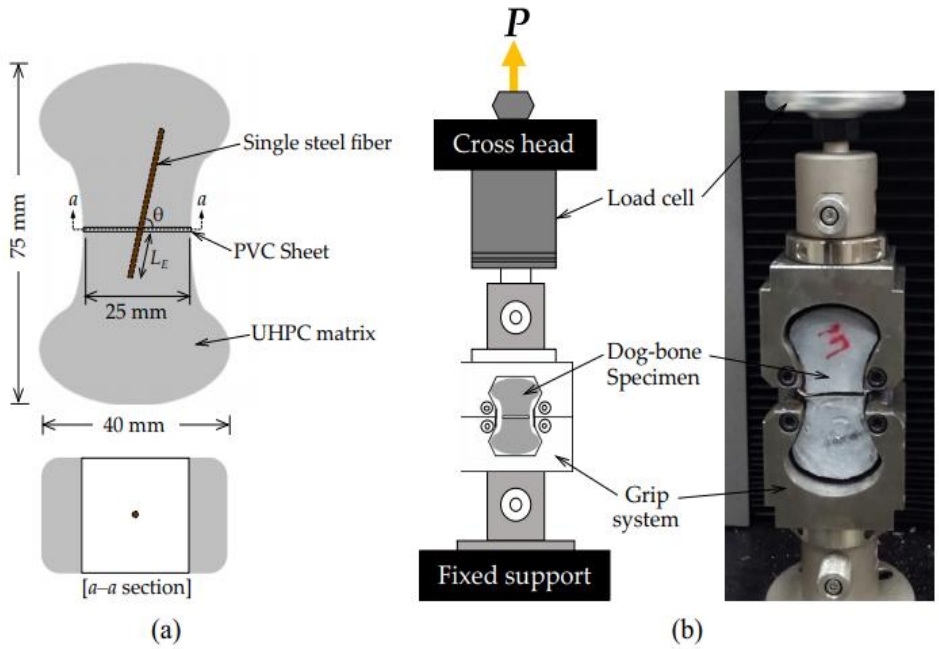

Figure 2.8: Fibre Pullout Test : (a) Schematic Geometry of Dog-bone Specimen and (b) Test Setup (Yoo, et al., 2019)

As shown in Table 2.6, the hooked fibre possessed the highest average bond strength at all inclination angle, followed by twisted fibre or half-hooked fibre and lastly the straight fibre. Due to the highest bond strength in hooked fibre, it possessed the highest maximum fibre tensile stresses among the other types of steel fibres.

Table 2.6: Summary of Pullout Test Results (Yoo, et al., 2019)

Fiber type	Inclination angle [°]	Avg. bond strength, τ_{av} [MPa]	Slip capacity, S_{max} [mm]	Max. fiber stress, $\sigma_{f,max}$ [MPa]
S-fiber	0	5.95 (3.015)	1.05 (0.958)	793.3 (344.726)
	30	6.91 (1.324)	2.28 (2.205)	921.3 (321.825)
	45	6.57 (2.377)	3.77 (1.929)	876.0 (372.943)
	60	5.92 (0.389)	3.05 (1.114)	789.3 (72.266)
T-fiber	0	18.65 (2.644)	1.28 (0.543)	1407.6 (234.855)
	30	19.02 (5.364)	1.46 (1.388)	1551.9 (472.166)
	45	18.14 (9.844)	1.53 (0.665)	1209.1 (656.296)
	60	17.16 (2.509)	1.84 (0.725)	1281.4 (187.350)
H-fiber	0	23.48 (0.548)	1.12 (0.205)	2806.3 (136.368)
	30†	24.42 (0.828)	2.49 (0.438)	2605.2 (88.306)
	45†	24.31 (0.492)	1.73 (0.398)	2593.1 (52.498)
	60†	21.39 (0.830)	3.19 (0.591)	2281.6 (88.522)
HH-fiber	0	15.58 (3.475)	1.25 (0.558)	1661.5 (370.625)
	30	20.77 (1.309)	1.96 (0.142)	2215.8 (139.605)
	45	21.01 (0.553)	3.40 (0.631)	2229.5 (60.971)
	60	16.50 (2.925)	3.66 (0.724)	1759.7 (312.036)

[Note] S-fiber = straight fiber, T-fiber = twisted fiber, H-fiber = hooked fiber, HH-fiber = half-hooked fiber, and () = standard deviation.
† Fiber is ruptured.

2.4.2.3 Stress-strain in steel fibre in SFRC members

By taking account of the detailed characteristic of steel fibre in SFRC members, shear behaviour models had been proposed in Jin-Ha, et al. (2013), which had been modified based on softened truss models (STM) instead of a discrete crack model to evaluate the shear stresses and strains in steel fibres. In the analytical models, steel fibres were modelled as independent reinforcing materials. The potency of the steel fibres as a shear reinforcement is evaluated by assessing the benefaction of the steel fibres to the total shear resistance of SFRC beams (Jin-Ha, et al., 2013).

The utilisation of the steel fibre tensile capacities with respect to the fibre rupture or slip behaviour during a pull-out test can be described with fibre efficiency in Equation 2.1 (Clifford, et al., 2016). Throughout the experimental investigation of Clifford, et al. (2016), it was found out that the scatter of steel fibre efficiency decreased when embedment depth increases for all fibre types. Besides, with greater depths of embedment, steel fibres perform better in shear resistance when the slip dependent shear stress decreased, and the slip displacement increased. This behaviour can be explained with the increase in adhesion wedge and bond effects due to the extra steel fibre contact surface in a concrete matrix.

By focussing on the effect of the steel hooked end shape fibre, the tangential stresses in hook act with bond stresses contemporarily, which bond stresses, τ_f can be explained in Equation 2.2 (Remigijue and Gediminas 2010).

$$\text{Fibre efficiency} = \sigma_{max}/f_y \quad (2.1)$$

where

σ_{max} = tensile stress in steel fibre, N/m^2

f_y = yield strength of steel fibre, N/m^2

$$\tau_f = \tau_1 + \tau_2 \quad (2.2)$$

where

τ_f = total bond stresses, N/m^2

τ_1 = bond stresses in the straight part of the fibre, N/m^2

τ_2 = bond stresses in hook, N/m^2

As discussed in Remigijue and Gediminas (2010), the ultimate force of steel fibre should be equivalent to the optimal pull-out force in fibre. There are three broadly used models of steel fibre anchoring in fibre reinforced concrete matric as presented in Figure 2.9.

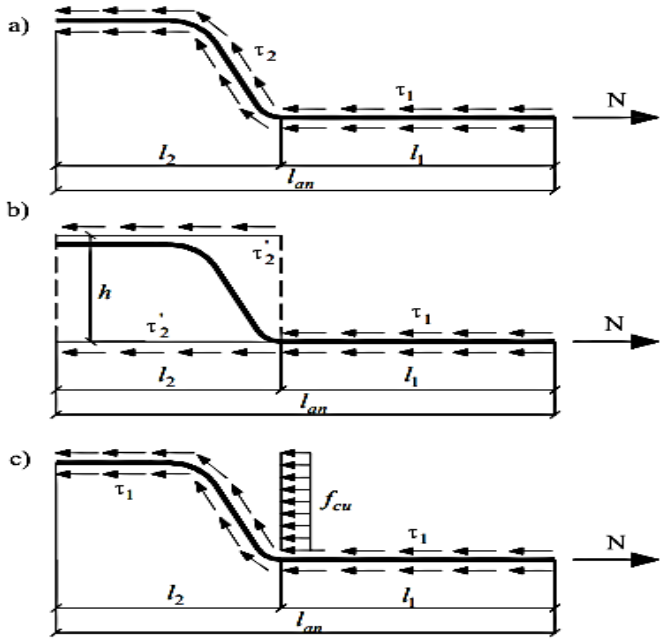

Figure 2.9: Estimation of Steel Fibres Shape Models at Single Hooked End: a) Estimation of bond stresses, τ_2 in hook of fibre in part of l_2; b) Estimation of bond stresses τ_2 by shape of fibre (h, l_2); and c) Estimation of hook by concrete bearing strength, f_{cu} (Remigijue and Gediminas, 2010)

(Note: N = pull-out force; l_{an} = anchorage length)

2.4.3 Advantages of SFRC

As discussed earlier, incorporation of steel fibres in reinforcing concrete enhances the tensile and fatigue flexural strength, increases impact resistance, spalling and also abrasion. Besides, homogeneous and isotropic properties are provided with the uniform dispersion of steel fibres throughout the mix of concrete at the same time increase the structural integrity of the concrete. These properties allow the crack free from stress accommodation throughout the concrete. Steel fibres function to mitigate cracking in concrete by ensuring the microcracks are intercepted in the matrix before they develop. Besides, steel fibres are delivering its bond strength when in contact with concrete matrix and act as a discrete reinforcing bar when extending across the cracks.

Application of steel fibre reinforcement could prospectively replace stirrup reinforcement by eliminating the shear size effect in beam depth and increasing in shear strength (Ranjan Sahoo and Abhimanyu, 2014). This can probably improve productivity and deliver cost efficiency with a reduced volume of concrete-making materials. Steel fibre reinforced concrete is an economical design alternative as it delivers an effective construction and lower labour costs.

2.4.4 Disadvantages of SFRC

Nonetheless, the complete replacement of traditional steel reinforcement with steel fibres is still debatable due to safety issues on loading capacity and the long-term durability of SFRC under exposure to chloride and carbonation. Specifically, the durability of cracked SFRC will reduce because of the chloride and carbonation-induced corrosion of steel fibres when subject to wet and dry cycles in the environment (Victor, et al., 2018). This will give negative impact on the structural integrity especially adverse implications on the mechanical behaviour of SFRC for a long-term perspective.

The disadvantages of SFRC also include workability reduction and water absorption during the mixing of concrete. The capacity of fibres in absorbing water can lead to volume changes in concrete which induce minor cracks. Besides, monitoring and strict control of concrete wastage should be emphasized to minimize the wastage as wasted concrete means wasted fibres.

2.5 Mechanical Properties of SFRC

This subsection discusses the influence of incorporation of fibres on mechanical properties of concrete. The mechanical properties of SFRC are influenced by fibre type, configuration, aspect ratio and content by volume fraction. The physical properties that SFRC exhibits upon the applied force include compressive strength, direct tensile strength, flexural tensile strength, flexural toughness in energy absorption as well as direct shear strength.

2.5.1 Compressive Strength of SFRC

Amit Rai and Joshi (2014) had addressed that the inclusion of fibres may change the failure mode of cylinders and give rise to little effect on the enhancement of compressive strength values with only 0 % to 15 %. The investigation reported by Thomas and Ramaswamy (2007) also stated that there was only a small increase in ultimate strength which less than 10% for addition of 1.5 % steel fibres in the composite concrete by volume fraction. Behbahani, Nematollahi and Farasatpour (2011) also presented that there was only 0 % to 15 % of increment in compressive strength with an addition amount of steel fibre up to 1.5 %.

There was no significant increase in strain at peak stress with the inclusive of steel fibres from the investigations of Thomas and Ramaswamy (2007). Figure 2.10 shows that there was a gradually descending slope in the stress-strain curves, where there was decelerating strength loss after the peak stress. These can indicate that RC was improved in terms of spalling resistance, toughness and ductility with the inclusion of steel fibres as the peak strain increased linearly with the increase of steel fibre volumetric percentage.

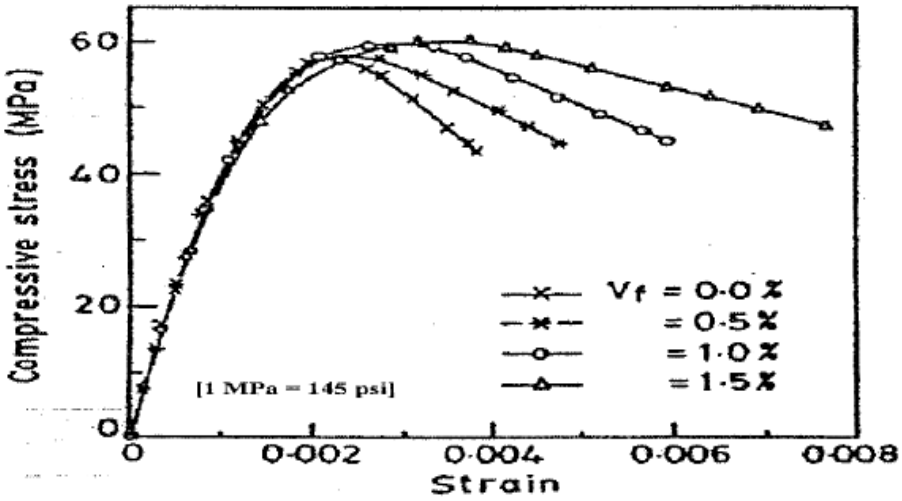

Figure 2.10: Compressive Stress-Strain Curve of SFRC with Different Volume Fraction of Fibres (Padmarajaiah and Ramaswamy, 2002 cited in Behbahani, Nematollahi and Farasatpour, 2011)

2.5.2 Direct Tensile Strength of SFRC

There is no standardized direct tension test method to be utilized in determining the stress-strain curve of SFRC (Hai, 2009). However, the curve can be observed to mainly depends on the fibre index, stiffness of testing machine, gauge length, the occurrence of cracking within the gauge length selected and so on (ACI Committee 544, 1999). Figure 2.11 shows the typical examples of SFRC with straight, hooked and enlarged-end steel fibres under stress-strain curves with strains measured using strain gauges.

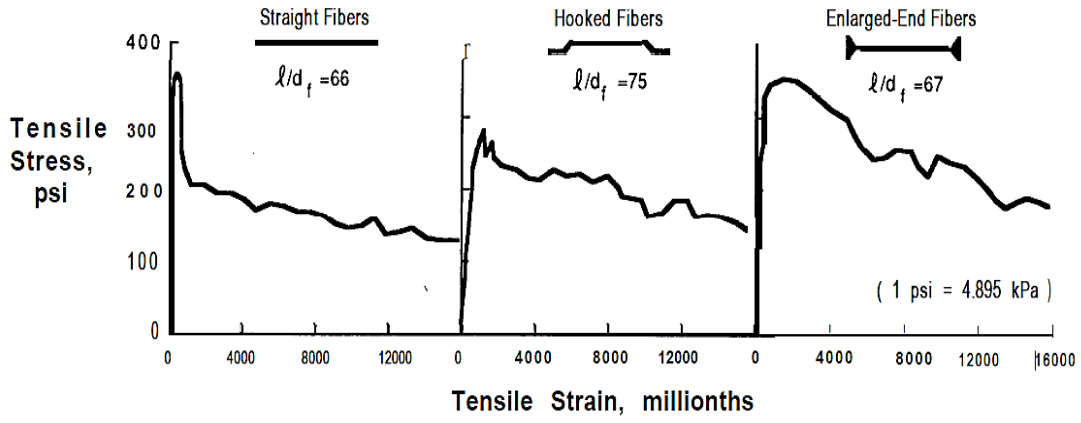

Figure 2.11: Direct Tensile Stress-stain Curves from SFRCs (ACI Committee, 1988)

From the investigation of ACI Committee 544 (1999), the ascending part of the stress-strain curves is found to be similar to normal concrete until the first cracking

occurred, which means that the strength of SFRC is generally similar to that of unreinforced concrete. However, the descending part is based on the fibre reinforcing parameters, fibre index, the volume fraction of fibre and its aspect ratio. ACI Committee 544 (1999) also stated that deformation at multiple cracks, higher frictional and development of fibre bending energy during pull-out of fibre can increase the magnitude of toughness.

As reported by Altaan and Anay (2015), the tensile strength of the FRC had mainly affected the cracking shear stress as compared to shear strength which is highly dependent on the shear span/effective depth ratio. Hence, steel fibres contribute more to shear strength than the first shear cracking at the onset. Behbahani, Nematollahi and Farasatpour (2011) also addressed that the inclusion of fibres barely increased the direct tensile strength but significantly increased in the toughness and post-cracking behaviour.

2.5.3 Flexural Tensile Strength of SFRC

As mentioned in Eleonora (2011), RILEM Technical Committee 162-TDF (Test and Design Methods for Steel Fibre Reinforced Concrete recommended the equivalent flexural tensile strength to be replaced by the residual flexural tensile strength. The equivalent flexural tensile strength is inferred from the energy absorption capacity based on the contribution of steel fibres and can be derived from the area under the load-deflection curve, while the residual flexural tensile strength is inferred from the load applied at a measured displacement of crack opening or midspan deflection.

Steel fibres have a much more significant influence on concrete's flexural strength rather than direct tension and compression. From Figure 2.12, flexural strength values can be determined at Point A, when the first crack occurred at the load at which the load-deformation curve start deviating off from linearity; and Point C where indicates the ultimate flexural strength or rupture modulus when maximum load achieved.

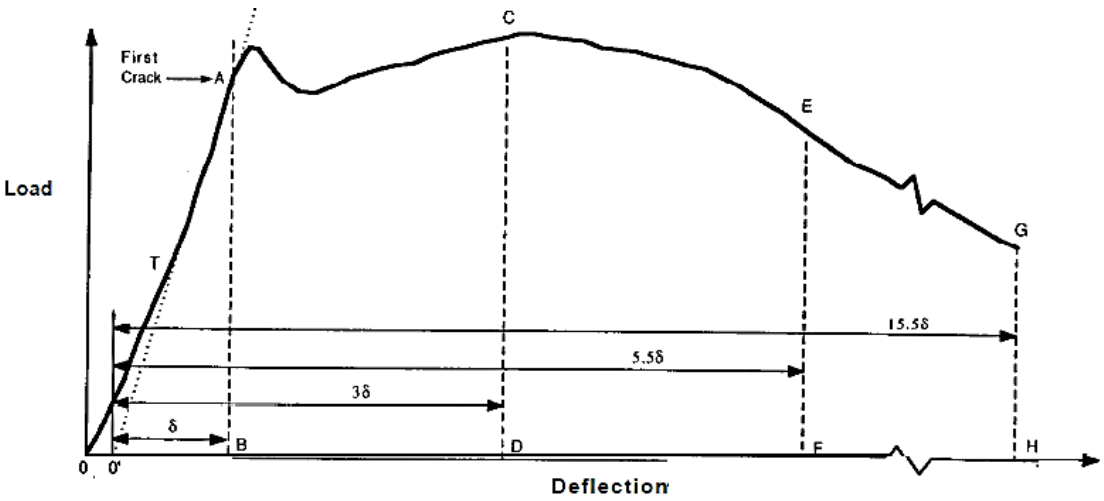

Figure 2.12: Significant Characteristic of Load-Deflection Curve in Determining Flexural Strength (American Society for Testing and Materials, 1997)

Ultimate flexural strength usually increases with the increase of fibre volume concentration (ACI Committee 544, 1999). Steel fibres with less than 0.5 % volume fraction of low aspect ratio less than 50 will have very little effect on static strength properties. Besides, fibres with better end anchorage like hooked end will enhance flexural strength over unreinforced matrices by much as 100% (ACI Committee 544, 1999).

2.5.4 Flexural Toughness of SFRC in Energy Absorption

Toughness is referred to a measure of the capacity in energy absorption at the deformation stage. It is derived from the area under load-deformation curves or stress-strain curves. Enhancement of toughness by fibres able to prevent sudden and accident failure under static loading or under dynamic loading in absorbing energy.

Figure 2.13 depicts the relationship between toughness and strength of fibre reinforced composite regarding the effect of fibre percentage from 0 % to 1.25 %. The increment in tensile strength and concrete toughness is linear with the increase of fibres volume. It shows that the effect fibres on the toughness are higher than on strength.

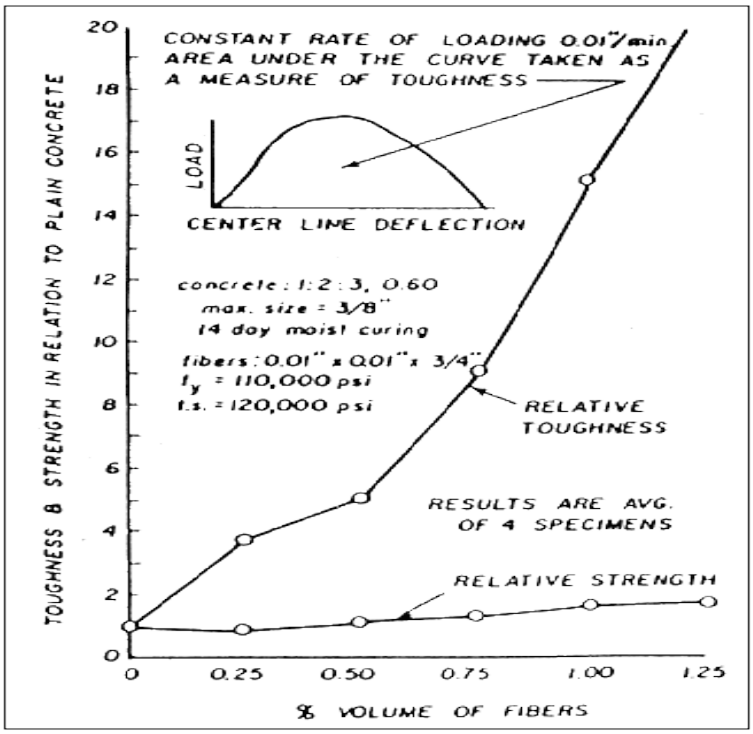

Figure 2.13: Effect of Fibre Volume Percentage on Toughness and Strength of Composite (Shraddhu, 2017)

Deformed fibres usually improve the toughness and capacity of energy absorption of concrete. As can be seen in Jean-Francois and Nemkumar (1994), fibres with end anchorage have more potent performance than fibres with deformations throughout the entire length. The matrix strength shows its influence on the characteristics of toughness when there is a steeper sudden drop after the first crack within the capacity of load carrying. However, this influence is fibre geometry dependent.

2.5.5 Direct Shear Strength of SFRC

Deficits in shear resistance which lead to shear failure in concrete member are preceded by any deflections or cracking. This problem may arise when stress-induced exceed the maximum shearing stress resistance. However, shear failure happens when there is sliding between layers of a structural element with the applied forces in the opposite direction. Therefore, the shear resisting actions will eventually be effectuated when the structural element is placed under a combination of flexure and shear, especially at the regions where initiation of multi-axial state and diagonal cracks appear (Mari, et al., 2014). This action allows the shear force to be propagated between

elements across the crack. The total shear transferred by compression chord of concrete reflects the shear strength of the structure.

As can be seen in the experimental research of Mari, et al. (2014), the evolution of cracking in a shear failing element without stirrups sequencing from the early stage of loading is shown in Figure 2.14 (a) until the loading was extended to cause the ultimate failure of element as shown in Figure 2.14 (d). At a specific load level before failure, the crack propagation at the first stage is slow with moderate critical crack width. This is due to the main role contributed by the interlocking of aggregate and residual tensile strength to allow an effective shear transfer. However, crack width increased significantly with increment of loading, hence shear resistance was devitalized at bigger crack widths as can be observed in Figure 2.14 (b) and Figure 2.14 (c). It can be evaluated that the combination of compression and shear stresses in the compression chord formed a new extension of crack from the tip of the web's crack, in the compression zone of a beam.

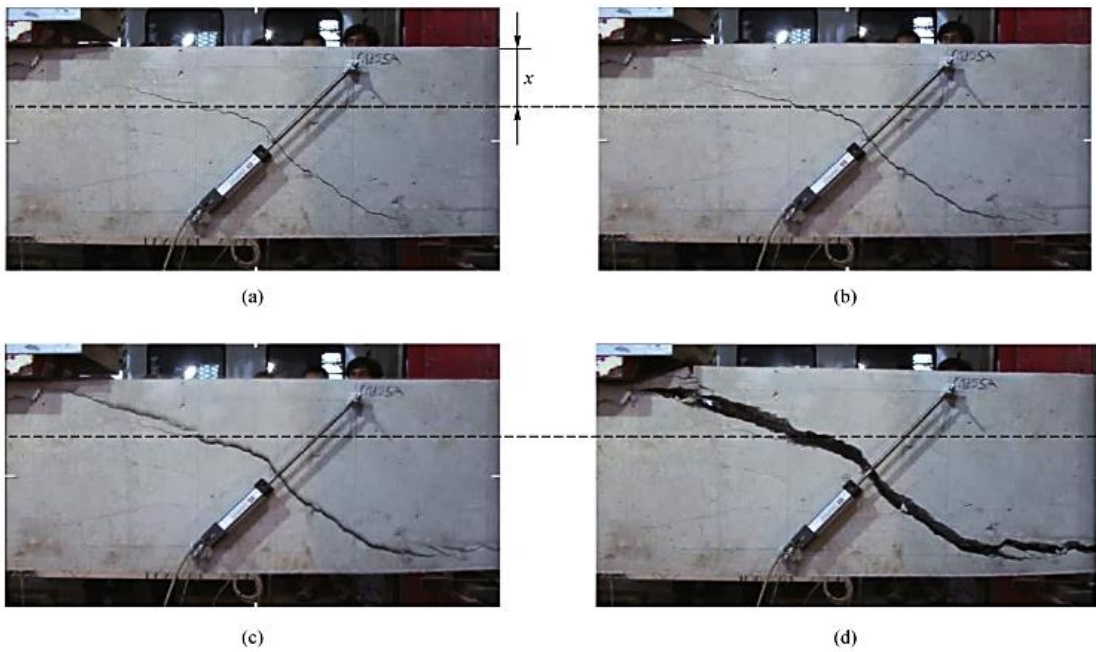

Figure 2.14: Sequence of Critical Shear Crack Propagation in a Shear Failing Element (Mari, et al., 2014)

As depicted in Figure 2.15, the tip at the first branch of critical crack referred to the most impotent section which came before the combination of shear-bending failure. By making a conservative assumption as in Equation 2.3, the critical crack was estimated to initiate at the intersection between the cracking moment of section and

bending moment diagram at failure (Mari, et al., 2014). Thus, there will be higher shear force resistance located at a deeper depth of the compression chord at the region which nearer to point of zero bending moment because of the inclination crack. In contrast, there will be higher shear transfer capacity at the section which located far away from support with the same compression chord depth but subjected to higher normal stresses (Mari, et al., 2014).

$$S_{cr} = M_{cr}/V_u \tag{2.3}$$

where

S_{cr} = Section where the critical shear crack initiated

M_{cr} = Cracking moment

V_u = Ultimate shear force

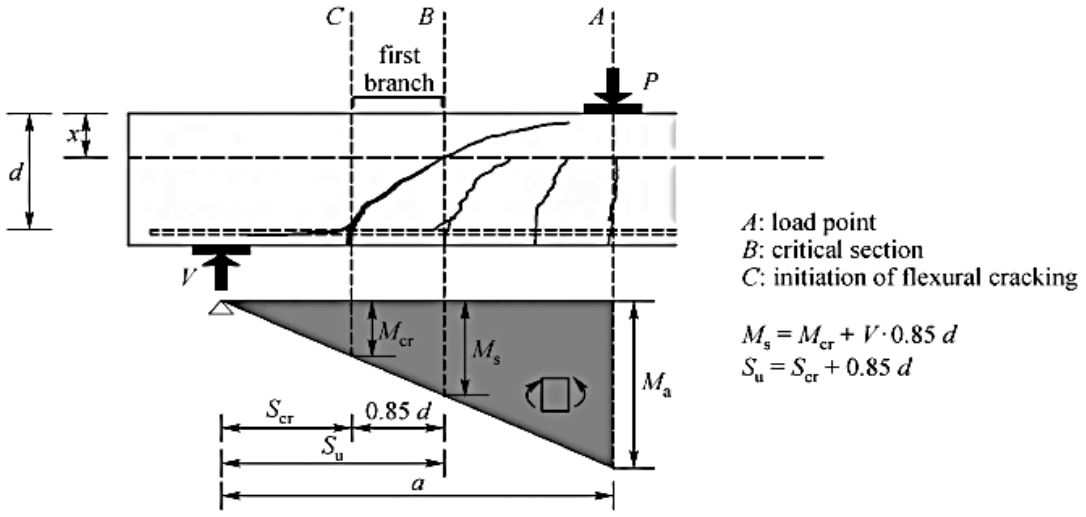

Figure 2.15: Section of Shear Critical in the Beam (Mari, et al., 2014)

From the experimental and numerical investigations made in Cladera and Mari (2014) and Cladera and Mari (2015), the inclination of the cracks can be related to Equation 2.4 based on the first branch of flexural-shear crack with respect to a horizontal projection which is equivalent to 0.85*d*.

$$\cot\theta = \frac{0.85}{1 - x/d} \tag{2.4}$$

2.5.5.1 Shear transfer mechanism

The equilibrium in the shear span of one side of a simply supported beam without shear reinforcement is illustrated in Figure 2.16. The shear transfer mechanism considers a constant shear force over the beam length. There are compression (C) in the top region and tension (T) in the bottom region of the beam. As both internal and external forces are maintained, there is a diagonal crack bounded on one side. The factors assumed to be carrying the external transverse force when there is no shear reinforcement is provided for the normal reinforced concrete beam are shear force over the uncracked compression zone, V_c; dowel action by flexural reinforcement, V_d and inclined shear stresses of aggregate interlocking, V_a across the inclined crack (Birgisson, 2011). In addition to beam action, shear contribution also includes arch action as well as fibres.

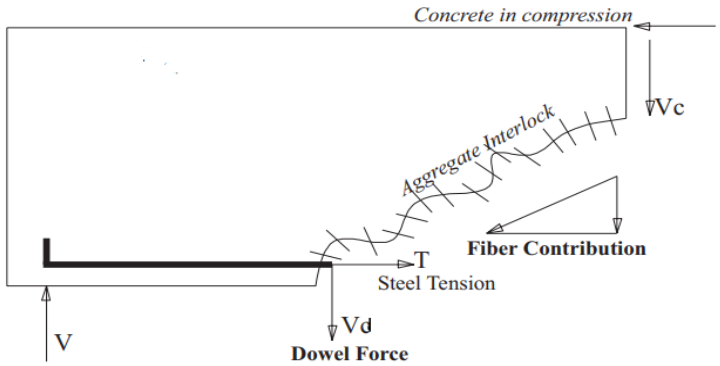

Figure 2.16: Mechanisms of Shear Transfer in a Cracked Beam Without Stirrups (Xia, et al., 2015).

However, the V_a action decreases in shear resistance when the inclined cracks gradually widen in the concrete while V_c and V_d increase. Upon the failure in aggregate interlocking, there is a great amount of shear force transmitted rapidly to the compression zone which causes sudden fracture of the beam when the contribution of arch action is relatively small (Birgisson, 2011). Furthermore, there are forces act on the longitudinal reinforcement due to the bar deflection at the crack face when there are inclined cracks across the dowel (El-Ariss, 2006). Hence, the total shear resistance of dowel action is the summation forces of aggregates try to interlock each other around the bar to resist the deflection. Furthermore, there are beam and arch mechanisms in shear resistance when beams develop a flexure-shear interaction (Birgisson, 2011). Therefore, the structural beam can achieve considerably higher load

than at diagonal cracking when there is more contribution from arch action than beam action.

Moreover, the shear resistance increased as crack continued to propagate in the compression chord until the ultimate shear failure occurred. The crack growth extends and followed by the reduction in aggregate interlocking during the loading process. However, this decrement in aggregate interlocking should compensate with the transferring of shear by the concrete chord in compression to accomplish the equilibrium state (Mari, et al., 2014). Figure 2.17 depicts the shear stress distribution during pre-incipient failure in the limit state of the critical section at a region close to the tip of the first branch crack which is away from the local stresses around the tip. Indications such as *x* refer to the depth of neutral axis while *d* refers to effective depth of the member section.

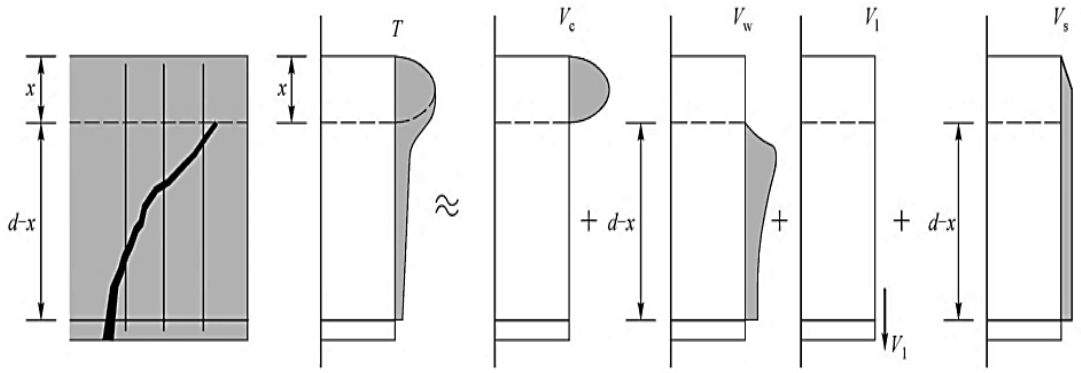

Figure 2.17: Profile of Combining Shear Stresses Distribution of Contributing Actions in Incipient Failing Situation (Mari, et al., 2014)

Note: T = Total shear resistance by concrete

V_c = Shear resistance by uncracked compression head

V_w = Shear transfer across web cracks

V_l = Shear resistance by longitudinal reinforcement

V_s = Shear resistance by transverse reinforcement

2.6 Shear Failure of SFRC Beam Structure

Beam is one of the structural members that initially encounters lateral loads. The total effect of reaction forces induced by the applied loads can leads to shear forces and bending moments in term of deflections, internal stresses and strain of the beam. However, a crack may occur and parallel with the principal compressive stress

direction or normal to the principal tensile stress direction when the principal tensile stress reached the concrete tensile strength at any point (Raju, 2014).

A resulting failure will give rise to a cut across cracking namely shear cracks and diagonal cracks if considering a beam under applied shear forces at ultimate loads. The actual behaviour of shear failure can be determined through two types of inclined cracks, namely flexural-shear cracks (crack extended from past flexural cracks) and web-shear cracks (cracks developed in the web of beams at highest shear stress region) as shown in Figure 2.18 (Neil, Daniel and Robert, 2005).

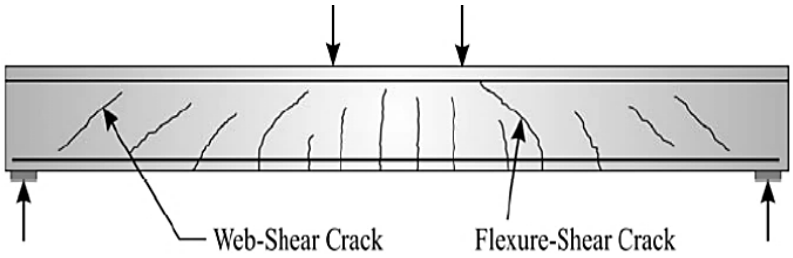

Figure 2.18: Types of Inclined Cracks Subjected to Shear Forces (Neil, Daniel and Robert, 2005)

With respect to the parameters of dimensions, configurations, loading types, longitudinal reinforcement and structural properties, diagonal failure modes caused by cracks are due to diagonal tension, shear compression, shear tension, web crushing and arch rib as shown in Figure 2.19 (Pillai et al., 2003 cited in Raju, 2014). As discussed in Raju (2014), diagonal tension failure normally takes place in concrete members which lack longitudinal reinforcement or less stirrups, it may be initiated from the past flexural cracks and expand quickly throughout the cross-section of member before collapse as illustrated in Figure 2.19 (a); shear compression failure occurs above the shear crack tip when there is crushing of concrete in compression zone, where compression zone is formed with less web reinforcement but adequate longitudinal reinforcement ratio as illustrated in Figure 2.19 (b); shear tension failure is usually caused by imperfect bonding of longitudinal reinforcement with concrete which leads to development of crack alongside the main dowel bars until they combine with a flexural shear crack as illustrated in Figure 2.19 (c); web crushing failure is normally found in I-beams due to the thickness of the slender web as illustrated in Figure 2.19 (d); and arch rib failure normally takes place when there is transference of direct force from loading to the bearings in short span beams or deep beams.

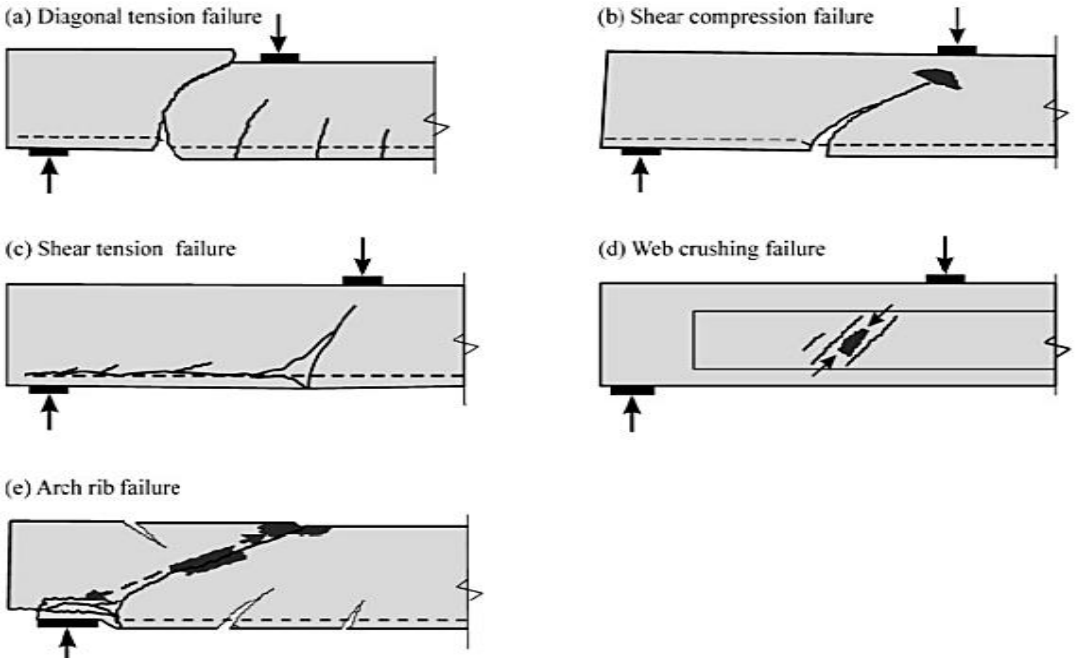

Figure 2.19: Shear Failure Modes and Crack Pattern of Beams (Pillai et al., 2003 cited in Raju, 2014)

2.7 Factors Influencing Shear Capacity

The shear capacity of reinforced concrete beams is influenced by a number of parameters. The main factors affect the shear failure occurrence are discussed in this section. The factors include the effect of depth of beam, the effect of shear span-to-depth ratio and effect of fibre percentage.

2.7.1 Effect of Depth of Beam on the Shear Crack Width

The deeper the member, the higher the shear resistance exhibited which allows longer diagonal shear cracks form upon to failure, and thus decrease the effective stress magnitude to be transmitted across the crack widths. This will require a greater force in magnitude to cause a deep beam to fail in shear than other beams with a smaller length of the inclined crack.

2.7.2 Effect of Shear Span-to-Depth Ratio (*a/d*) on the Behaviour of Beams

The assumption was made that a RC beam without stirrups would undergo the diagonal tension failure when the principal tensile stresses in line with the shear span exceed the concrete tensile strength (Guray, Riza Secer and Semih, 2017). As the moment and shear force magnitude have influence in the development of the inclined

shear cracks in the RC beam, they will control the shear capacity as well as the failure mode. The beam will act as a deep beam with a smaller value of *a/d*, which is less than 2.5 and possess a higher shear capacity than the beam with higher *a/d* value of more than 2.5 (Harvinder, 2017). This can be explained that in the case of a deeper beam, compression strut is formed between the two adjacent inclined shear cracks at which shear can be transmitted to the support directly.

As defined in Harvinder (2017), the beam with smaller *a/d* value of less than 2.5 normally fails when there are inclined cracks being initiated and followed by crushing of the reduced concrete section happening at the crack tip which is known as a shear-compression failure. Final failure can also be occurred when the inclined crack extends in the downward direction, approaching the beam tensile face until it joins the longitudinal tension steel. This failure is known as a shear-tension failure. However, for the beam with *a/d* value more than 2.5, vertical flexural shear cracks will form in the maximum moment region causing flexure failure.

Diagonally reinforced short beams with shear span ratio range from 0.89 to 1.25 are subjected to cyclic loading. Flexural capacity, bond strength and shear strength can then be evaluated by equations in the American Concrete Institute (ACI) Code conservatively for diagonally reinforced short beams. However, Yuji and Hideki (1996) had discussed that the failure mode of most specimens was sliding shear failure at short span beam end after yielding.

2.7.3 Effect of Fibre Percentage

The shear stress has a linear proportional relationship with the fibre percentage, indicates that shear strength increases with the greater fibre volume fraction. However, the relationship between shear stress and fibre percentage showed a more consistent trend than the relationship between normalized shear stress and fibre percentage as shown in Figure 2.20. As explained in Hai (2009), the increase in fibre content can reduce its effectiveness when its volume fraction exceeds 1 %. Besides, the strain of SFRC increases according to peak compressive strength as the volumetric percentage of fibres increase. The outcome of the research by Jin-Ha, et al. (2013) showed that the estimated optimized volume fraction of steel fibres was 1 %-1.5 % in the aspect of shear performance.

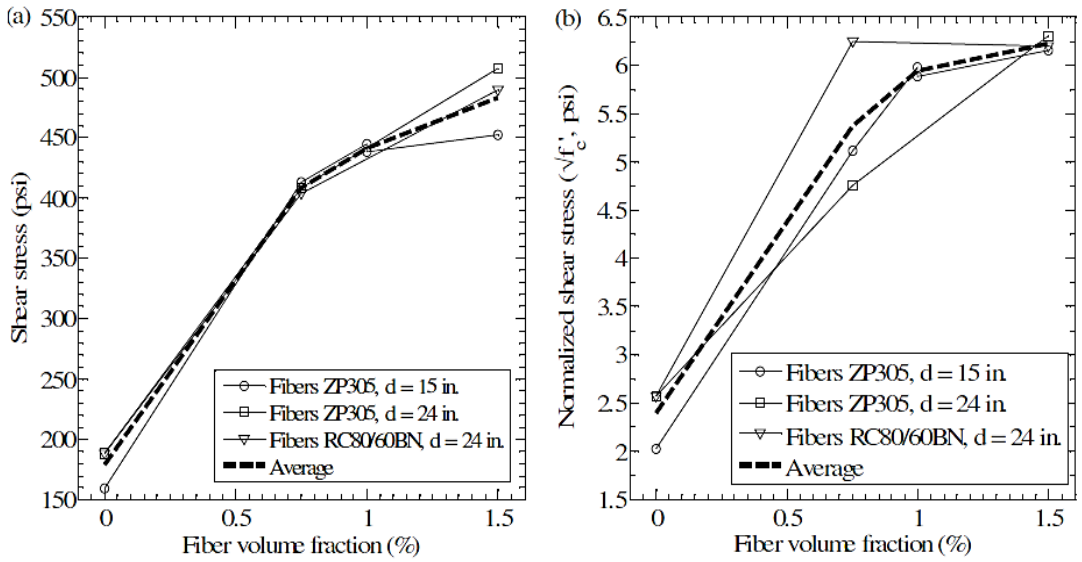

Figure 2.20: Effect of Fibre Percentage on Shear Stress and Normalized Shear Stress (Hai, 2009)

2.8 Previous Research Related to SFRC

Mello, Ribellato and Mohamedelhassan (2014) had investigated the improvement of concrete properties with the inclusion of steel fibres with respect to compressive, tensile and flexural strength of concrete along with the cracking ductility. An aspect ratio of 60 with 33 mm long of 0.55 mm diameter hooked end steel fibres were used in this research. It had a density of 7.84 g/cm^3 with 1200 MPa of tensile strength.

Mello, Ribellato and Mohamedelhassan (2014) also discussed that the mix was found to segregate with more than 1200 ml/m^3 plasticizer added and remained workable even though the mix did not achieve the desired slump. It showed that the mix workability decreased with the increase of fibre percentage as fibres absorb more cement paste to be coated due to the large surface area in high content. Besides, the slump loss is due to the increase of the mixture viscosity. Even though 0.5 % and 1.5 % of steel fibre by volume reduced the concrete compressive strength, fibres at higher concentration improved this strength by up to 20 %. The experimental results as shown in Figure 2.21 presented the increase in concrete tensile strength with the addition of steel fibres except at 0.5 % steel fibres. Moreover, it had been shown by Amit Rai and Joshi (2014) that fibre reinforced concrete with the inclusion of fibre volume fraction as low as 1 % or lower, had an insignificant effect on compressive and tensile strength (Amit Rai and Joshi, 2014).

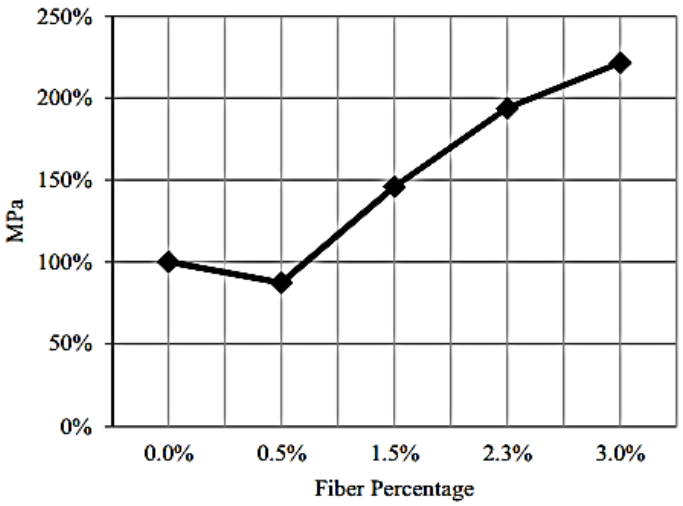

Figure 2.21: Tensile Strength for Concrete with addition of Steel Fibres (Mello, Ribellato and Mohamedelhassan, 2014)

There was an increase of 121 % of concrete's original tensile strength with 3.0 % of fibres added. Besides, concrete flexural strength was improved when steel fibres were incorporated at the studied volume fraction. The fact that at 2.3 % had higher improvement than at 3.0 % can be explained by the difficulty in rodding the concrete and the steel fibres were not as dispersed with the latter percentage. Table 2.7 shows all the results obtained for concrete strength with the inclusion of steel fibres at different volume fraction.

Table 2.7: Changes in Concrete Strength with Different Fibres Addition (Mello, Ribellato and Mohamedelhassan, 2014)

STEEL RESULTS

	Workability		Compressive		Flexural		Tensile	
	Plasticizer (mL)/m³	Slump (mm)	Strength (MPa)	Δ in Compressive Strength	Strength (MPa)	Δ in Flexural Strength	Strength (MPa)	Δ in Tensile Strength
Plain Concrete	0	85.0	42.9	-	6.46	-	3.75	-
Steel Fibers 0.5%	0	75.0	39.0	-9.0%	6.88	6.4%	3.27	-12.8%
Steel Fibers 1.5%	1145	20.0	41.0	-4.4%	9.43	45.9%	5.47	45.8%
Steel Fibers 2.3%	1135	0.0	45.2	5.3%	11.68	80.7%	7.27	93.3%
Steel Fibers 3%	1127	0.0	51.4	19.9%	10.85	67.9%	8.30	121.5%

Furthermore, several laboratory experiments on mechanical properties of SFRC had been carried out by researchers and the data on the percentage increment in strength from their investigation is summarized in Table 2.8. It was found that there will be an increase in the modulus of elasticity up to 3 % for every 1 % increment in fibre content by volume. Moreover, Table 2.9 shows the summary of laboratory testing which had been carried out by previous researchers for different types of concrete with the addition of steel fibres.

Table 2.8: Summary of the Implemented Approaches on Mechanical Properties of SFRC from the Previous Study

Author(s) (year)	**Increment in strength in percentage throughout the evaluation tests on SFRC (%)**			
	Compressive strength	**Split tensile strength**	**Flexural strength**	**Modulus of Elasticity**
Shah Suendra and Rangan (1994)	6-17	18-47	22-63	8-25
Byung Hwan (1992)	6-17	14-49	25-55	13-27
Barrows and Figueiras (1992)	7-19	19-48	25-65	7-25

Table 2.9: Summary of Laboratory Test Conducted for Different Types of Concrete with Incorporation of Steel Fibres

Author(s) (year)	Types of concrete	Type of Fibre	Work-ability	Hardened Concrete Properties Test							Durability		MF
			ST[1]	CT[2]	SPT[3]	FPBT[4]	TPBT[5]	CFT[6]	MoE[7]	MoR[8]	CPT[9]	WAT[10]	SEM[12]
Abbass, Khan and Mourad (2018)	NWRC	H	✓	✓				✓					
Afroughsabet and Ozbakkaloglu (2015)	HSC	H		✓	✓	✓						✓	
Altun, Haktanir and Ari (2007)	NWRC	H		✓	✓	✓		✓	✓				
Balendran, et al. (2002)	NWHSC & LWHSC	H		✓	✓		✓	✓		✓			
Banthia and Sappakittipakorn (2007)	NWRC	C		✓		✓		✓	✓				

Table 2.9 (Continued)

Hassanpour, Shafigh and Mahmud (2012)	LAC	H	✓	✓	✓			✓		✓			
Khaloo, et al. (2014)	SCRC	H	✓	✓	✓	✓		✓					
Selvi and Thandavamoorthy (2013)	NWRC	C		✓	✓						✓	✓	
Yehia, et al. (2016)	SCRC	H		✓	✓				✓		✓		✓

Note: NWRC = Normal Weight Reinforced Concrete, HSC = High Strength Concrete, LAC = Lightweight Aggregate Concrete, SCRC = Self-compacting Concrete, H = Hooked Fibre, C= Crimped Fibre, [1]ST = Slump Test, [2]CT = Compressive Test, [3]SPT = Splitting Tensile Test, [4]FPBT = Four-point Bending Test, [5]TPBT = Three-point Bending Test, [6]CFT = Compressive and Flexural Toughness, [7]MoE = Modulus of Elasticity, [8]MoR = Modulus of Rupture, [9]CPT = Chloride Permeability Test, [10]WAT = Water Absorption Test, [11]SEM = Scanning Electron Microscope

2.9 Existing Theoretical Models and Empirical Formulas

Concrete elements itself have sufficient shear capacity in resisting their self-weight and external imposed load. The resulting shear forces will normally be highest towards the support and there are combine factors of resistance. Shear stresses caused by torsional moments on a beam will impose diagonal cracking. Hence, reinforcement is necessary which is additional to that required for bending and shear. The action of a reinforced concrete beam in shear was illustrated as an analogous truss as shown in Figure 2.22 in compliance of EC2. The concrete plays its role to be both top and diagonal compression members, where the diagonal angle inclined at an angle to the horizontal. The combination of strut model also consists of the longitudinal tension reinforcement as bottom chord and vertical shear links as transverse tension members. However, without considering the direct contribution from the shear capacity of the concrete itself, all the shear should be resisted by the transverse links provision in this model.

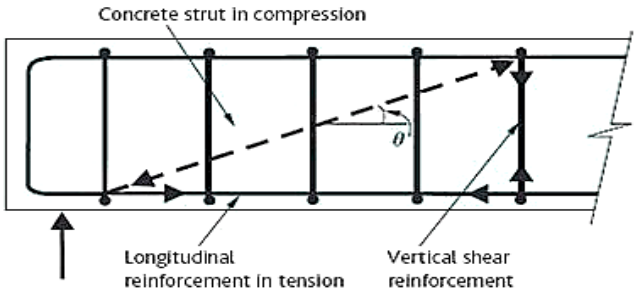

Figure 2.22: Analogous Truss Model Based on Variable Strut Inclination Method

Assumption was made in Pruijssers (1986) that the entire cross section of the beam contributes to the shear resistance, V_{cu} for the theoretical modelling of the shear failure mechanism in beams without stirrups. This assumption is valid for uncracked beams and the ultimate shear stress, τ_u is presented as Equation 2.5, where b is the beam width and d is the effective depth of beam.

$$\tau_u = V_{cu}/bd \tag{2.5}$$

Shear design model was addressed in Babar, Joshi and Shinde (2015) to verify the strength of SFRC deep beams for present investigations. The proposed ultimate shear strength of SFRC is as Equation 2.6.

$$v_{uf} = e\,[0.24\,f_{spfc} + 80\,\rho\frac{d}{a}] + 0.41\,\tau F \text{ (MPa)} \quad (2.6)$$

where,

e = 1.0 when $a/d > 2.8$; $2.8\,d/a$ when $a/d < 2.8$

f_{spfc} = computed value of split cylinder strength of fibre concrete

= $f_{cuf} / (20 - \sqrt{F}) + 0.7 + 1.0\sqrt{F}$, where f_{cuf} is fibre concrete cube strength

ρ = Longitudinal reinforcement ratio

d = effective depth of beam

a = shear span

τ = average fibre matrix interfacial bond stress, taken as 4.15 MPa (Kwak, et al., 2002)

F = $V_f \frac{l_f}{d_f}$, fibre factor in which V_f = fibre volume fraction ; l_f = length of fibre and d_f = diameter of fibre.

2.10 SFRC Application

The versatility of SFRC in the construction industry has various applications. SFRC has been successfully applied in highway and airfield pavements by overlaying to the beneath slab in bounded or unbounded form as it enhances the flexural strength and decreases the thickness of pavement required. Besides, the greater capacity of tensile strain in SFRC minimizes the crack widths efficiently as compared to plain concrete because it is more resistant to impact and repeated loading.

SFRC also generally used in offshore or hydraulic structures as the incorporation of fibres in concrete can regulate control crack as well as plastic and drying shrinkage due to its random distribution throughout the concrete. It manages to reduce the permeability of concrete, leading to higher resistance to cavitation and erosion when exposed to the high velocity of water flow than a conventional RC. Besides, SFRC also applicative in thin-walled structures and tunnels. Fibre shotcrete is applied extensively in slope stabilization, bridge maintenance and tunnel lining in the protection of steel structures.

Moreover, precast application with the use of SFRC can be found from concrete piping, manhole covers and machine frames as bases due to its auxiliary reinforcement when subjected to temporary load in controlling shrinkage cracks,

preventing cracking during transportation or installation of precast members. SFRC can also be found in refractory concrete as they are more durable when exposed to high thermal stress, thermal shock and mechanical abuse as SFRC imparts the combination of enhanced toughness, cracking control, and abrasion and spalling resistance.

2.11 Summary

Steel fibres are hard intrusion materials. The use of this, short and randomly distributed steel fibres in concrete have a distinct advantage in their physical properties, especially with high tensile strength, impact resistance and elastic modulus. Besides, they are easily deformed and indented to improve their geometry in the anchorage end to have a stronger bond contacting with surrounding cementitious matrix. The concept of including steel fibres helps to compensate for concrete's brittle behaviour by enhancing its tensile strength, fracture toughness, durability, post cracking response and shear strain capacity. However, the capacity of water absorption in fibres can cause low workability during mixing and potentiality of corrosion stains whenever the fibres are exposed at the surface.

SFRC which under uncracked state has similar elastic mechanical properties as conventional concrete with the same mix proportions. Steel fibres pledge excellent crack resistance due to its performance in increasing toughness and energy absorption capacity of the concrete. Bridging fibres which possess bond-slip characteristics and fibre bridging transition effect play the main role in delaying further crack opening and also resisting complete fibre pull-out to fibre fracture across a crack. The material and structural properties of SFRC are mainly focused on compressive strength, direct tensile strength, flexural tensile strength, flexural toughness in energy absorption, direct shear strength and shear failure on beam members. Factors influencing the shear capacity in SFRC beam includes the depth of beams, shear-to-span ratio and fibre volume fraction.

SFRC is mostly adopted in the structural application of slab and pavements, hydraulic structure, fibre shotcrete, precast application and so on. Application of steel fibre reinforcement could possibly replace stirrup reinforcement by eliminating the shear size effect in beam depth and increase in shear strength. This can probably improve productivity and deliver cost efficiency with a reduced volume of concrete-making materials. Steel fibre reinforced concrete is an economic design alternative as it delivers an effective construction and lower labour costs.

CHAPTER 3

METHODOLOGY AND WORK PLAN

3.1 Introduction of Experiment Work

The experimental methodologies which implemented in this experiment program with a devised work plan are discussed in Chapter 3. The experimental program involved the concrete trial mix design process, collection, preparation and handling of raw materials and equipment, followed by mixing procedures of reinforced concrete. Next, it describes the beam specimens' design in dimension and reinforcement detailing as well as construction and production. In addition, laboratory testing to obtain fresh state and mechanical properties of RC which includes steel tensile test, slump test, compressive test, splitting tensile test, water absorption test four-point loading bending test are discussed in this chapter.

3.2 Experimental Work Flow Chart

In general, the experimental program consists mainly of the design, construction and testing of simply-supported concrete short beams. The outline of the trial mix selection process is shown in Figure 3.1 to achieve the mix proportion of concrete with 30 MPa characteristic compressive strength. This is then followed by the overall process of beam construction, concrete mixing, casting and curing as well as a program of laboratory testing which presented in Figure 3.2 in the manner of a flow chart.

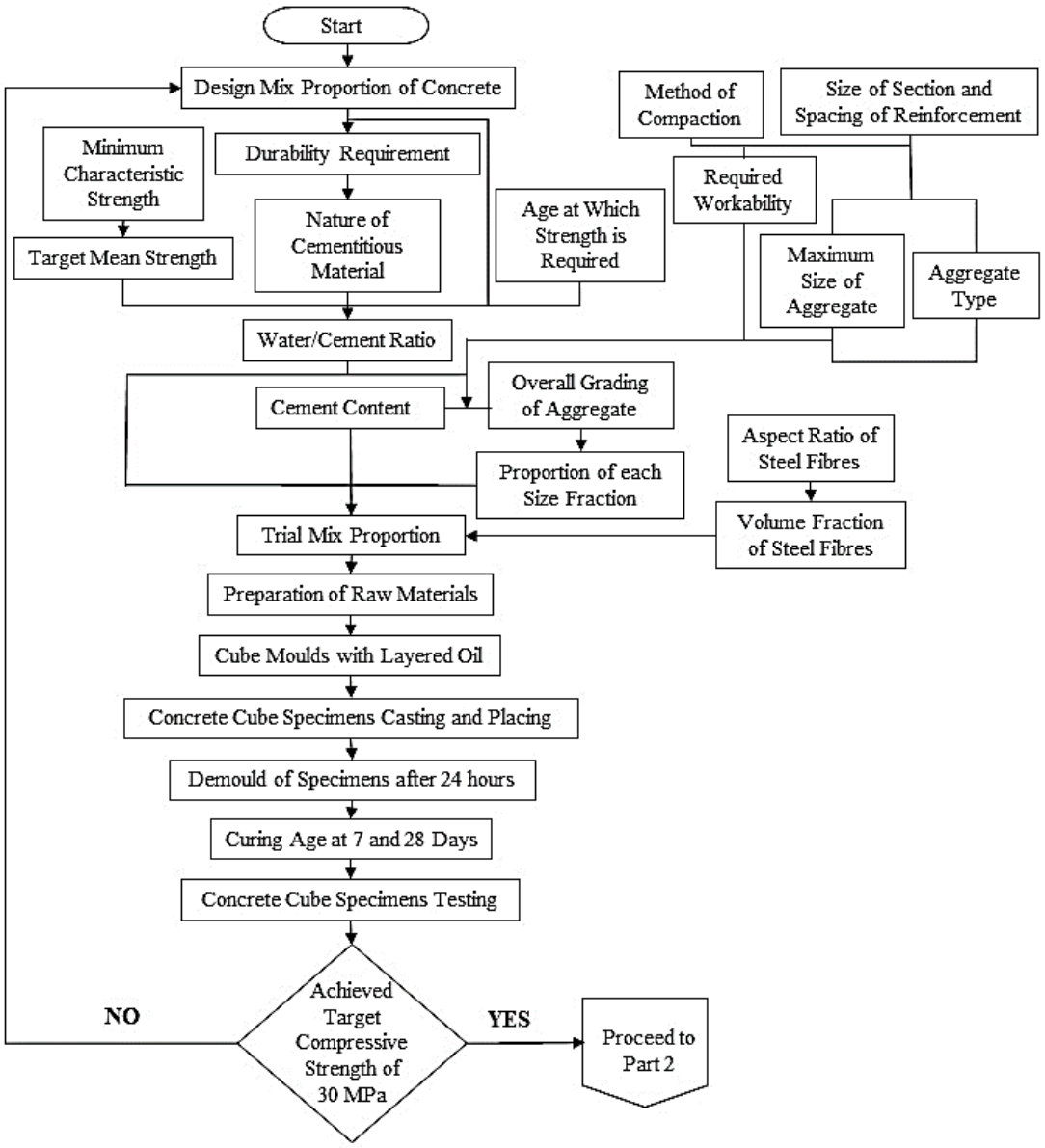

Figure 3.1: Experimental Workflow Chart (Part 1)

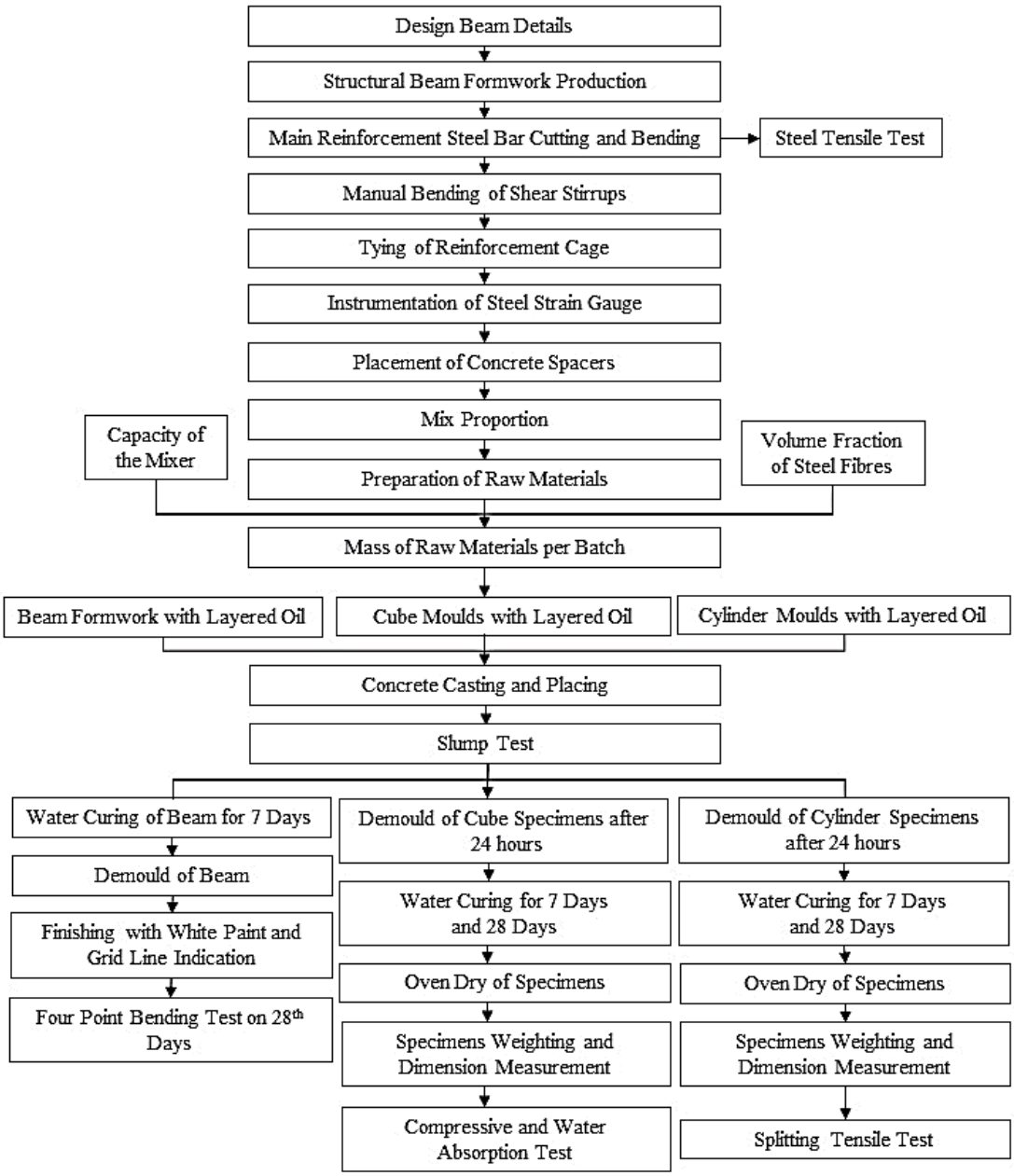

Figure 3.2: Experimental Workflow Chart (Part 2)

3.3 Constituent Materials of Steel Fibre Reinforced Concrete

SFRC in this experimental study was based on mix design of Portland cement binders, fine and coarse aggregates, water and steel fibre. It had similar mix-proportions as conventional concrete except for the incorporation of steel fibre.

3.3.1 Ordinary Portland Cement (OPC)

"Orang Kuat" which is one of the OPC brand with 3.15 specific gravity, manufactured by YTL Cement (M) Sdn. Bhd. was used in this research work. It complies with all

the Type 1 Portland Cement Standards according to ASTM C150 (2007) with cement strength class of 52.5. Figure 3.3 shows the "Orang Kuat" OPC with its primary chemical composition as illustrated in Table 3.1. The OPC was allowed to pass through 300 µm opening sieve size to separate all the cement clinker and kept in an airtight container to avoid contact with moisture in the air as hydrated cement particles will affect the calcium silicate hydrate gel formation.

Figure 3.3: Orang Kuat Brand OPC Manufactured by YTL

Table 3.1: Primary Constituent of OPC

Constituent	Ordinary Portland cement % by weight
Lime (CaO)	64.64
Silica (SiO_2)	21.28
Alumina (Al_2O_3)	5.60
Iron oxide (Fe_2O_3)	3.36
Magnesia (MgO)	2.06
Sulfur trioxide (SO_3)	2.14
N_2O	0.05
Loss of ignition	0.64
Lime saturation factor	0.92
C_3S	52.82
C_2S	21.45
C_3A	9.16
C_4AF	10.2

3.3.2 Aggregate

This subsection further discusses the construction aggregate for grained particulate material such as coarse aggregate and fine aggregate. Those aggregates are the mined materials which also as an important component of concrete composite materials. The aggregates are one of the reinforcements in adding strength to the concrete matrix.

3.3.2.1 Coarse aggregate

The crushed coarse aggregate was used in the saturated surface dry condition and was prepared in accordance with ASTM C33 (2006) in the production of concrete. The aggregate was sieved using 20 mm, 10 mm and allowed to retain on 4.75 mm sieve. Subsequently, washing of coarse aggregate was carried out to remove dust on surfaces of aggregate and let to be sun-dried for a minimum of five hours. Figure 3.4 shows the sieved coarse aggregate with size of 4.75 mm to 10 mm and 10 mm to 20 mm which stored separately in the container.

(a) (b)

Figure 3.4: Storage of Sieved Coarse Aggregate : (a) 10 mm; (b) 20 mm

3.3.2.2 Fine aggregate

Fine sand which is in compliance with ASTM C33 (2006) was used as fine aggregate for the constitution of concrete. The uncrushed fine aggregate used was saturated surface dry in moisture content. The sand sieving method was either done by manually or mechanically in compliance with ASTM C136 (2004) and was sieved to pass through No. 4 sieve (4.75mm opening) and retained at No. 200 sieve (75μm opening). Figure 3.5 shows the fine aggregate with particle diameter of 56 % passing 600 μm which employed in this study.

Figure 3.5: Fine Aggregate

3.3.3 Water

The water used in this study was directly from municipal water tap in compliance with ASTM C1602 (2006) in the production of hydraulic cement concrete. Soft water which was free from acids, alkalis, oils or organic impurities was used in mixing. The *w/c* ratio applied in this study is 0.60 by referring to Department of Environmental (DOE) method in achieving target strength.

3.3.4 Steel Fibre

Stahlcon hooked-end steel fibre was used in this study and was distributed by Oriental Housetop. The steel fibres which were glued in bundles in order to facilitate the concrete mixing process is shown in Figure 3.6. However, those glued units were scattered into a single unit during the concrete mixing.

Figure 3.6: Stahlcon Steel Fibre

It has standard compliances which conform to BS EN 14889-1:2006 and MS 2388: 2010 under Group 1 type made of cold drawn wire. The detailed profile of hooked-end steel fibre provided by the manufacturing company is shown in Table 3.2. The amount of fibres incorporated in the concrete mix was measured as 0.6 % and 0.7 % in volume fraction of the composite of fibre reinforced concrete in this study.

Table 3.2: Profile of Stahlcon Short Hooked-End Steel Fibre

Profile	HE 0.55/35
Fibre Diameter, d (mm)	0.55 (±0.03)
Fibre Length, L (mm)	35 (±1.75)
Aspect Ratio	65(±4.5)
Density (kg/m^2)	7800
Elastic Modulus, E (MPa)	205 000
Tensile Strength (MPa)	Min 1200 (±5%)
Quantity (pc/kg)	±14 490

3.4 Concrete Mould

Moulds for specimens or fastenings in compliance with ASTM C470/ C470M (2002) were reusable steel cubic and cylinder moulds. For aggregate size equal or more than 20 mm, the required dimension of cubic and cylindrical mould used in conforming the specifications set by British Standard and ASTM is shown in Table 3.3. The inner surface of moulds was cleaned to be free from residue or dust. Besides, bolts were tightened in holding the mould structure firmly to avoid dismantle of moulds easily. The last step was greasing and coating the inner surface of moulds for ease of demoulding after the hardening of concrete.

Table 3.3: Size of Mould for Different Test Method

Testing Method	Type of Mould	Dimension of Mould
Compressive Strength Test & Water Absorption Test	Cubical	150 mm × 150 mm × 150 mm (Width × Depth × Length)
Splitting Cylindrical Tensile Strength Test	Cylindrical	100 mm × 200 mm (Diameter x Length)

3.5 Trial Mixtures

Trial mix in this study was a pre-stage to achieve a target characteristic strength of 30 MPa in concrete. The procedure in preparing concrete cube and cylindrical samples were performed for the short beams as well from concrete mixing, casting to curing.

3.5.1 Trial Mix Proportions

The common method of expressing the mix proportions of concrete ingredients is in terms of ratios or parts of cement, water, coarse and fine aggregates. The *w/c* ratio used was determined to be 0.60 according to British Standard, using DOE method while the steel fibres percentage added was determined based on the total volume fraction of composite mix. Mix design of the study was performed using DOE mix design form as shown in Appendix B. Table 3.4 shows the mix proportion of each type of concrete mix where NWRC indicated as Mix 1, SFRC-0.6 and SFRC-0.7 indicated as Mix 2 and Mix 3 respectively.

Table 3.4: Concrete Mix Proportions

Raw Materials (kg/m^2)	**Control**	**Variables**	
	Mix 1 (NWRC)	**Mix 2 (SFRC-0.6)**	**Mix 3 (SFRC-0.7)**
Cement	341.67	341.67	341.67
Fine Aggregate	748.47	748.47	748.47
Coarse Aggregate			
-4.75 mm – 10 mm	359.02	359.02	359.02
-10 mm – 20 mm	718.04	718.04	718.04
Water	205	205	205
Steel Fibre	-	46.8	54.6

3.5.2 Concrete Mixing, Casting and Curing Procedure

The mixing and curing test specimen procedure of concrete were under control which carrying out a standard practice in the laboratory in compliance with ASTM C192 (2006). A concrete mixer with a capacity up to 0.3 m^3 was used instead of hand mixing as hand mixing should be limited to a maximum volume of 0.007 m^3. A concrete machine-mixer is as shown in Figure 3.7 for large amount mixing.

Figure 3.7: Concrete Machine-Mixer with Capacity of 0.3 m^3

Before the starting of the mixer, all the dry constituents such as coarse aggregate, fine aggregate and cement was in turn added into the concrete mixer. All the dry materials were allowed to mix thoroughly and followed by adding water into the mixture. The mixer was allowed to run for each time when each portion of water was poured separately to ensure homogenous mixing.

In order to avoid segregation or formation of agglomerate during the process of adding fibres, well concrete mixing should be accomplished with a uniform dispersion of the steel fibres. However, the agglomerate formation tendency will be intensified with the increase of volume percentage of fibre, decreasing workability at the same time. The fibres-concrete mixture was prepared by adding the fibres gradually to the fresh concrete until the desirable fibres percentage by volume was reached. The fibres were slowly added to the thoroughly mixed concrete (cement, water, coarse and fine aggregates) while the mechanical mixer is rotating. After all the constituent materials of concrete were placed into the mixer, it was allowed to rotate for three minutes with a three minutes subsequent rest, and lastly, undergo a two minutes final mix as in accordance with ASTM C192 (2006).

The homogeneity of the concrete mix was evaluated visually, and the concrete mixtures were uniformly mixed and well prepared after the mixing process was done. Next, the inner mould and formwork surface was well lubricated with a layer of oil before the placing of fresh concrete. Then, fresh concrete was poured with divided three layers into mould and formwork subsequently. The concrete cube and cylinder

specimens were compacted by rod tamping for 25 times, whereas the beam specimens were consolidated using a concrete vibrator to eliminate the air bubbles in the pour. The outermost layer of concrete was finished using a trowel to level off the slightly overfilled concrete at the top of the mould and formwork to give smooth surface flush.

Concrete specimen of cube and cylinder were left to set after casting as shown in Figure 3.8 and demoulded after 24 hours. The cube and cylindrical specimens were allowed to cure by immersing in a water curing tank to undergo hydration process for curing age of 7 days and 28 days respectively as illustrated in Figure 3.9. In accordance with ASTM C511, the water curing tank used was a non-corroding material and always maintained a water temperature at 23.9 $\pm$ 2.0 °C.

(a) (b)

Figure 3.8: Sample of Concrete Specimen Left for Setting: (a) Cube Specimen; (b) Cylinder Specimen

Figure 3.9: Curing of Concrete Cube and Cylinder Specimens in Water Tank

Whereas the beam specimens were left to set after casting as shown in Figure 3.10 and demoulded after seven days to allow sufficient setting. There were fully covered with wet gunny bags to prevent evaporation of water. As stated in Punmia, et al. (2007), the exposed concrete surface shall always be kept in a wet condition for at least seven days especially for OPC.

Figure 3.10: Concrete Beam Specimens

3.6 Reinforced Concrete Structural Beam

The production of NWRC and SFRC beams included the construction of formwork panels, steel reinforcement cage, hand-tied reinforcement and installation of strain gauge.

3.6.1 Reinforced Concrete Structural Beam Design and Details

The design of beam in the aspect of beam size, shear span-to-depth ratio and stirrups spacing is computed in Appendix A. Figure 3.11 and Figure 3.12 show the detailing of the structural beam with and without stirrups respectively at dimensions of 125 mm in width × 200 mm in depth × 800 mm in length under four-point loading. The effective depth was to be 163 mm. By justification, the steel reinforcements used for the top and bottom rebar were 2R8 and 2H8 respectively; R8 was used for the shear link with a spacing of 100 mm, indicated in R8-100. However, shear links do not apply to full span of beams but only located at shear span to avoid the delay of concrete crack at the flexure zone. This allowed the steel to yield first before crushing of concrete.

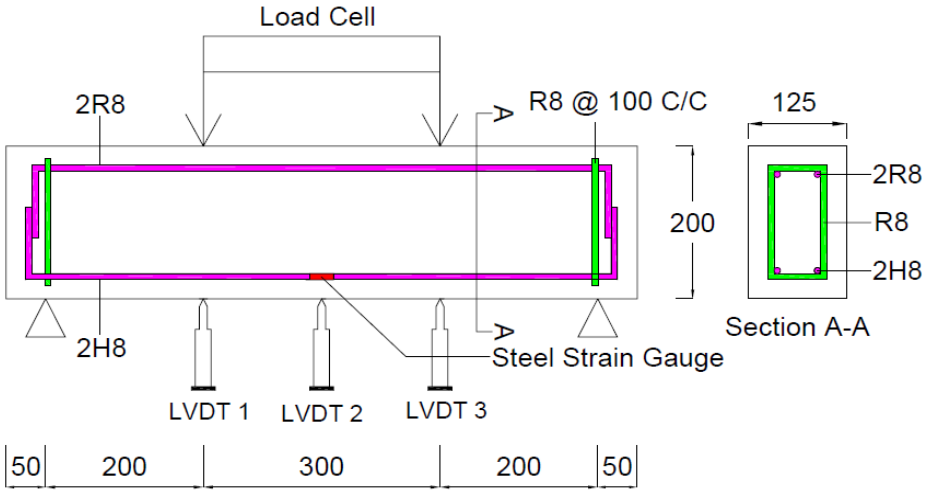

Figure 3.11: Detailing of NWRC-W/OS, SFRC-0.6 and SFRC-0.7 Beam (Note: all dimension in mm)

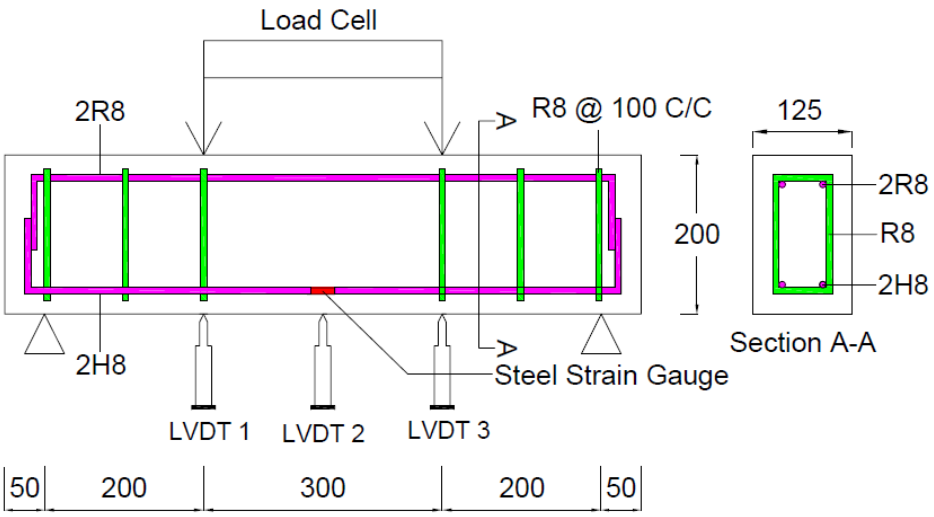

Figure 3.12: Detailing of NWRC-W/S Beam (Note: all dimension in mm)

3.6.2 Construction of Reinforced Concrete Beam

Preparations of concrete formwork panels, reinforcement cage and installation of strain gauge were performed in advance before the casting of RC beam specimens.

3.6.2.1 Production of structural beam formwork

Concrete formwork was built using plywood material where plywood was sawed and assembled in a prismatic form. Structure of formwork was constructed by simple mechanical work such as nailing and screwing as shown in Figure 3.13.

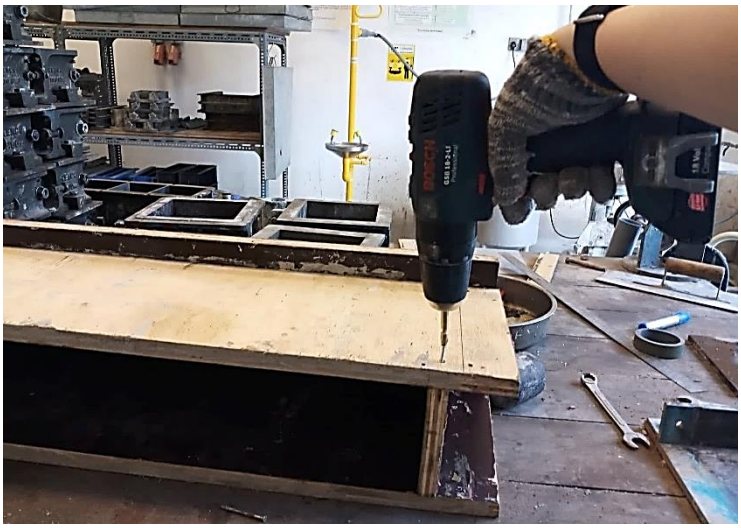

Figure 3.13: Formwork Making According to Dimension of Beam

3.6.2.2 Preparation of steel main reinforcement and shear link

The readily available steel bar was longer than required and cutting was needed to prepare a bar of the desired length. Steel bar cutter machine was then operated to cut the steel reinforcement precisely as illustrated in Figure 3.14.

Figure 3.14: Cutting of Steel Bar Using Steel Bar Cutter

Next, the steel bar was then bent into the desired angle to produce the anchorage by using steel bending machine as shown in Figure 3.15. The bending

machine was used only for bending of high tensile strength steel reinforcement Besides, manual bending was performed for bending of mild steel reinforcement at the bending platform as shown in Figure 3.16. The shear link was prepared to be 90 degree anchored.

Figure 3.15: Bending of Main Reinforcement at Bending Machine

Figure 3.16: Manual Bending of 90^{o} Anchored Shear Link at Bending Platform

3.6.2.3 Preparation of steel reinforcement cage

As illustrated in Figure 3.17, a steel reinforcement cage was produced by tying the shear links vertically to the individual main reinforcement into a cage form with galvanized steel wire. Stirrups were put vertically for ease of installation. All the connections should be rigid enough to form a beam skeleton system to prevent any bar movement during the process of concreting. The reinforcement was cleaned to remove any loose rust on the surface during fixing and handling of bars to make sure the

adequate bonding with the concrete. Sample of reinforcement cage for beam with and without stirrups are shown in Figure 3.18.

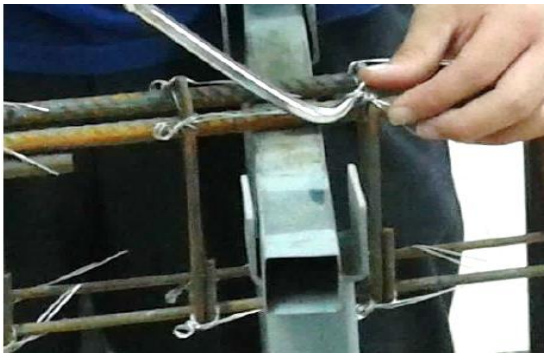

Figure 3.17: Tying of Reinforcement in Conjoining Main Reinforcement and Shear Links

(a)

(b)

Figure 3.18: Steel Reinforcement Cage: (a) Beam Cage With Stirrups; (b) Beam Cage Without Stirrups

3.6.2.4 Instrumentation of steel strain gauge

The chosen steel strain gauge was a FLK-6-11 type, TML load cell, as shown in Figure 3.19. A steel strain gauge was attached at the bottom part of rebar located at the beam's mid-span to evaluate the strain behaviour of the steel bar. Prior to the installation of the strain gauge, the steel bar was grounded at where the gauge installation position was marked. The strain gauge wire was then fixed in position using masking tape and

the bonding surface of the specimen was made sure to be free from rust, grease or dust before the cyanoacrylate adhesive was applied on the gauge cell. Next, subsequent layers of coatings using coating material were applied directly to the surface of the strain gauge until it fully covered the strain gauge for gauge protection. The coating was left for at least 24 hours for complete dry before the sheathing of Vinyl Mastic Tape for insulating and moisture sealing purpose. Figure 3.20 shows the overall process of basic bonding procedure of strain gauge.

Figure 3.19: TML Steel Strain Gauge, Type of FLK-6-11-3LJC

Figure 3.20: Instrumentation of Steel Strain Gauge

3.6.2.5 Reinforced concrete structural beam casting and curing procedure

Preparation works were needed before the casting of concrete. The first step was to place and tie the concrete spacers at the bottom and corner side of the steel reinforcement to keep the reinforcing in place and create a free space as cover. The samples of concrete spacers were made of mortar and became a permanent part of the concrete structure after the placement as shown in Figure 3.21. The steel reinforcement cage was then placed in the formwork as shown in Figure 3.22. Besides, the fresh concrete mix was consolidated by vibrator during the casting of the RC beam to release trapped air, allow concrete settled firmly in place and avoid fibre segregation as shown in Figure 3.23. Metal trowels were used to finish the surface for the last step of casting.

Figure 3.21: Concrete Spacers Made of Mortar

Figure 3.22: Placement of Steel Reinforcement Cage in Beam Formwork

Figure 3.23: Using of Vibrator to Consolidate Fibre Reinforced Concrete Mix

After the placement and setting of concrete for 24 hours, the curing of beam specimens was done by covering the surrounding surface using wet gunny bags for hydration process as shown in Figure 3.24. This was to maintain the moisture content and surrounding temperature in preventing rapid loss of moisture due to evaporation.

Figure 3.24: Curing of Beam Specimens

3.6.2.6 Stripping of formwork and finishing

The RC concrete specimens were set and left for a period of seven days with the props left under before the stripping of formwork. The RC beams were painted with white paint so that propagation of cracking is more evident. Besides, 50 × 50 mm grid indication was drawn on the surface of the concrete beam to ease the coordination of cracking as shown in Figure 3.25.

Figure 3.25: Surface Painting and Grid Drawing on Beam Surface

3.7 Material Testing and Properties

The same equipment and procedure used for conventional concrete can also be applied on fibre reinforced concrete in determining the mechanical properties. Material tests were performed for steel, fresh state and hardened concrete properties.

3.7.1 Direct Steel Tensile Test

In accordance with ASTM E8, the direct steel tensile test was conducted to identify the yield and ultimate tensile strength of the steel reinforcement bar. Instron Universal Tensile Tester was used to apply the direct tensile load at a controlled deformation rate as shown in Figure 3.26. A Linear Variable Differential Transformer, as abbreviated as LVDT was used as an extensometer to measure the deformation of the specimen. The behaviour of deformation and load was indicated by a dial gauge and recorded in chart recorder. A digital Vernier Calliper was used to measure the dimensions of specimens accurately.

Figure 3.26: Steel Tensile Test : (a) Instron Universal Tensile Tester: (b) Tensile Testing of Steel Bar until Fracture

The yield strain, yield strength from 0.2 % strain and ultimate tensile strength of steel bar were determined by Equation 3.1 and Equation 3.2 respectively.

$$\text{Yield strain of Steel Reinforcement, } \mu\varepsilon = \frac{\text{Elastic Tensile Stress}}{\text{Modulus of Elasticity}} \tag{3.1}$$

$$\sigma_{0.2\%y} = \frac{P_{0.2\%y}}{\mathrm{A_o}} \tag{3.2}$$

$$\sigma_{TS} = \frac{P_{max}}{\mathrm{A_o}} \tag{3.3}$$

where

$\sigma_{0.2\%y}$ = Yield Strength from 0.2 % Strain, MPa

σ_{TS} = Ultimate Tensile Strength, MPa

$P_{0.2\%y}$ = Load at yield (offset 0.2 %), N

P_{max} = Load at Maximum Tensile Stress, N

A_o = Original Cross-sectional Area of Specimen, mm^2

3.7.2 Fresh Concrete Testing Method–Slump Test

Slump test was carried out in accordance with ASTM C143 (2008) to obtain the workability of fresh normal weight concrete as well as conventional concrete. The fresh concrete was tested using a metal conical frustum mould, namely slump cone, where the cone had a dimension of 300 mm in height with 100 mm top opening diameter and 200 mm bottom opening diameter. The slump cone was placed on an impermeable and flat surface followed by pouring of fresh concrete in three equal layers subsequently. Stroking of 25 times was required using the tamping rod on each layer to ensure compaction. Once the fresh concrete had fully occupied the cone at the last layer, the slump cone was lifted vertically upward by care with a height of about 300 mm within 3 to 7 seconds in a steady state without any lateral or torsional motion. The cone was then made an about-turn to be inverted and put next to the slump as a height denotation. The measurement of the slump was taken immediately at which the value is referred to the drop in height between the cone and slump. The ideal slump value to control the workability of concrete was maintained between 60 mm to 80 mm.

3.7.3 Destructive Hardened Concrete Strength Test

Mechanical properties of concrete can be determined through several destructive testing. In this context, the concrete crushing and failure is the usual destructive test in determining the concrete strength and behaviour under different loads. Destructive testing methods include compressive test, splitting tensile test and four-point bending shear test.

3.7.3.1 Compressive strength test

The concrete cube specimens with a side length of 150 mm were tested for its compressive strength when the required testing age had achieved by using AD300/EL Digital Readout 3000 kN Compression Test Machine as shown in Figure 3.27. Compressive axial load was applied until reaching the peak load which allow the failure to occur in accordance with BS EN 12390-03 (2009). Prior to the compressive test, the concrete cube specimens were oven-dried for at least 24 hours after being taken out from the water curing tank as shown in Figure 3.27. The physical measurements such as weight and cube's dimensions were taken before the compression testing. A constant loading rate was applied using 2.0 ± 0.2 MPa/s. The compressive strength of the test specimen was determined by Equation 3.4.

$$f_c = \frac{P}{A} \tag{3.4}$$

where

f_c = compressive strength, MPa

P = peak load sustained by specimen, N

A = cube specimen's cross-sectional area at which uniform load applied, mm^2

Figure 3.27: Concrete Cube Testing using General Compression Test Machine

3.7.3.2 Splitting tensile strength test

Prior to the split-tension test, the concrete cylindrical specimens were oven-dried for at least 24 hours after being removed from the water curing tank. The physical measurements such as weight and dimensions of the cylinder were taken similar to the compressive strength test. The specimen was then tested with 1.0 ± 0.2 MPa/min at constant loading rate using the AD 300/EL Digital Readout 3000 kN Compression Test Machine as shown in Figure 3.28. Generally, the split-tension test was to measure the concrete tensile strength according to ASTM C496 (2004) by applying a diametric compressive force, which induces the tensile stresses at a constant rate along the vertical diameter until failure. A cylindrical specimen was placed aligned on the plywood strip where the strips was placed at centred along the lower bearing block, while another plywood strip were placed lengthwise on the cylinder to ensure uniformly loading.

Figure 3.28: Concrete Cylinder Testing Using General Compression Test Machine

Since the tension was developed in the transverse direction, the specimen would also fail along its vertical diameter. The split tensile magnitude or known as indirect tensile strength acting perpendicularly to the line of action of the applied load was computed with Equation 3.5.

$$T = \frac{2P}{\pi LD} \tag{3.5}$$

where

T = splitting tensile strength, MPa

P = peak load, N

L = effective length, mm

D = average height/length, mm

3.7.3.3 Four-point bending shear test

The four-point bending shear test was carried out using the standard test method according to ASTM D6272 using a simple supported beam. RC beam with a dimension of 125 mm × 200 mm × 800 mm was used as a test specimen. 300 kN Structural Reaction Frame Machine with load sensor was used to test the shear strength of a beam with a loading rate of 1.0 ± 0.2 MPa/min. Three LVDTs were placed at three different

locations of the bottom beam to determine the degree of deflection corresponding to a gradual increment of loading by controlling a pressure valve. The LVDTs were placed symmetrically about the midspan at the interval spacing of 150 mm. Besides, Data Logger TDS-540 was connected with LVDTs and strain gauges wires for data acquisition in generating the output of strain value. The specimen was tested to be deflected until fracture occurs and rupture in the outer fibre. The shear strength can be computed in term of shear stress using the following Equation 3.6:

$$v = \frac{V}{2bd} \tag{3.6}$$

where

v = shear strength, MPa

V = maximum load applied, N

b = beam width, mm

d = beam effective depth, mm

Photograph in Figure 3.29 depicts the details of the test set-up and arrangement of the external instrumentation such as LVDTs and data logger.

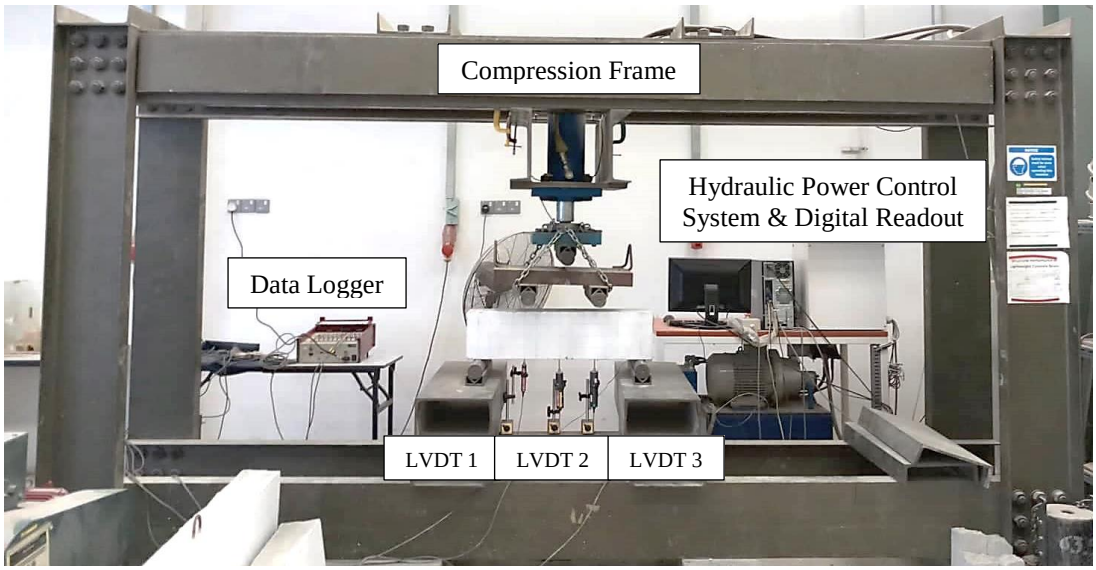

Figure 3.29: Test Set-up and Arrangement of External Instrumentation

3.7.4 Durability Concrete Testing Method–Water Absorption Test

The standard water absorption test method for density, absorption and voids in hardened concrete was performed in accordance with ASTM C642 (2006). Concrete cube specimens with a side length of 150 mm were used for this test. The mass of the surface-dried specimens after the immersion in water curing tank was determined as shown in Figure 3.30. Then, the specimens were oven-dried for 24 hours at a temperature of 100 to 110 ℃ as shown in Figure 3.31. The specimens were then removed from the oven on the following day and allowed to cool down to a room temperature in a desiccator followed by physical measurement of its mass. The percentage of water absorbed can thus be calculated from the increment in the specimen's mass divided by the oven-dried sample's mass as shown in Equation 3.4.

$$WA = \frac{W_{sat} - W_{dry}}{W_{dry}} \times 100\ \% \tag{3.7}$$

where

WA = water absorption of hardened concrete specimen, %

W_{sat} = Weight of saturated surface dry specimen, kg

W_{dry} = Weight oven-dried of specimen, kg

Figure 3.30: Measurement of Specimen's Mass Using Digital Weight Machine

Figure 3.31: Oven-dried of Concrete Specimens for 24 Hours

3.8 Summary

An experimental program was conducted from the mix selection process, mix design proportion, mixing procedures of concreting, design of structural beam, collection, preparation and handling of raw materials and equipment, construction in casting, curing process to laboratory testing in obtaining the fresh state and mechanical properties of SFRC. The tests in determining the quality of concrete included slump test, compressive test, splitting tensile test, four-point bending test and water absorption test. The experimental work was discussed by applying the methodologies to ensure a systematic and orderly work plan.

There were twelve RC beams cast for this experiment with three normal weight reinforced concrete beams with stirrups (NWRC-W/S), three normal weight reinforced concrete beams without stirrups (NWRC-W/OS), three 0.6 % steel fibre reinforced concrete beams (SFRC-0.6) and three 0.7 % steel fibre reinforced concrete beams (SFRC-0.7).

CHAPTER 4

MATERIAL TEST RESULTS AND DISCUSSION

4.1 Introduction

Chapter 4 basically presents the properties of the material which determined from the experimental raw data of testing, followed by discussion on data analysis. Subchapter 4.2 mainly focuses on tensile testing to determine the engineering properties of steel reinforcement used in this research. As it is described in Chapter 3 of this report, the hardened concrete data for compressive strength, splitting tensile and water absorption tests have been presented in the remaining part of this chapter.

4.2 Steel Tensile Test

The steel tensile test was carried out with the steel reinforcement using Instron Universal Tensile Tester. Figure 4.1 shows the tensile specimens of H8 and R8 respectively under tension testing until fracture failure.

Figure 4.1: Tested Cylindrical H8 and R8 Steel Bar Specimens Under Uniaxial Tensile Loading

The characteristic stress-strain curve diagram for H8 and R8 steel specimens are shown are illustrated in Figure 4.2 and Figure 4.3 respectively. From these curves, the behaviour of materials can be identified depending on the strain amount induced at four distinct intervals of tensile stress.

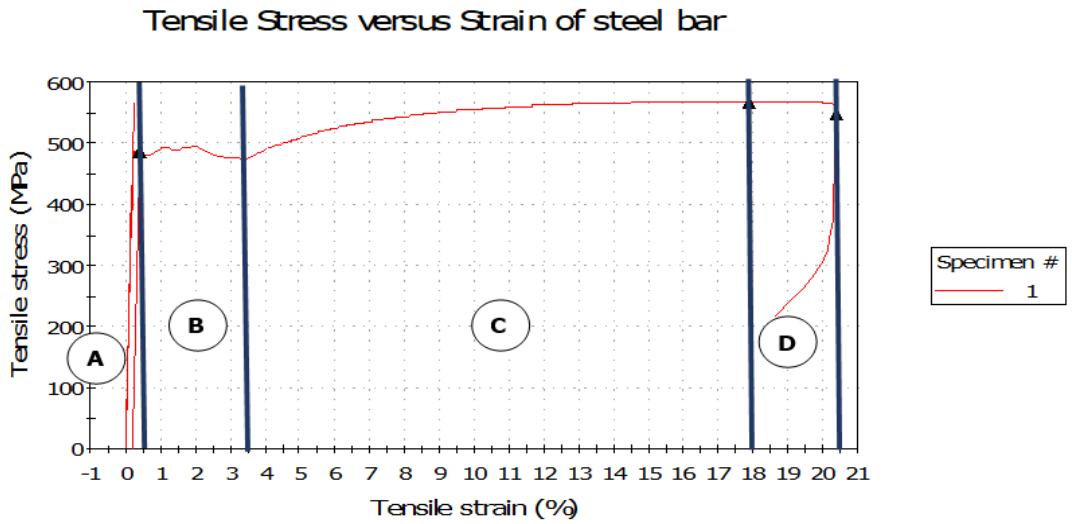

Figure 4.2: Tensile Stress-strain Curve of H8 Steel Bar

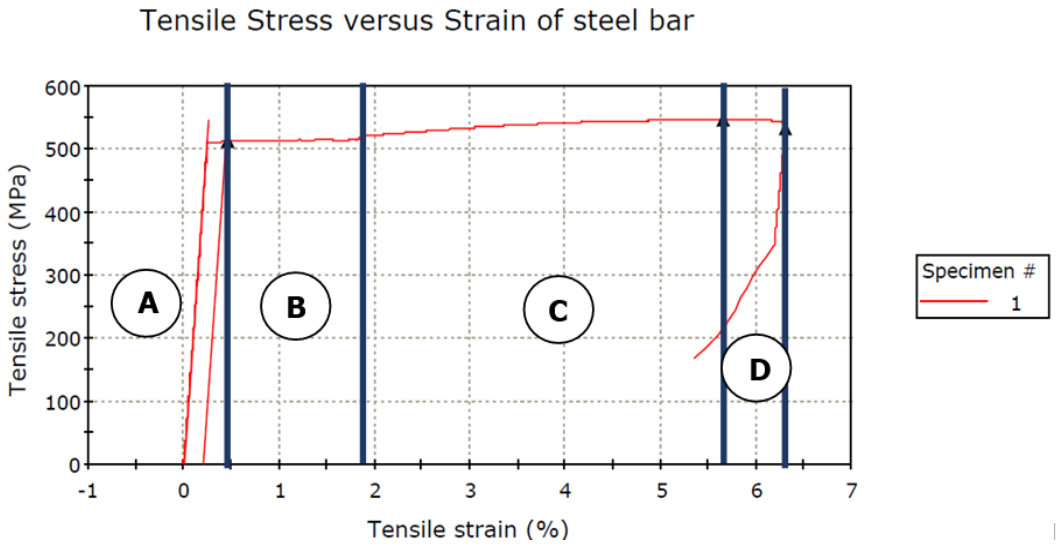

Figure 4.3: Tensile Stress-strain Curve of R8 Steel Bar

The resulting tensile stress-strain curve exhibits mechanical properties through the stress-strain characteristic of steel reinforcement when direct tensile force was applied. The nominal stress was identified by dividing the applied tensile load by the original cross-sectional area of the specimen. The computation assumed that the stress is constant throughout the cross-section and over the gauge length. As shown in Figure 4.2 and Figure 4.3, the graphs were subdivided into four stages, Region A to Region D for each deformation behaviour of steel reinforcement.

At the initial stage, Region A shows the elastic deformation or elastic strain of steel bar which gives a linear relationship of load and extension. The gradient of the

linear curve at this stage indicates the elasticity modulus, Young's modulus which is also a degree of stiffness of steel bar. From the stress-strain curve, there is a defined offset yield point of 0.2 % plastic strain at which yield point is not easy to determine from the curve. There was a breakdown of material when the steel bar was subjected by a slight increase in stress above the elastic limit in the flow Region B. This behaviour is known as yielding. Hence, yield strength is determined when the first plastic deformation start to occur. At this region, the upper yield point happens first followed by a lower yield point where there is a reduction in load-carrying capacity.

When the yielding has ended, the strain hardening commences and the rise in the curve in Region C is where an increase in load can be sustained by the steel bar. The curve becomes flatter later until it reaches the maximum point of stress, referred to as the ultimate tensile strength. This is the point where the steel bar can sustain the maximum load capacity before failure. Beyond this point, a constriction tends to form in Region D due to necking in which the cross-sectional area decreases in a localized region of mid-length of the steel bar. Hence, the stress-strain diagram exhibits to curve downward until the fracture occurs and the steel bar breaks at fracture stress.

Table 4.1 shows the summary of mechanical properties computed from the tensile testing of the H8 and R8 steel bars based on the experimental data shown in Appendix C and Appendix D respectively.

Table 4.1: Material Properties of H8 and R8 Steel Bars

Steel Bar	**Notation**	**Yield Strength (MPa)**	**Ultimate Tensile Strength (MPa)**	**Modulus of Elasticity (MPa)**	**Yield Strain (με)**
Longitudinal tensile steel bar	H8	485.33	568.25	214 980.30	2257.56
Longitudinal compressive steel bar	R8	511.16	546.12	203 231.74	2515.16
Transverse stirrups	R8	511.16	546.12	203 231.74	2515.16

4.3 Fresh Concrete Testing Method-Slump Test

The fresh properties of the produced NWRC, SFRC-0.6 and SFRC-0.7 were determined by the slump test as shown in Figure 4.4 to determine the mixture workability. Figure 4.4 (a), (b) and (c) show the permissible slump where the three types of concrete mixture remained intact and retained a symmetric shape of "true" slump. Table 4.2 depicts the results of slump test for plain concrete, 0.6 % and 0.7 % steel fibre additions in concrete.

(a) (b) (c)

Figure 4.4: Slump Test on Fresh Concrete Properties: (a) Slump Test of Plain Concrete; (b) Slump Test of 0.6 % Steel Fibre Addition in Concrete; and (c) Slump Test of 0.7 % Steel Fibre Addition in Concrete

Table 4.2: Slump Value Recorded for Each Fresh Concrete Mix Batch

Nomenclature	**Volume Fraction of Steel Fibre, V_f (%)**	**Slump (mm)**	**Variation as Compared to Control (%)**
NWRC (Control)	0	63	-
SFRC-0.6	0.6	54	-14.29
SFRC-0.7	0.7	52	-17.46

From the test results, it is shown that the slump loss occurs with the increase of fibre percentage in the concrete mix. Slump control can be difficult as concrete incorporated with steel fibre tends to hang together. The reason for lower slump is that the introduction of steel fibres created a network structure in concrete, which can limit

mixture flow. Besides, the increment of fibre percentage absorbed more cement paste to coat around because of large surface area in high content. When higher fibre consumptions are applied, the mixture presents a much stiffer consistency and the increase of the mixture viscosity makes the slump loss. The stiff steel fibres push the aggregates apart, produce an increasing difficulty of relative movement of coarse particles and restricting of mixture mobility which can lead to workability loss turning the compaction process more difficult. However, the slump does not intimate how well the fibres will be distributed in the mix, how the consolidation of fibre reinforced mix or finishing properties of concrete mix.

4.4 Destructive Hardened Concrete Mechanical Strength Test

For each batch of beam specimens, there were at least three concrete cubes for compressive strength test and three cylindrical specimens for splitting tensile test were cast from the same batch of the concrete mix during casting of the beam. The physical measurement and compressive peak load of each concrete specimen were taken and recorded in Appendix E and Appendix F. The main destructive tests on hardened concrete are the compressive test and splitting tensile test.

4.4.1 Compressive Strength Test

Concrete characteristic was determined by characteristics compressive cube strength test of concrete. Figure 4.5 shows the average compressive cube strength taken from the result of three cube specimens after the curing age of 7 days and 28 days.

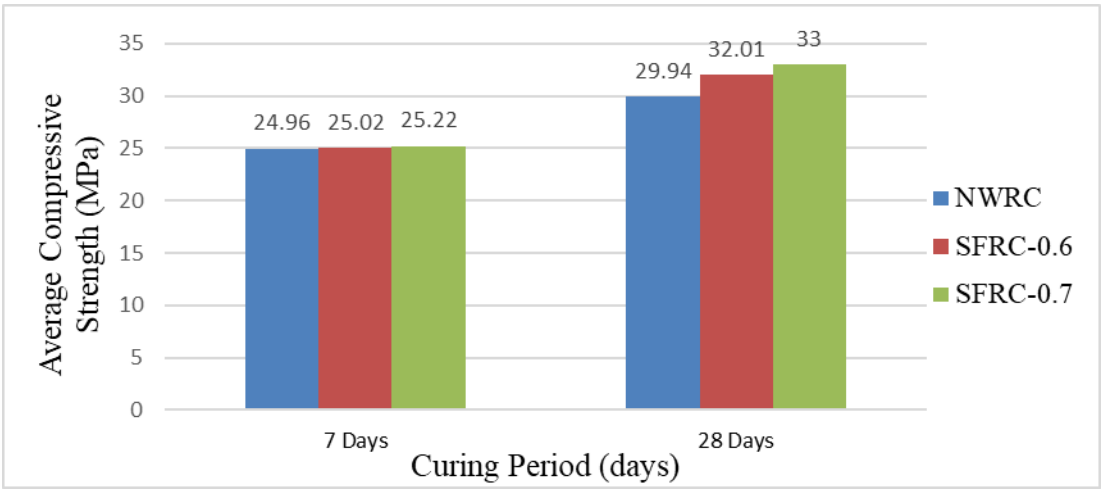

Figure 4.5: Average Compressive Cube Strength of Concrete Specimens at Curing Periods of 7 Days and 28 Days

Moreover, Figure 4.6 shows the average compressive cylinder strength obtained from the compressive cube strength with a multiple factor 25/30 for concrete characteristic strength of C25/30 without considering the partial safety factors. A variation percentage in compressive strength between two volume fraction fibre concrete as compared to control concrete is tabulated in Table 4.3.

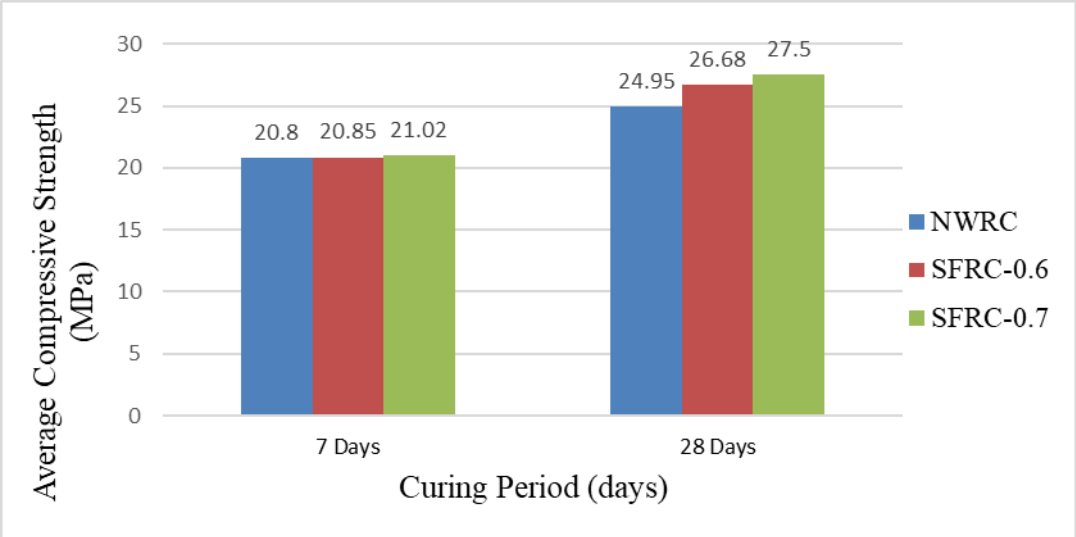

Figure 4.6: Average Compressive Cylinder Strength of Concrete Specimens at Curing Periods of 7 Days and 28 Days

Table 4.3: Variation in Compressive Strength as Compared to Control Specimens at Curing Period of 7 Days and 28 Days

Nomenclature	**Variation in Compressive Strength (%)**	
	7 Days	**28 Days**
NWRC (Control)	-	-
SFRC-0.6	0.25	6.93
SFRC-0.7	1.05	10.23

From Figure 4.5 and Figure 4.6, it shows a direct proportionality of compressive strength to curing age. Typically, the compressive strength of concrete at 7^{th} day curing age in this study reached around 70 % to 80 % of the compressive strength of concrete at 28^{th} day curing age. It can be noticed that the concrete developed a high early strength in seven days.

Besides, it can be seen that there is an insignificant increasing trend in compressive strength with the increment of fibre percentage. The compressive strength of concrete specimens with the inclusion of 0.6 % and 0.7 % increased from 6.93 % and 10.23 % respectively as compared to plain concrete. As mentioned in Kumutha and Vijai (2009), there would have an insignificant increase in the concrete compressive strength with the addition of steel fibre in concrete mixture beyond 0.5 % volume fraction.

Normal concrete easily fails when subjected to compression as stress block at 45 degree in angle is heavily sheared due to its brittleness. Hence, the increase in compressive strength can be explained that the introducing of fibres can reduce the shear stress in concrete against this shear plane. Besides, concrete with the inclusion of steel fibre is likely to be confined and slightly take more load.

Figure 4.7(a) and Figure 4.7(b) illustrates the crack patterns of plain concrete cube specimen and steel fibre concrete cube specimen respectively. It can be observed that the crack width of plain concrete cube is much larger than that of the steel fibre concrete cube. Besides, there was seriously crushing and spalling of plain concrete as compared to steel fibre concrete. Plain concrete also developed with major cracks on the surface as compared to steel fibre concrete. This can be explained as steel fibres in the concrete provide bridging effect by distributing the stress among concrete cracks to limit the propagation of cracking or breaking of concrete.

(a) (b)

Figure 4.7: Crack Pattern of Concrete Cube Specimens under Compressive Test: (a) Plain Concrete; (b) Steel Fibre Concrete

4.4.2 Splitting Tensile Strength Test

The tensile strength was determined indirectly in splitting tensile test where the load was applied over the specimen diametrically and uniformly along the cylinder length. Figure 4.8 shows the average tensile strength taken from the result of three cylinder specimens after 7 days curing and 28 days curing. A variation percentage in splitting tensile strength between two volume fraction fibre concrete as compared to control concrete is tabulated in Table 4.4.

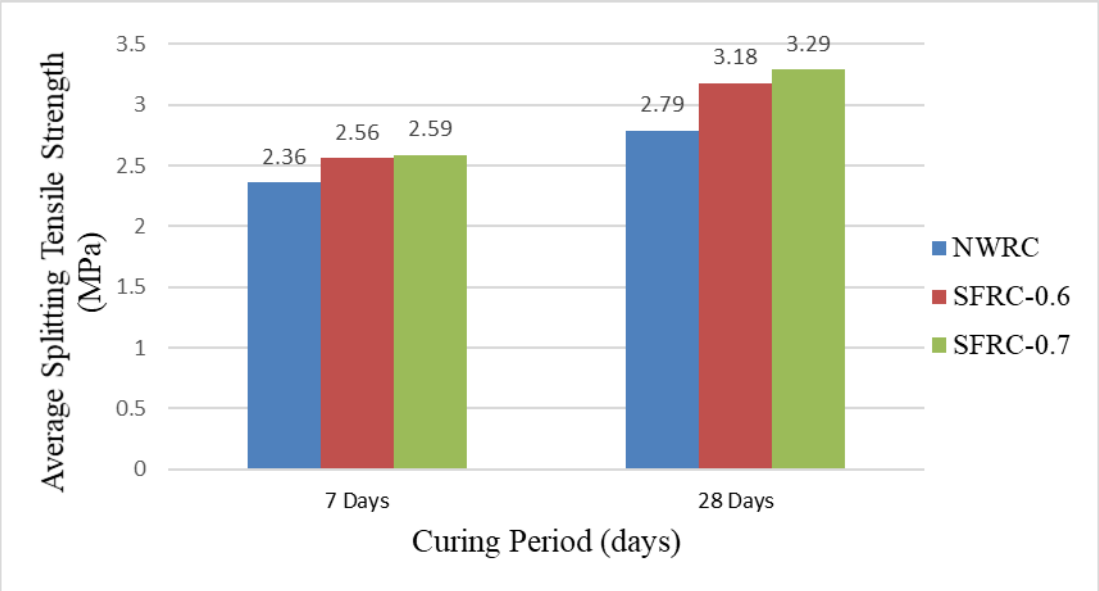

Figure 4.8: Average Splitting Tensile Strength of Cylinder Specimens at Curing Periods of 7 Days and 28 Days

Table 4.4: Variation in Splitting Tensile Strength as Compared to Control Specimens at Curing Period of 7 Days and 28 Days

Nomenclature	Variation in Splitting Tensile Strength (%)	
	7 Days	28 Days
NWRC (Control)	-	-
SFRC-0.6	8.47	13.98
SFRC-0.7	9.75	17.92

As depicted in Figure 4.8, the splitting tensile strength is directly proportional to the curing age, which similar to the development of compressive strength in concrete. Typically, the splitting tensile strength of concrete at 7th day curing age in this study

reached around 80 % of the splitting tensile strength of concrete at 28th day curing age. It can be noticed that the development of tensile strength of steel fibre concrete is higher at later strength with high increment percentage as compared to plain concrete.

The same trend also exhibited in splitting tensile strength that tensile strength improved with the increment of fibre percentage. The tensile strength of concrete specimens with the inclusion of 0.6 % and 0.7 % increased from 13.98 % and 17.92 % respectively as compared to plain concrete. This strength enhancement is due to the fibre-bridging mechanism possessed by fibres with the concrete matrix and act as a multi-dimensional reinforcement. It absorbs energy and transmitted the energy to other parts of concrete from applied load. Therefore, there was a distribution of applied load uniformly throughout the concrete specimen instead of concentration of local load on one region.

Figure 4.9 and Figure 4.10 depict the crack patterns of plain concrete cylinder specimen and steel fibre concrete cylinder specimen respectively. The failure of the cylinder was determined along the diameter in a vertical direction. The tensile stress induced split the plain concrete cylinder into two halves during the progress of load applied. The splitting took place along the vertical plane as the indirect tensile stress had been induced. However, the steel fibre concrete cylinder was held in position and remained intact with smaller crack width. It can be found that strong interlocking force between the concrete matrix and steel fibres contributes in transferring stress and distributing load uniformly to region around, hence increase the splitting tensile strength.

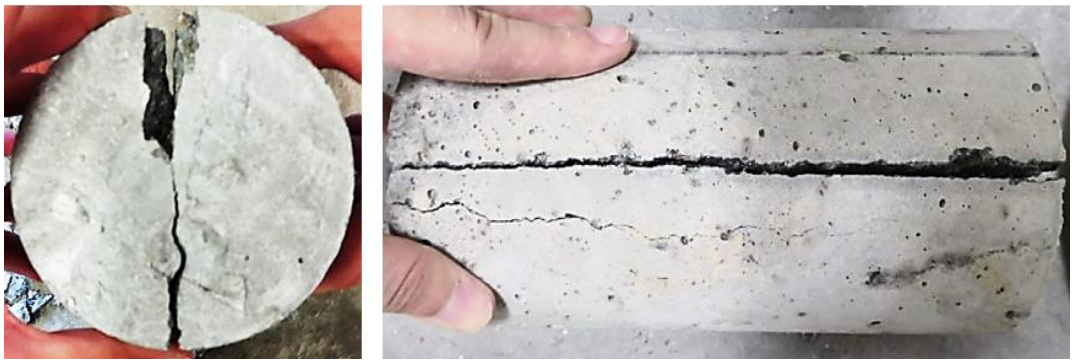

(a) (b)

Figure 4.9: Crack Pattern of Plain Concrete Cylinder Specimen: (a) Plan View of Concrete Cylinder; (b) Side Elevation of Concrete Cylinder

(a) (b)

Figure 4.10: Crack Pattern of Steel Fibre Concrete Cylinder Specimen: (a) Plan View of Concrete Cylinder; (b) Front Elevation of Concrete Cylinder

4.5 Durability Concrete Testing-Water Absorption Test

The water absorption test was performed by submerging the concrete cube specimens in water until the weight became constant. Figure 4.11 shows the average water absorption taken from the result of three concrete cube specimens after 7 days and 28 days. A variation percentage in water absorption between two volume fraction fibre concrete as compared to control concrete is tabulated in Table 4.5.

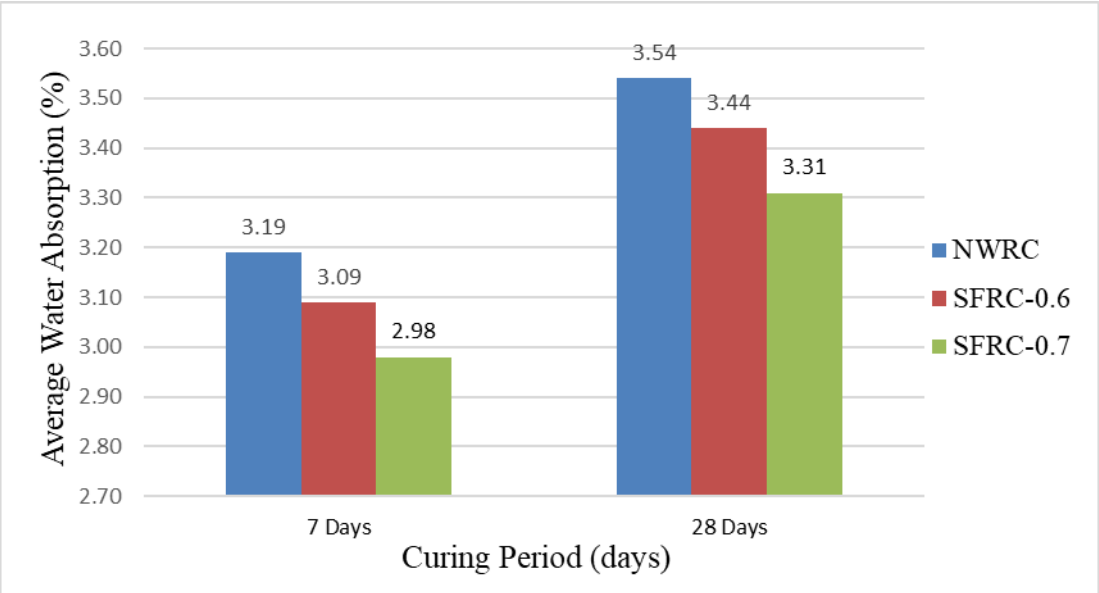

Figure 4.11: Average Water Absorption of Cube Specimens at Curing Periods of 7 Days and 28 Days

Table 4.5: Variation in Water Absorption as Compared to Control Specimens at Curing Period of 7 Days and 28 Days

Nomenclature	Variation in Water Absorption (%)	
	7 Days	28 Days
NWRC (Control)	-	-
SFRC-0.6	-3.13	-2.82
SFRC-0.7	-6.58	-6.50

From the result shown, the percentage of the water absorption decreased steadily with the increment of volume fraction of steel fibre in the normal curing regime. The water absorption of concrete at 7^{th} day curing age in this study reached about 90 % of the water absorption of concrete at 28^{th} day curing age. However, the water absorption of concrete specimen with the inclusion of 0.6 % and 0.7 % decreased from 2.82 % and 6.50 % respectively as compared to plain concrete. This can be explained that steel fibre concrete shows improved durability as compared to normal concrete.

The same steel fibre influence on water absorption in concrete performed in the experimental research conducted by Velayutham and Cheah (2014) in studying the durability of steel fibre reinforced high strength concrete subjected to normal curing. Steel fibre concrete has lower water absorption and lower permeability than plain concrete as steel fibre in concrete resist movements, therefore affecting permeability to decrease. Steel fibre concrete able to limit pore connectivity and reduce the porosity of the concrete mix since it is coated by cement paste in the surrounding area and it does not absorb moisture. Besides, the addition of fibres can enhance crack control through crack bridging, allowed closely spaced microcracks, which reduce the permeability of concrete at the same time.

4.6 Summary

In summary, material testing such as steel direct tensile test, slump test, compressive test, splitting tensile test and water absorption test were conducted to study the mechanical and engineering properties in this research. The experimental yield strength value presented is 485.33 MPa for H8 and 511.16 MPa for R8, whereas yield

strain value is 2257 με for H8 and 2515 με for R8. There was slump loss with the increase of fibre percentage in the concrete mix as an increment of fibre percentage absorb more cement paste to coat around due to the large surface area in high content. The compressive strength and splitting tensile strength of concrete with the inclusion of 0.6 % and 0.7 % steel fibre increased insignificantly from 6.93 % to 10.23% and 13.98 % to 17.92 % respectively as compared to plain concrete. It can be explained that increase in the fibre content results in an enhancement in concrete mechanical properties as bridging effect induced by fibres form a network structure in concrete and tend to reduce crack propagation and distribute stress among the cracks. Besides, the introduction of steel fibre in concrete can improves durability due to its lower water absorption and lower permeability than plain concrete.

CHAPTER 5

SHEAR STRENGTH BEAM TEST RESULTS AND DISCUSSION

5.1 Introduction

Chapter 5 discusses the experimental result and data obtained from the shear strength test and provide analysis of the behaviour of each tested beam. Each performance of the beam will be discussed separately in term of load response deflection relationship, load-strain response in longitudinal rebar in conjunction with crack pattern and failure mode. A comparison between the shear beam test results will be discussed to study the effect of variables on beam behaviour.

5.2 Shear Strength Beam Test Subjected to Four-point Loading

During the four-point bending test, tested beams were subjected to two point loads which applied in uniform increments and deflections were imposed. The applied load, the beam deflection and longitudinal rebar strain were recorded continuously up to failure is shown in Appendix G and plotted as load-deflection curves. Table 5.1 shows the peak shear load applied on each of the beam specimens at ultimate failure, ultimate shear strength and failure mode on tested beams. The maximum shear that can be resisted by the concrete strut is calculated in Appendix H for NWRC and Equation 2.5 is used to compute the ultimate shear capacity for SFRC.

Table 5.1: Tested Beams Details

Nomenclature	**Ultimate Load Applied, P (kN)**	**Experimental Ultimate Shear Strength, $v_{ULT,exp}$ (MPa)**	**Computed Ultimate Shear Strength, $v_{ULT,cal}$ (MPa)**	**Shear Strength Ratio, $\frac{v_{ULT,exp}}{v_{ULT,cal}}$**	**Failure Mode**
NWRC-W/OS	88	2.16	2.02	1.07	Shear
NWRC-W/S	126	3.09	2.38	1.30	Shear
SFRC-0.6	116	2.85	3.01	0.95	Shear
SFRC-0.7	120	2.94	3.18	0.92	Shear

The results obtained from the experimental investigation shows that the ultimate shear strength increased from 2.16 MPa to 2.85 MPa (31.94 %) and 2.94 MPa (36.11 %), when 0.6 % and 0.7 % of steel fibres were introduced respectively. However, the results show that the NWRC-W/S increased the shear strength of NWRC-W/OS beam up to 45.15 %. NWRC-W/S beam can sustain greater load as compared to the beams with the inclusion of steel fibres content at 0.6 % and 0.7 %. This is because incorporation of steel fibres in the concrete matrix can exhibit the ductile tensile behaviour even after cracking during the load resisting phase due to the bridging mechanism of fibre pull-out behaviour. The steel fibres that intersected in the cracking plane absorb the residual strength improving the post-crack compressive behaviour. Hence, steel fibres can improve durability and the behaviour at serviceability limit state as they are able to permit effective stress transfer and reduce crack width as well as crack spacing. The following subsection explains further the experimental behaviour of each beam specimen in term of deflection, crack pattern and failure type.

The following subsection explains further the experimental behaviour of NWRC-W/OS as control and a comparative conventional beam of NWRC-W/S which both beams without the inclusion of steel fibre as well as SFRC-0.6 and SFRC-0.7 in term of deflection, steel strain, crack pattern and failure mode.

5.2.1 Normal Weight Reinforced Concrete Beam Without Stirrup (NWRC-W/OS)

The following section explains further the experimental behaviour of NWRC-W/OS beam specimen in terms of load-deflection, steel strain, crack pattern and failure mode. NWRC-W/OS is acted as plain concrete control beam without shear reinforcement to isolate the results by testing the fibre volume as the variable.

5.2.1.1 Load response deflection

The load response deflection relationships of NWRC-W/OS is presented graphically in Figure 5.1.

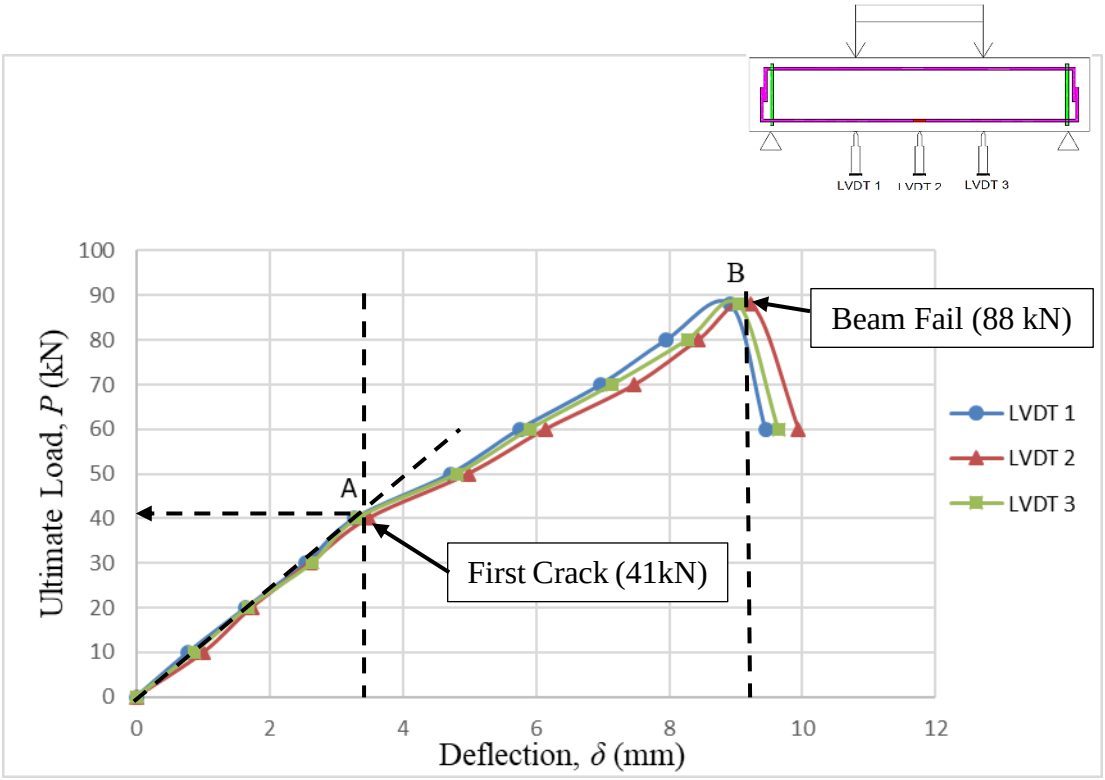

Figure 5.1: Load-deflection Behaviour of NWRC-W/OS Beam

As shown in Figure 5.1, the schematic diagram shows the location of LVDT 2 to be monitored at midspan of the beam to measure the deflection of the beam at midspan. There are LVDT 1 and LVDT 3 at the interval spacing of 150 mm placed symmetrically about the midspan at the loading points to examine the symmetricalness of the beam at both sides during the testing.

41 kN was the first cracking load determined experimentally with the midspan deflection of 3.63 mm. At Point A, the first cracking load can be defined as the first point, where the linearity of the load-deflection curve started to lose. The gradient under the linearity of load-deflection relationship can be explained in term of stiffness, which the beam can resists deformation in response to an applied force. Beyond Point A, the deflection of beam continued to increase upon further loading and reached Point B. The concrete beam reached its ultimate state and failed with an ultimate shear load of 88 kN causing the crushing of top compressive concrete. The beam failed and met a midspan deflection of 9.23 mm.

5.2.1.2 Load response steel strain

The load-steel strain curve for longitudinal compressive dowel bar of the NWRC-W/OS beam is illustrated in Figure 5.2.

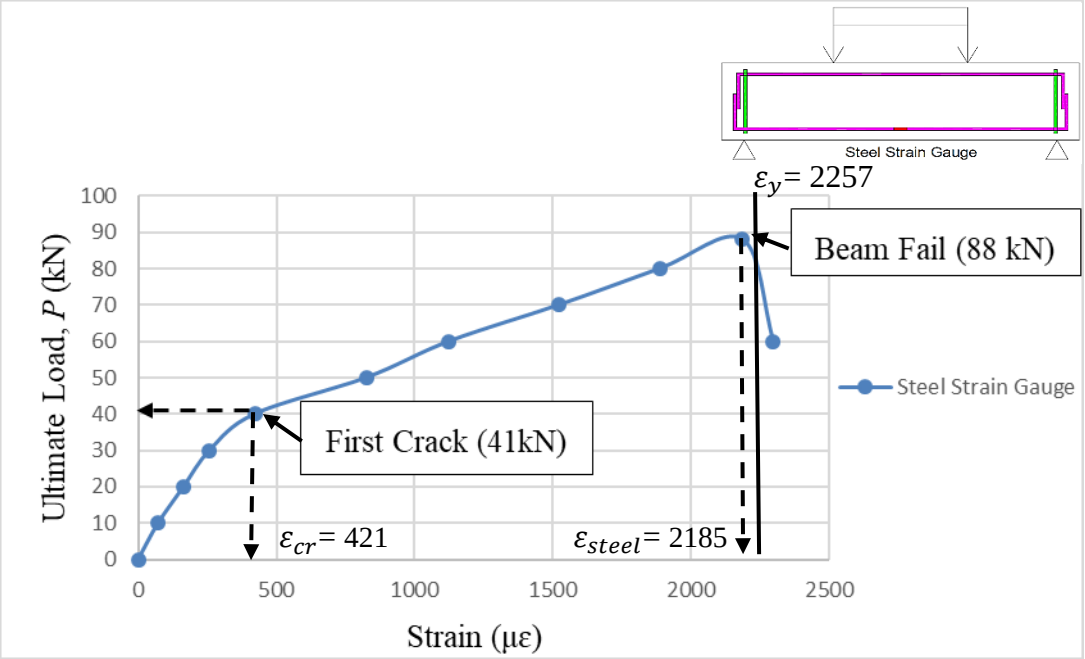

Figure 5.2: Load-steel Strain Curve for NWRC-W/OS Beam

As presented in Figure 5.2, the steel strain gauge installed was used to measure strain behaviour of steel reinforcement at every interval of loadings. At the beginning of the loading, the concrete beam sustained a large portion of load and the increment of steel strain performed slowly. The first crack occurred at 41 kN with the steel strain value of 421 με and the stress induced by the applied load was transferred to the dowel bar beyond this point. Then the steel strain of beam, ε_{steel} beyond this load level increased linearly and greatly to 2185 με at which the beam failed before the reaching of the yielding strain, ε_y. Hence, it can be concluded that the beam is not failing at the excessive yielding of the steel reinforcement but in excessive cracking in concrete.

5.2.1.3 Crack pattern and failure mode

As indicated in Figure 5.3, the first crack location can be determined at the bottom face of the tested beam. The ultimate failure of the beam took place at 88 kN and followed by the crushing of concrete in the compression zone. The crack pattern of NWRC-

W/OS beam at load intensities of 60 kN, 70 kN and 80 kN were presented in Autocad as shown in Figure 5.4.

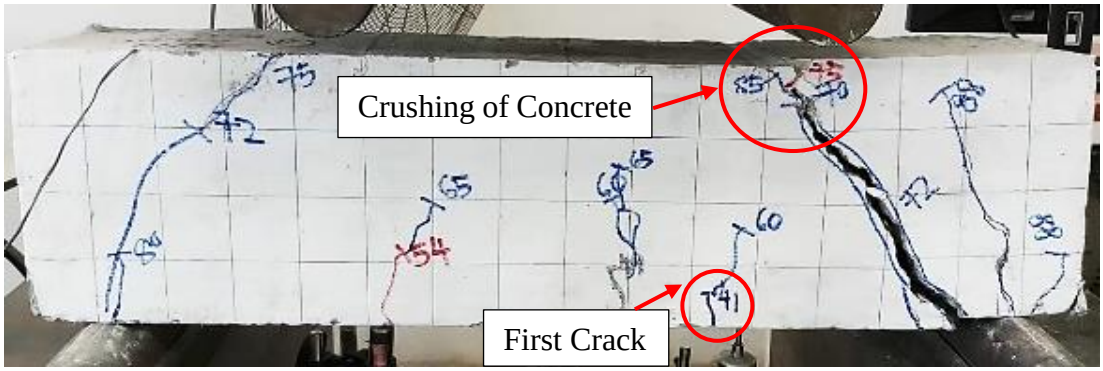

Figure 5.3: First crack and Crushing of NWRC-W/OS Beam

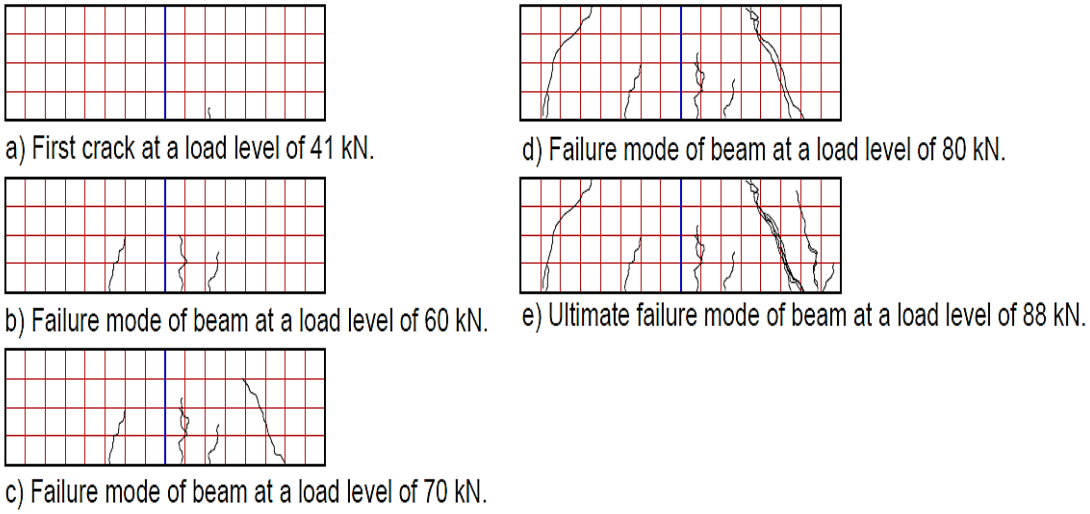

Figure 5.4: Crack Pattern of NWRC-W/OS Beam

As depicted in Figure 5.4, the first vertical tension crack developed at the tension zone of the tested beam in the region between midspan beam and right loading point, nearly to where the maximum degree of moment occurred. As shown in section (b), the flexural-shear cracks occurred at 60 kN which extended from past flexural cracks. Upon further loading, these cracks were widened, increased in number and propagate upward and toward the support. As can be observed in section (d) of Figure 5.4, a numerous of cracks emerged and the diagonal shear cracks with a large slope outside the two loads and closer to them were formed when further loading applied. The crack propagated through the beam until it reached the compression zone. These cracks were developed in the web of beams at the highest shear stress region. Finally,

the beam failed in shear at 88 kN, due to the major crack in diagonal splitting. Besides, all the cracks were observed to propagate parallel to one another which can be represented by an analogous truss. According to Mosley, Hulse and Bungey (2012), the truss model is assumed, and the shear force is transferred by the compressive strut of concrete and longitudinal tension steel.

A critical incline shear tension crack was formed resulted from the diagonal tension near the support where the shear stresses were acting on the surface. For beams without stirrups with an *a/d* ratio of less than 2.5, which tested until failure, develop inclined cracks, are able to withstand an additional load after the internal force redistribution due in part to the action of arch (Cladera Bohigas, 2003).

At the load level of 88 kN, the beam reached a critical point and failed due to the splitting of the compression concrete. The study of Raj and Rao (2015) showed that this type of failure was compression strut failure or shear compression, where there was local crushing near the loading points or support. Overall, the failure mode observed was a combination of diagonal tension failure, shear compression failure and arch rib failure. The arch rib failure took place as there was a transference of direct force from loading to the bearings in short span beam.

5.2.2 Normal Weight Reinforced Concrete Beam With Stirrup (NWRC-W/S)

The following section explains further the experimental behaviour of NWRC-W/S beam specimen in terms of load-deflection, steel strain, crack pattern and failure mode. NWRC-W/S is acted as a conventional beam with shear reinforcement. The shear capacity which can be resisted by transverse shear reinforcement is compared with concrete with steel fibres addition in term of shear strength.

5.2.2.1 Load response deflection

The graph of the load-deflection curve of the NWRC-W/S is presented in Figure 5.5.

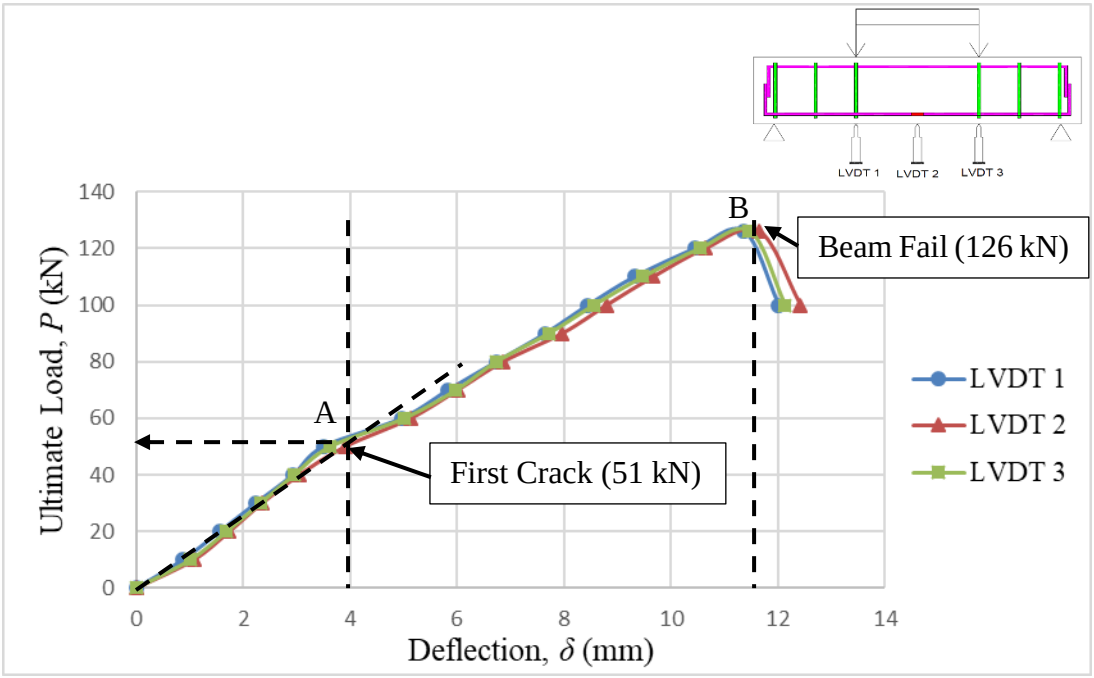

Figure 5.5: Load-deflection Behaviour of NWRC-W/S Beam

As presented in Figure 5.5, the deflection behaviour shown by LVDT 1 and LVDT 3 indicates that the beam was tested symmetrically about the midspan at the loading point. 51 kN was the first cracking load determined experimentally with the midspan deflection of 4.03 mm. The change in stiffness was determined at Point A, where was the occurrence of the first crack. After the first crack, the linearity of the load-deflection relationship lost, and the deflection of the beam continued to increase gradually upon further loading where the tensile stress in concrete had transferred to the steel reinforcement. Eventually, the load stopped increasing at 126 kN when it reached its ultimate state and failed with ultimate shear. This was followed by the crushing of top compression concrete where midspan deflection was 11.645 mm.

5.2.2.2 Load response steel strain

The load-steel strain curve for longitudinal compressive dowel bar for the NWRC-W/S beam is presented in Figure 5.6.

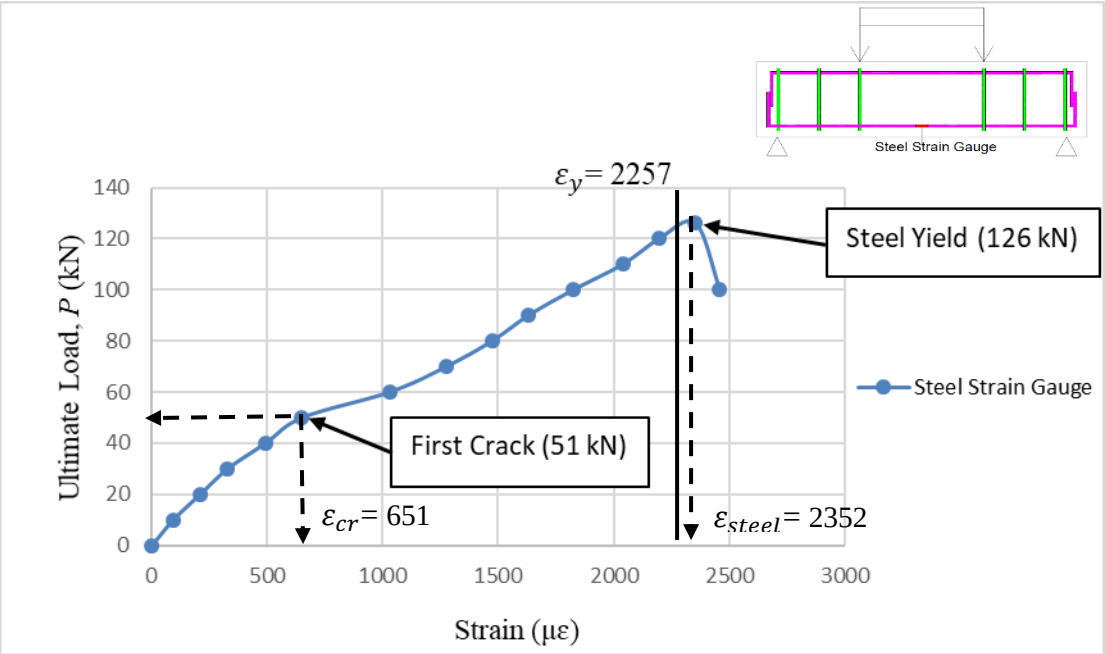

Figure 5.6: Load-steel Strain Curve for NWRC-W/S Beam

As depicted in Figure 5.6, the load-strain curve for NWRC-W/S beam has only one refraction point. Prior to the first tension crack occurred at 51 kN, the concrete beam handled large portion of the applied stress where the increment of steel strain performed slowly. The first crack had a value of 651 με in steel strain value and followed by a gradually elongation in steel reinforcement where the stress induced by the applied load was transferred to the steel reinforcement. When the load reached 126 kN, the steel strain value had achieved 2352 με where the beam failed after the yielding of steel at 2257 με which determined through material testing. The beam could said to fail at where there were excessive crack in concrete and yielding of the steel reinforcement. Shear failure was expected as steel reinforcement had not yield in excessive.

5.2.2.3 Crack pattern and failure mode

Figure 5.7 indicates the first crack location at the bottom face of NWRC-W/S beam. The ultimate failure of beam met at 126 kN and followed by the crushing of concrete. The crack pattern of NWRC-W/S beam at load intensities of 60 kN, 80 kN, 100 kN and 120 kN were presented in Autocad as shown in Figure 5.8.

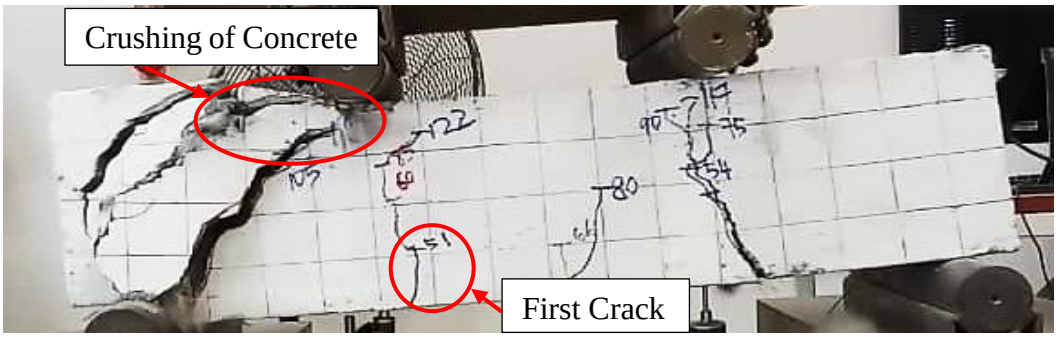

Figure 5.7: First Crack and Crushing of NWRC-W/S Beam

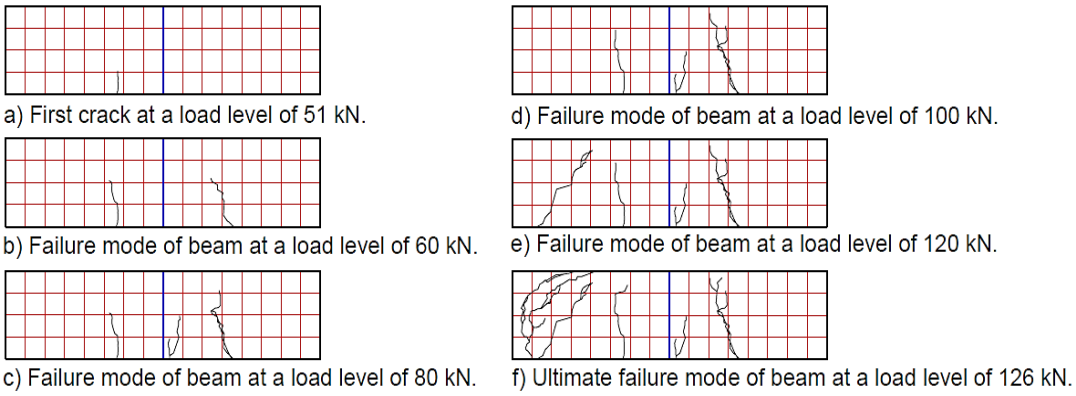

Figure 5.8: Crack Pattern of NWRC-W/S Beam

At load level of 51 kN, the first vertical tension cracks were formed near the left loading point and within the constant moment zone. By increasing the load, additional cracks generated and extended toward the shear span region. Far ahead, large shear crack with nearly 45^{o} from left supports was induced at the load of 120 kN. Due to capacity failure in the shear stress region, the beam was finally failed at the load of 126 kN. More cracks appeared more parallel to that which was propagated toward the supports to the loading points during the crushing of compressive concrete. This was followed by the beam failure in diagonal splitting. Besides, experimental observations also showed that the cracks in NWRC-W/OS beam open perpendicularly to the crack direction. Hence, no direct contribution from the shear capacity of the concrete itself and dowel action is to be expected but all shear will be resisted by the stirrups provision when truss model is assumed (Mosley, Hulse and Bungey, 2012).

By comparing Figure 5.6 (e) and (d), the diagonal tension failure was followed by bearing failure where the bearing stresses exceeding the concrete bearing capacity. As shown in Figure 5.7, the concrete spalling next to the crack upon failure can be seen. Besides, the failure happened in sudden and brittle due to the diagonal tension

failure. For NWRC-W/S beam, the diagonal shear mode caused by cracks were due to diagonal tension failure, shear compression failure and arch rib failure.

5.2.3 0.6 % Steel Fibre Reinforced Concrete Beam (SRFC-0.6)

The following section explains further the experimental behaviour of SFRC-0.6 beam specimen with the inclusion of 0.6 % steel fibre in NWRC mix by volume fraction in terms of load-deflection, steel strain, crack pattern and failure mode.

5.2.3.1 Load response deflection

The deflection of the SFRC-0.6 beam is depicted in the graph as shown in Figure 5.9.

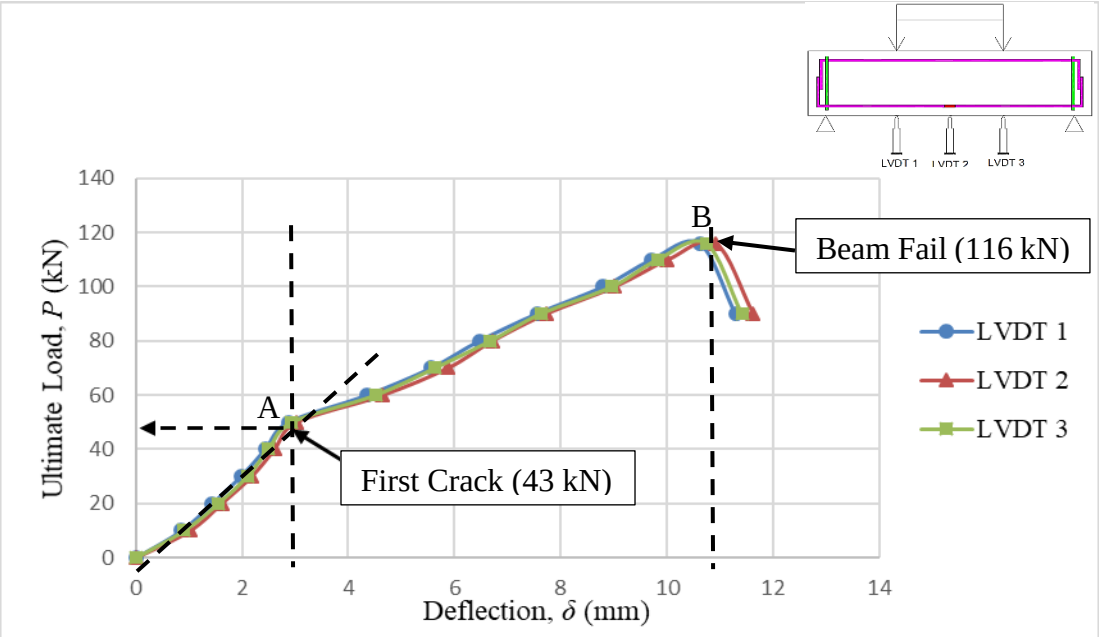

Figure 5.9: Load-deflection Behaviour of SFRC-0.6 Beam

As shown in Figure 5.9, the deflection behaviour is said to be symmetric on tested beams. At the beginning stage before the first crack Point A, the curve is observed to possess a mild gradient as the stiffness of the concrete beam itself. 43 kN was the first cracking load with a midspan deflection of 2.73 mm. After the first crack, there was a reallocation of stress to the steel reinforcement and steel bar from the concrete itself. Due to the refinement of ductility by steel fibres, the distribution of stress allowed the beam to deflect stably from Point A to Point B. In the fullness of testing period, the beam failed in shear mode at a load level of 116 kN where the midspan deflection was 10.91 mm.

5.2.3.2 Load response steel strain

The load-steel strain curve for longitudinal compressive dowel bar for SFRC-0.6 beam is plotted in Figure 5.10.

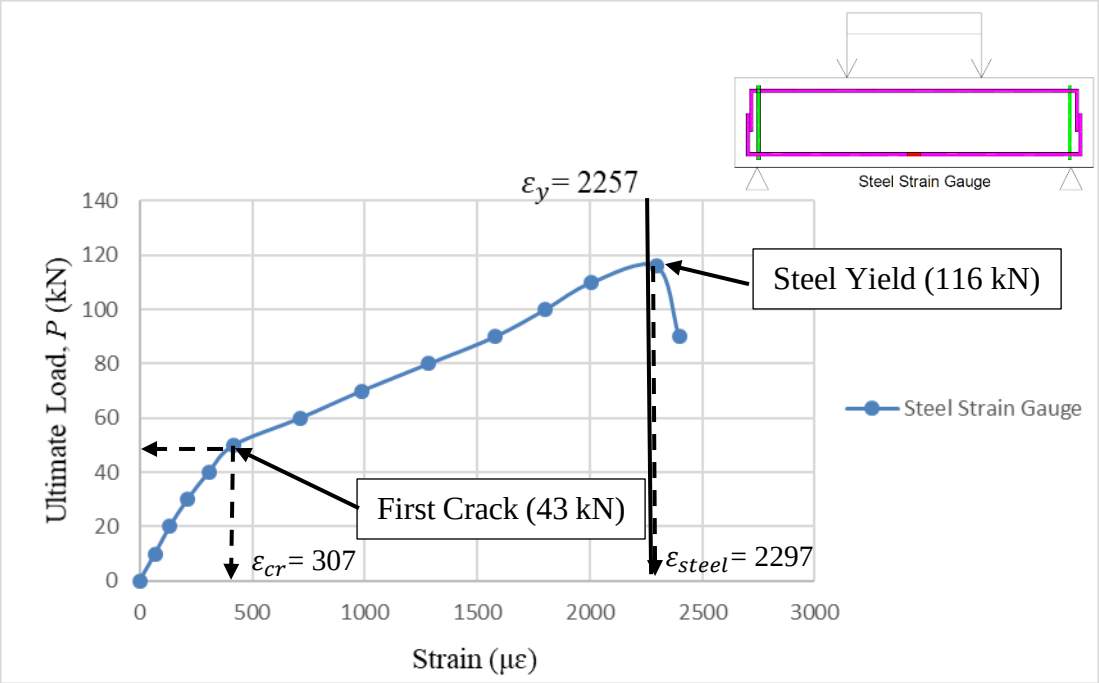

Figure 5.10: Load-steel Strain Curve for SFRC-0.6 Beam

Figure 5.10 illustrates the full behaviour of load-strain in steel reinforcement bar similar to the previous NWRC beam. At the beginning of the loading stage, the concrete beam sustained a higher portion of load the steel strain increased steadily. The first crack occurred at 43 kN with the steel strain value of 307 με. Upon further loading, the steel reinforcement bent steadily due to the combined effect of steel fibres and main reinforcement. The induced stress was shared with steel fibres, alongside with steel reinforcement, therefore the beam sustained greater load prior to the yielding of dowel bar. At the load level of 116 kN, the steel strain value had achieved 2297 με after the theoretical yield point of 2257 με. The beam is said to fail due to excessive crack in concrete with the yielding of the steel reinforcement.

5.2.3.3 Crack pattern and failure mode

Figure 5.11 shows the location of first crack on SFRC-0.6 beam when it was subjected to loading. The ultimate failure of the beam took place at 116 kN and followed by the

crushing of concrete. The crack pattern of SFRC-0.6 beam at load intensities of 60 kN, 80 kN and 100 kN were drawn by using Autocad and presented in Figure 5.12.

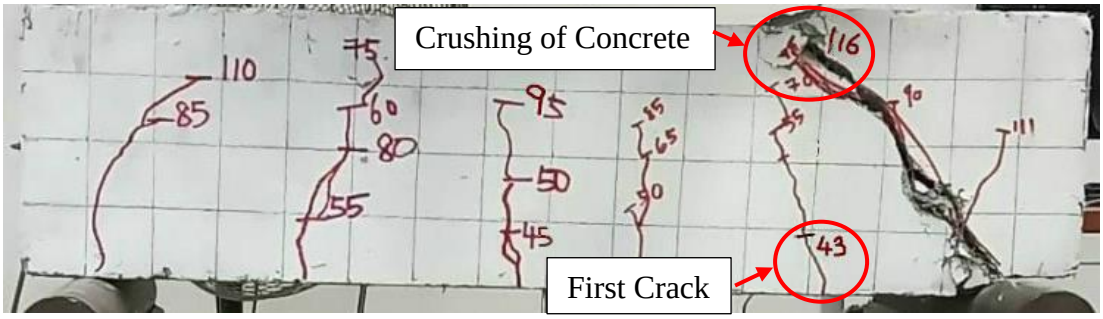

Figure 5.11: First Crack and Crushing of SFRC-0.6 Beam

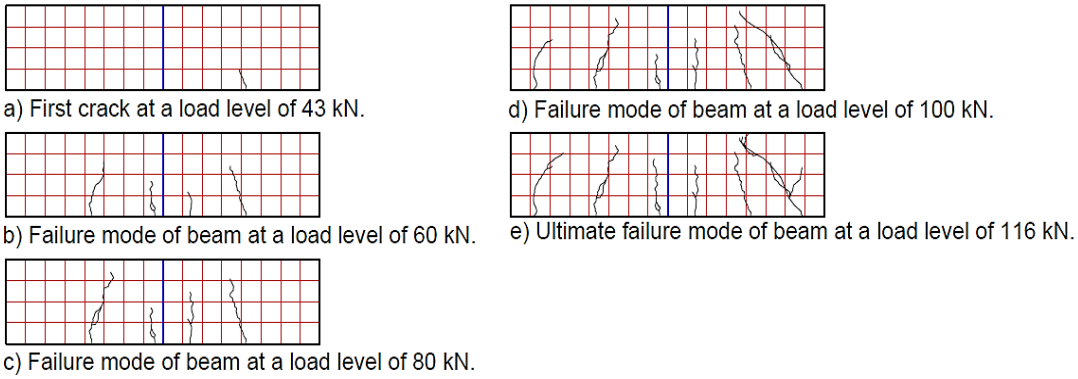

Figure 5.12: Crack Pattern of SFRC-0.6 Beam

For beam specimen SFRC-0.6, it can be seen that the critical shear crack formed prior to failure where the crack surface passed through aggregates. Besides, the formation of cracks was distributed uniformly and the bottom part of the beam. When the load level increased up to 43 kN, more vertical tension cracks appeared, and the existing cracks elongated upward slowly into compression zone but gradually. This is due to steel fibre in the beam reduce the development of stress concentration at the tip of cracks and delay the cracks growth rate. Steel fibres also distributed the stress from critical region to other parts of the concrete.

At the later stage of loading, the major cracks emerged and the diagonal shear cracks with a large slope outside formed. Finally, the bonding of steel fibres with the composite concrete at critical region was undermined at 116 kN ultimate load and failed in diagonal splitting when the compression region was crushed. Moreover, the diagonal shear crack propagated and reached the compression zone without any

secondary cracks sign. In diagonal compression failure, the beam specimen was able to sustain additional load after the first fully developed inclined tension crack was formed. The ultimate failure load is considerably higher at diagonal cracking due to arch action and this shear compression failure mode applies to short beam (Birgisson, 2011).

5.2.4 0.7 % Steel Fibre Reinforced Concrete Beam (SFRC-0.7)

The following section explains further the experimental behaviour of SFRC-0.7 beam specimen with the inclusion of 0.7 % steel fibre in NWRC mix by volume fraction in terms of load-deflection, steel strain, crack pattern and failure mode.

5.2.4.1 Load response deflection

The deflection of SFRC-0.7 beam has been presented graphically in Figure 5.13.

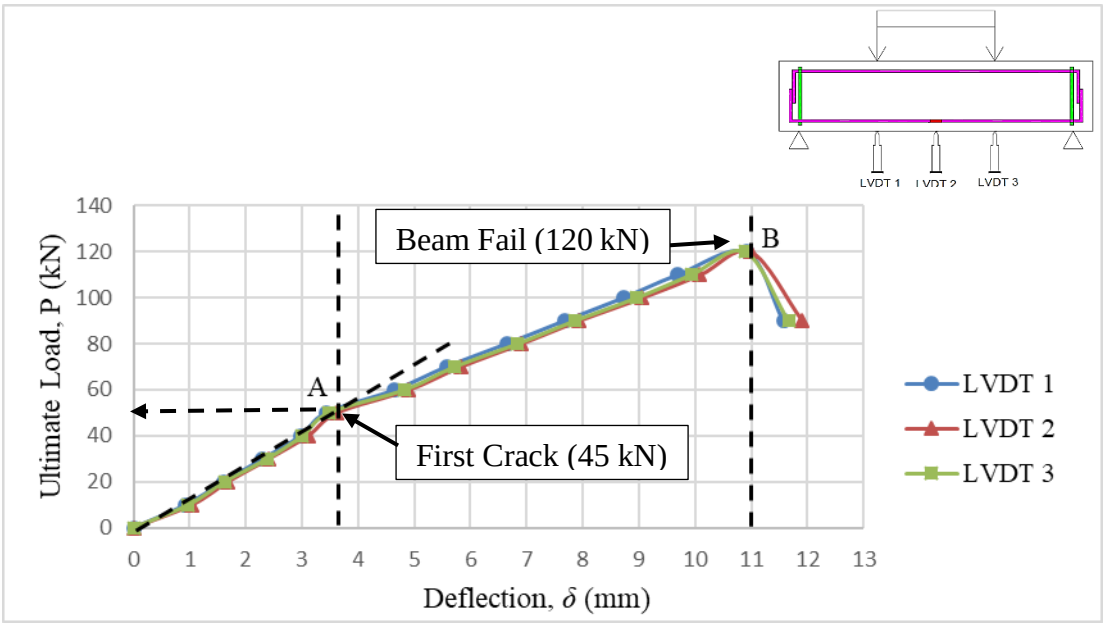

Figure 5.13: Load-deflection Behaviour of SFRC-0.7 Beam

As shown in Figure 5.13, the slope of the graph remains unchanged until the first crack load at 45 kN and reached Point A. The concrete remained its stiffness until the midspan deflection reached 3.36 mm. However, the cracks formed during early stage do not bring adverse effect to the beam integrity. This was then followed by the deflection increment in almost linear trend instead of a sudden rise in deflection upon further loading. This is because of the contribution of steel fibre in transferring stress

uniformly to the region around the concrete to avoid any concentration of local stress and allow steady deflection. This fibre-bridging mechanism allows the beam to reach its ultimate shear failure at Point B. 120 kN was the ultimate shear load tested on the beam with the midspan deflection of 10.98 mm.

5.2.4.2 Load response steel strain

The load-steel strain curve for longitudinal compressive dowel bar for the SFRC-0.7 beam is presented in Figure 5.14.

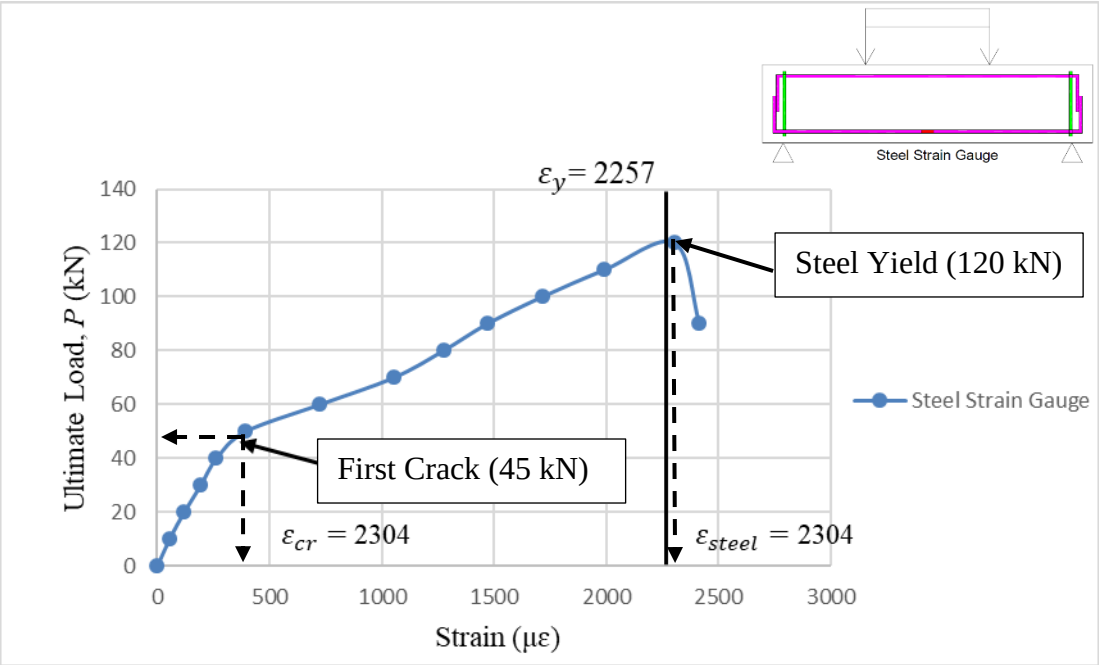

Figure 5.14: Load-steel Strain Curve for SFRC-0.7 Beam

As depicted in Figure 5.14, the behaviour of load-strain in steel reinforcement bar is similar to the curve as in Figure 5.10. Prior to the first tension crack occurred at 45 kN, the concrete beam able to sustain a large portion of applied stress where the increment of steel strain occurred slowly. The first crack had a value of 328 με in steel strain value where the steel fibre possessed its bridging effect to delay the macrocracks by distributing the applied stress due to the enhanced stiffening in the SFRC beam. At the load level of 120 kN, the steel strain value had achieved 2304 με, where the beam had sustained a greater amount of load before the steel yielded. The beam is said to fail due to excessive crack in concrete together with the yielding of the steel reinforcement.

5.2.4.3 Crack pattern and failure mode

Figure 5.15 indicates the location of the first crack at the bottom face of the tested beam. Meanwhile, Figure 5.16 shows the crack pattern of SFRC-0.7 beam at the failure load of 60 kN, 80 kN, 100 kN and 120 kN in Autocad drawing.

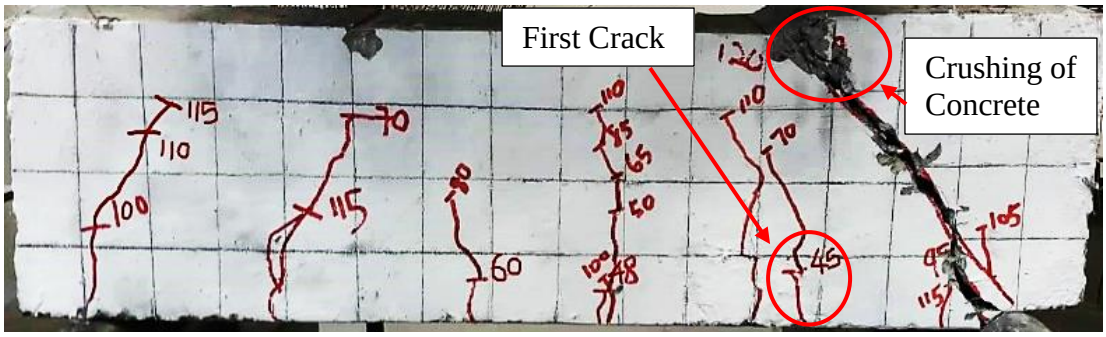

Figure 5.15: First Crack and Crushing of SFRC-0.7 Beam

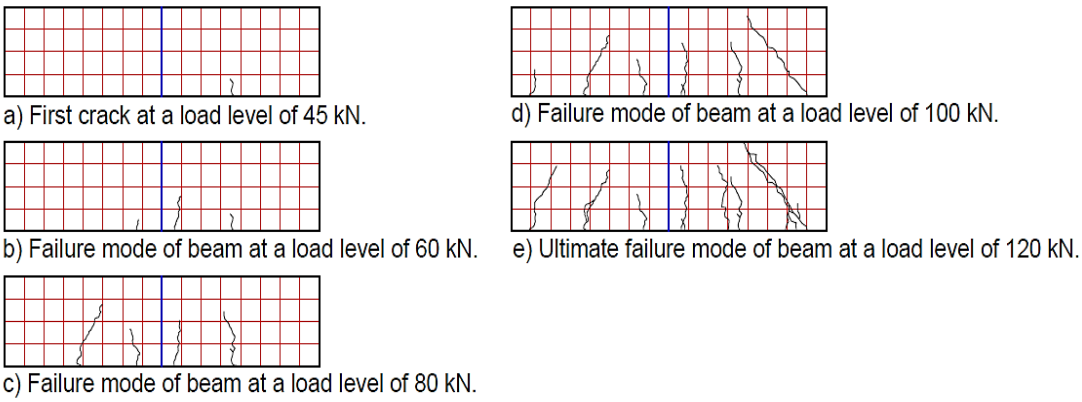

Figure 5.16: Crack Pattern of SFRC-0.7 Beam

For beam specimen SFRC-0.7, the cracking shear behaviour was similar to that observed in SFRC-0.6. In the full time of SFRC-0.7 failure, it can be seen that the crack propagation was slow in an earlier stage during the progressive debonding of the fibres. The slow propagation of cracks ultimately led to unstable crack propagation at the later stage and caused the failure of the beam specimen. As shown in Figure 5.15, the first vertical tension crack occurred at the tension zone of the tested beam in the area of right loading point with the first crack load of 45 kN. As depicted in Figure 5.16, it can be noticed that steel fibres contributed to improve the tensile resistance as well as post-cracking. At load level of 80 kN, the steel fibres inhibited the extension of crack width and propagation of cracks to compression zone. After the beam bent adequately, some minor cracks were noticeable around the major cracks. The evenly

dispersed steel fibres held the concrete through the bridging mechanism and mitigating the concrete from disintegrating.

Over soon, large shear crack with nearly 45 degree from right supports was induced at a load of 120 kN. hence the web shear cracks formed at highest shear stress region when cracks developed in the web of the beams. As mentioned in Russo and Zingone (1991) cited in Birgisson (2011), the failure mode of a beam can be predicted that shear compression failure is expectable when arch action governs whereas diagonal tension is expectable for the governance of beam action. Therefore, the SFRC-0.7 beam is said to fail of major crack in diagonal tension failure and shear compression failure of concrete.

5.3 Comparison of Structural Performance between NWRC Beam with SFRC-0.6 and SFRC-0.7

The results of each tested beam in the previous section were discussed and all of the beam specimens were diagnosed to be failed in shear failure mode in diagonal splitting. The shear behaviour is critical in beam specimens with the shear span-to-depth ratio of less than 3. Following the experimental work, parametric studies were worked out incorporating the content of shear stirrups and volume fraction of steel fibres. The comparison between NWRC-W/OS, NWRC-W/S, SFRC-0.6 and SFRC-0.7 beams is summarized in Table 5.2 and is further discussed in the following subsection in aspects of load-deflection behaviour, load-steel strain curve relationships, followed by crack pattern and failure mode of the beams.

5.3.1 Load response Deflection

The deflection was measured at mid-span section of the tested beam and recorded along with the whole range of loading until failure and plotted as load-midspan deflection curves. For comparison purpose, Figure 5.17 illustrates the midspan deflection behaviour variations of the NWRC-W/OS, NWRC-W/S, SFRC-0.6 and SFRC-0.7 beams subjected to the applied load. Table 5.2 shows that the first crack strength and failure consistently increased with the increment of steel fibres content.

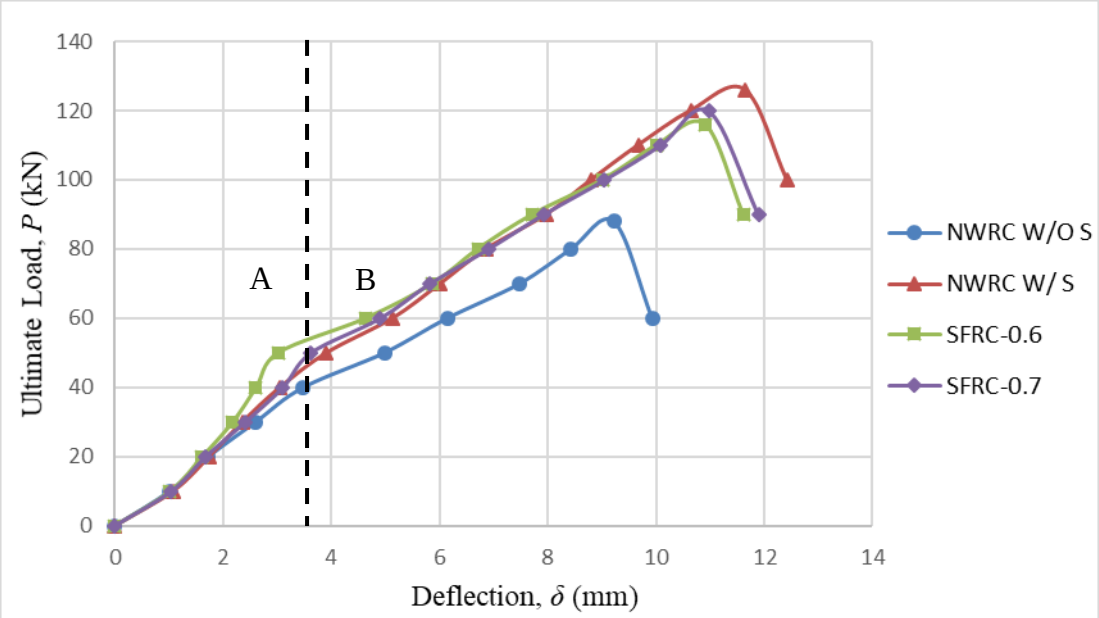

Figure 5.17: Load-deflection Behaviour of Beam Specimens at Midspan

Table 5.2: The Values of First Crack Strength, First Crack Deflection and Stiffness Indices of Bending Beam Specimens

Nomenclature	First Crack Strength		First Crack Deflection		Stiffness Indices	
	Strength, v_{cr} (MPa)	Δ (%)	δ_{cr} (mm)	Δ (%)	$\frac{P_{cr}}{\delta_{cr}}$ (kN/mm)	Δ (%)
NWRC-W/OS	1.01	-	3.63	-	11.29	-
NWRC-W/S	1.25	23.76	4.03	11.02	12.66	13.13
SFRC-0.6	1.06	4.95	2.73	-24.79	15.75	39.50
SFRC-0.7	1.10	8.91	3.36	-7.44	13.39	18.60

To evaluate the load-midspan deflection response of the beams, the behaviour of each beam is compared with others based on first cracking load and ultimate shear load. The points which the curvature increases sharply at the beginning are identified and the slope of the curve exhibits a definite change. Linear behaviour was observed for all beams up to the initiation of the first crack followed by a non-linear behaviour with a varying reduction in stiffness subjected to failure. However, the curves tended towards steadily and this may be attributed to the fibre effect in arresting cracking.

Study of Jothi (2008) stated that the first crack strength determined the FRC behaviour up to the onset of cracking in the concrete composite, whereas toughness indices characterize the toughness which up to specified end-point deflections. According to the graphic in Region A, as the fibre volume increased, the first cracking load increased. Especially, the introduction of steel fibre has higher first cracking load than control beam without stirrups but lower first cracking load than beam with stirrups. Stiffness reflects the resistance of an elastic body to deformation or deflection when subjected to the applied force, hence the addition of steel fibres enhanced the stiffness of the beam itself. SFRC-0.6 possessed the highest degree of stiffness indices where improvement of stiffness up to almost 40 %. However, NWRC-W/S possessed highest first crack deflection which reflected that beam with stirrup improved the pre-cracking by delay the appearance of the first cracks for flexure shear cracks due to its high efficiency in energy absorption.

Besides, the toughness of concrete beam can be determined from the area which under the load-deflection curve. Toughness is a property used to describe as the energy absorption capacity of reinforced concrete beams which is significant for the behaviour after the onset of cracking before rupturing. As shown in Figure 5.17, when fibre volume fraction increased, the toughness of beam specimens significantly increased as well as compared to NWRC-W/OS beam. This is because the addition of a volume fraction of hooked steel fibre as shear reinforcement imparts ductility and substantially increases the shear strength of a concrete beam. Fibres served as crack arrests or barriers which improve the tortuosity of the advancing crack. However, it can be seen that NWRC-W/S beam still has the highest first cracking strength with the improvement of 23.76 % as compared to NWRC-W/OS as well as toughness with the highest shear resistance due to its significant role as a source of energy dissipation and high ductility.

By referring to the later stage in Region B based on Figure 5.17, the corresponding maximum midspan deflection were 9.23 mm (at 88 kN), 11.65 mm (at 126 kN), 10.91 mm (at 116 kN) and 10.98 mm (at 120 kN) for NWRC-W/OS, NWRC-W/S, SFRC-0.6 and SFRC-0.7 beams respectively. With the inclusion of 0.6 % and 0.7 % steel fibres, the deflection had increased by 18.2 % and 19 % respectively. In general, the maximum deflection in SFRC beams is found to be increased with the increase in the fibre content, which infers that the steel fibre addition in a beam improves the post-peak ductility and maintains the ultimate load through further

deflection. Steel fibres have the ability to improve the bendability of the concrete structures and improve the effective stiffness of the beam after the occurrence of diagonal tensile cracking and decrease the beam deflection (Choi, Hong-Gun and Wight, 2007). This can be explained when steel fibres act as a medium in bridging existing macrocracks by limiting them from extending in the opening, as well as improving the strength in post cracking and thus improve the tensile strength. The mechanism works when steel fibres take up a large portion of tensile stress, allow the beam structure to sustain the higher ultimate load, until the weakening of anchorage between steel fibres and concrete.

5.3.2 Load response Steel Strain

Figure 5.18 illustrates the full behaviour of load-steel strain in midspan steel reinforcement bar for all four tested beams.

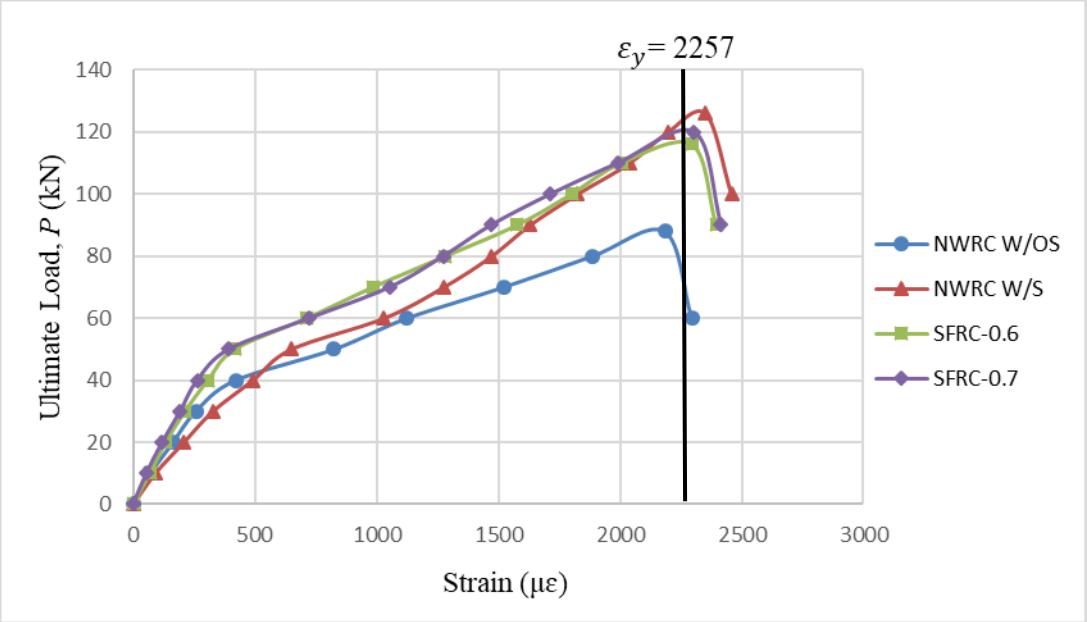

Figure 5.18: Load-steel Strain Curve of Beam Specimens

As shown in Figure 5.18, the first crack of NWRC-W/OS beam happened at 41 kN and lead to sudden elongation of the bottom concrete. The bottom steel reinforcement in NWRC-W/OS tended to deform in higher strain than other beams as the tensile stress in NWRC-W/OS beam was solely restrained by steel reinforcement which transferred from concrete. Upon further loading after the first crack load, the steel strain of NWRC-W/OS beam at the ultimate load of 88 kN was 2185 με (yield

strain equals to 2257 με) and this indicated that the failure of the beam was not due to excessive yielding of the steel reinforcement but in an excessive crack in the concrete.

As compared to NWRC-W/OS beam, SFRC-0.6 and SFRC-0.7 beams have higher steel strain value of 2297 με and 2304 με with an increment of 5.13 % and 5.45 % respectively. This is because the tensile stress in the concrete was shifted to the steel fibres instead of direct transferred to steel reinforcement, thus the elongation of steel reinforcement had been delayed when steel fibres started to withstand the stress immediately in preventing radical deflection in the beam as compared to NWRC-W/OS beam. Hence, the higher fibre content in concrete structure can improve the tensile stress capacity in concrete.

For NWRC-W/S beam, the steel strain value had achieved was 2352 με at the load level of 126 kN. Except for NWRC-W/OS beam which failed due to crushing of concrete before the yielding of steel, NWRC-W/S, SRFC-0.6 and SFRC-0.7 were failed due to both excessive cracks in concrete and yielding of the steel reinforcement. Shear failure was expected as steel reinforcement had not yielded in excessive. Steel fibres used in the reinforced concrete beam act as a secondary reinforcement can improve post-cracking tensile resistance and prevent instantaneous crack width development after the yielding of reinforcement. It can also be noticed that NWRC-W/S had a steeper gradient in load-steel strain prior to the failure as compared with SFRC-0.6 and SFRC-0.7. NWRC-W/S beam has a better property in energy absorption and higher load bearing capacity as compared to SFRC-0.6 and SFRC-0.7.

5.3.3 Crack Pattern and Failure Mode

Figure 5.19, 5.20, 5.21, 5.22 and 5.23 illustrate distinctive cracks development between NWRC-W/OS, NWRC-W/S, SFRC-0.6 and SFRC-0.7 at consistent loading interval.

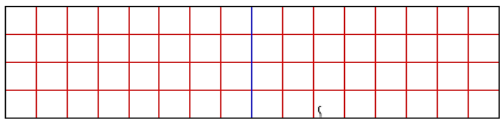

a) First crack of NWRC W/OS beam at 41 kN.

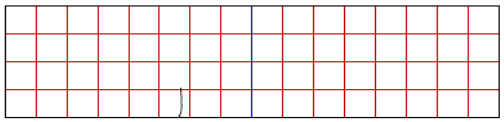

b) First crack of NWRC W/S beam at 51 kN.

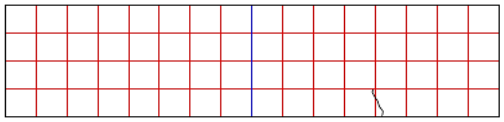

c) First crack of SFRC-0.6 beam at 43 kN.

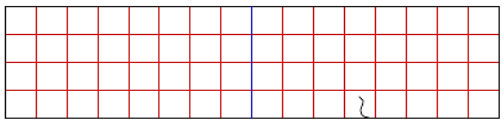

d) First crack of SFRC-0.7 beam at 45 kN.

Figure 5.19: Comparative First Crack

The first crack formation which induced near the region of load cell applied indicated that the development of moment by the loading was greater than the moment capacity of cracking of the beams. Figure 5.19 depicts the first tension crack of both NWRC beam specimens appeared as flexural-shear crack and about 100 mm away from the midspan. Besides, the initial crack of the SFRC-0.6 and SFRC-0.7 beams had delayed to 43 kN and 45 kN respectively as compared to NWRC-W/OS beam. The first diagonal crack was observed at which load no significant stiffness reduction was observed.

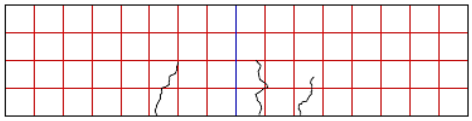

a) Failure mode of NWRC W/OS beam at 60 kN.

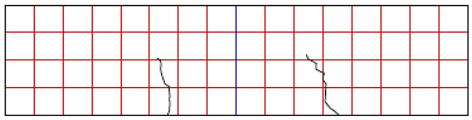

b) Failure mode of NWRC W/S beam at 60 kN.

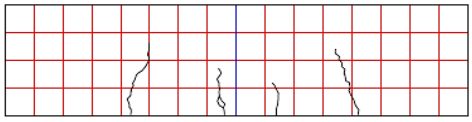

c) Failure mode of SFRC-0.6 beam at 60 kN.

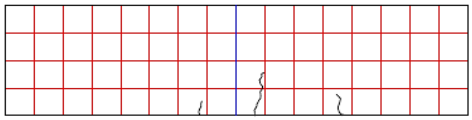

d) Failure mode of SFRC-0.7 beam at 60 kN.

Figure 5.20: Comparative Crack Pattern at 60 kN Failure Mode

As referred to Figure 5.20, flexural-shear cracks were spread throughout the shear span when there was an increment of loading continuously. Those cracks were extended from past flexural cracks. Besides, few inclined cracks started to be induced at the applied load of 60 kN at each of the beams. By comparing Figure 5.19 and Figure 5.20, it can be seen that the propagation of first cracks in SFRC-0.6 and SFRC-0.7 beams were slower than NWRC-W/OS beam. There was an increase of about 100 mm of crack length in NWRC-W/OS, whereas an extension of roughly 50 mm in NWRC-W/S, SFRC-0.6 and SFRC-0.7. The presence of steel fibres which bonded at the tensile surface of the concrete beam helped in arresting the macrocracks from propagating whereas the stirrups in RC beam absorbed energy and distributed the stress induced.

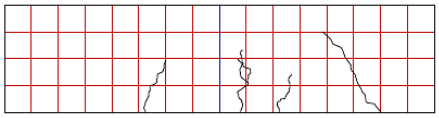

a) Failure mode of NWRC W/OS beam at 80 kN.

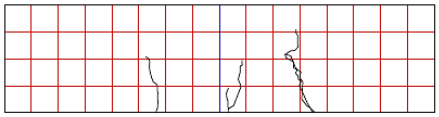

b) Failure mode of NWRC W/S beam at 80 kN.

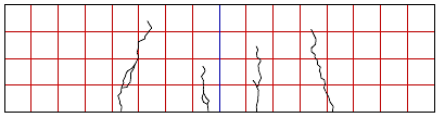

c) Failure mode of SFRC-0.6 beam at 80 kN.

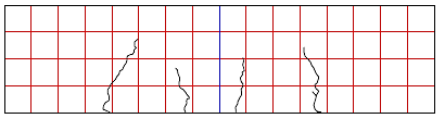

d) Failure mode of SFRC-0.7 beam at 80 kN.

Figure 5.21: Comparative Crack Pattern at 80 kN Failure Mode

As can be observed in Figure 5.21, the diagonal cracks started from the last flexural-shear crack and turned more and more inclined under shear loading. Similar to NWRC-W/S beam, only a few inclined cracks were observed from NWRC-W/OS beam. These inclined cracks, except for the critical one, stayed below the mid-depth level of the beam. The web-shear cracks started to form and noticeable in NWRC-W/OS, SFRC-0.6 and SFRC-0.7 beam, indicated that the shear stress was high at the shear span region. SFRC-0.7 beam had the overall shorter crack length as compared to the other three beams due to the higher steel fibre content as a medium of bridging mechanism.

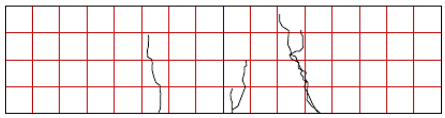

b) Failure mode of NWRC W/S beam at 100 kN.

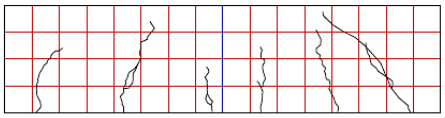

c) Failure mode of SFRC-0.6 beam at 100 kN.

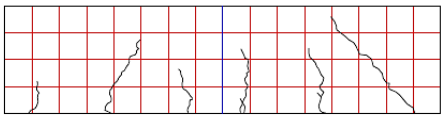

c) Failure mode of SFRC-0.7 beam at 100 kN.

Figure 5.22: Comparative Crack Pattern at 100 kN Failure Mode

As shown in Figure 5.22, there were only NWRC-W/S, SFRC-0.6 and SFRC-0.7 beams were tested up to the load level of 100 kN. These beams were able to exhibit several major inclined cracks prior to a complete failure. With splitting cracks having developed along with the upper layer of compression bar, the NWRC-W/S, SFRC-0.6 and SFRC-0.7 beams are said to approach a combination failure mode of diagonal tension and shear compression failure. The beams with the inclusion of steel fibres and stirrups were subjected to energy absorption which enabled it to resist additional loading after the formation of inclined cracks. However, NWRC-W/S beam had a better serviceability performance in controlling crack formation.

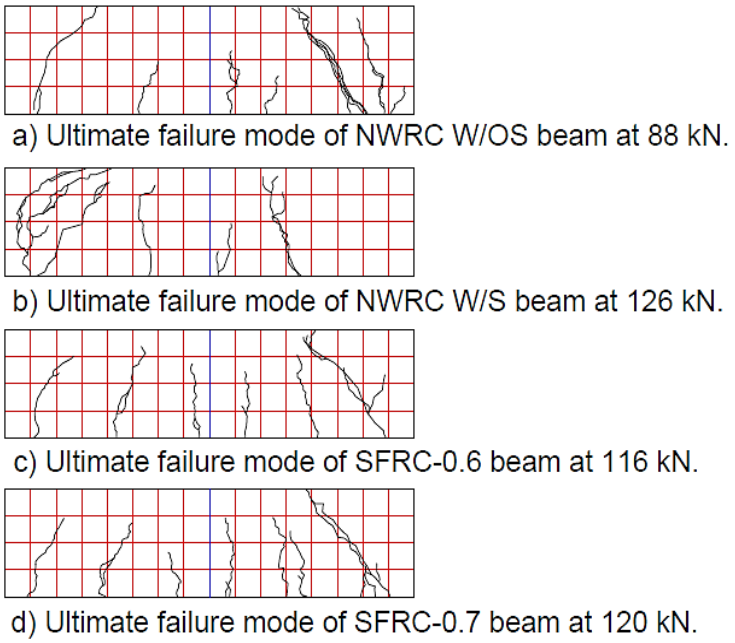

Figure 5.23: Comparative Ultimate Failure Mode

There was a distribution of principal stresses along the homogeneous concrete beam and it was illustrated in Figure 5.24. It can be noticed that the principle compressive stresses within the beam were imposed to be in arch form, whereas tensile stresses took the form of a curve assumed by a cord or suspended chain. The bending stresses were dominant with minimum shear at the mid-span of the beam, hence the stresses direction was more likely to be a counterpart to the beam axis (Mosley, Hulse and Bungey, 2012). Since the shearing forces were greater at supports, the principle stresses were more likely to be inclined. Hence, the diagonal cracking was formed near the supports due to the tensile stresses subjected to shear. Therefore, greater shear

force imposed a greater inclination angle. The failure mode which illustrated in Figure 5.25 shows the bending behaviour of the beam for midpoint deflection and possible critical crack section due to the incremental rotation angle from supports.

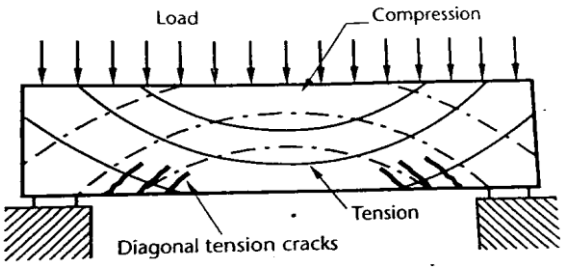

Figure 5.24: Distribution of Principle Stresses in a Beam (Mosley, Hulse and Bungey, 2012)

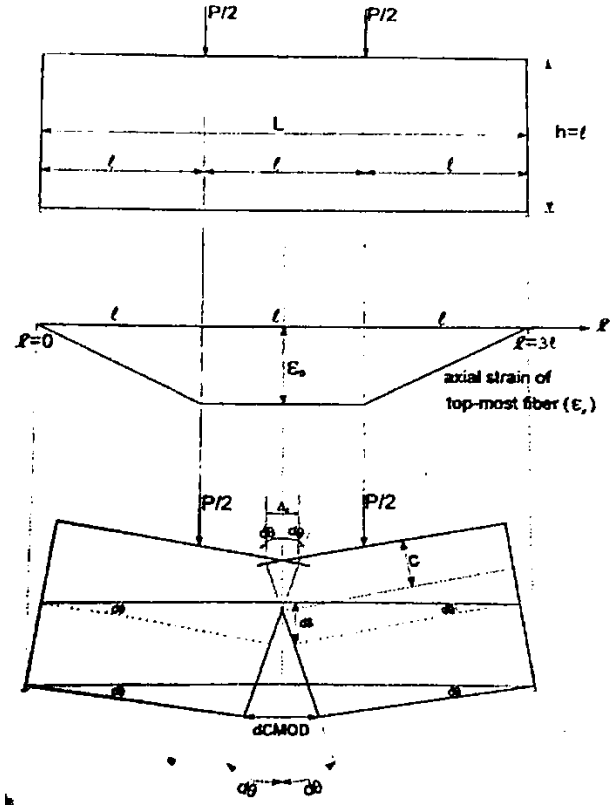

Figure 5.25: Failure Mode of Mid-span Deflection (Prudencio, et al., 2006)

Once the load which was sufficient to impose a diagonal tension was greater than the concrete tensile strength, a critical inclined crack occurred and followed by failure of beam immediately. It can be noted that the last critical crack developed fully. NWRC-W/S beam sustained with the highest ultimate shear load at a load level of

120 kN, followed by SFRC-0.6, SFRC-0.7 and lastly the control beam, NWRC-W/OS with 120 kN, 116 kN and 88 kN respectively.

Besides, much of the true shear cracks were also occurred at the lower half region of the beam especially for SFRC-0.6 and SFRC-0.7 beams where the tensile stress was distributed uniformly and minimize in crack width as well as reduction of crack spacing between two adjacent cracks. As compared with NWRC-W/OS beam, both SFRC-0.6 and SFRC-0.7 beams have higher shear strength, as steel fibres manage to transfer tensile stress across the surfaces of crack, which is known as crack-bridging stress as stated in Choi, Hong-Gun and Wight (2007). Besides, prior to collapse, a significant deformation was detected where the cracks appeared on beams with the incorporation of fibres substantially increased in number and were spaced more closely. Tantary, Upadhyay and Prasad (2012) explained that this type of cracking pattern increased further energy absorption capacity where the shear failure mode was gradual enough in dissipating sufficient energy before fracture. Hence, there is a better redistribution of internal stresses where additional diagonal cracks were observed.

Crack bridging which possessed by steel fibres within SFRC took place at a wake behind the crack front. When subjected to extra pressure during the crack opening, the bridging ligaments held the crack surfaces and minimize the intensity of stress around the crack tip and hence toughen the brittle material. Figure 5.26 depicts where the stress at those the critical section, such as compression zone, uncracked tension zone as well as crack tension zone.

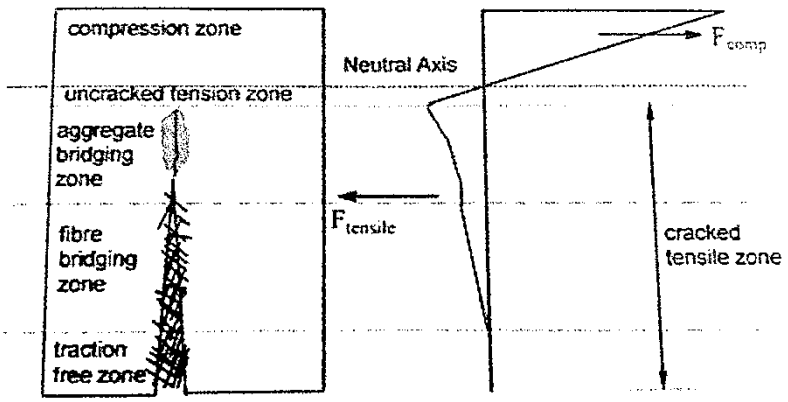

Figure 5.26: Simple Stress Block at Critical Cracking Zone of SFRC (Prudencio, et al., 2006)

The behaviour was explained with the aggregate bridging zone which initiated the fibre-matrix debonding zone from matrix-micro cracking. However, there was traction free zone at which fibre was partially pulled out from the concrete matrix. Figure 5.27 shows the fibre behaviour on localized beam crack surface. It can be seen that there was some non-straightened steel fibre anchorage within the damage matrix due to the resistance of pullout in the concrete composites was not develop fully. Hence, they were pulled prematurely from the matrix under tensile force.

Figure 5.27: Steel Fibre Behaviour on Localized Crack Surface

The shear failure mode of all beams was about to similar with the diagonal failure modes with about 45 degree of inclined diagonal crack. Hence, they can be reasonably considered as a combination of diagonal tension failure and shear compression failure at the shear crack tip when there is concrete crushing in the compression zone.

5.4 Summary

From the four-point bending shear test on the concrete beams, the results showed that concrete with hooked steel fibre provided higher post-cracking stiffness, an increase

in the shear capacity and energy absorption than plain concrete. Test results also indicated that the fibres have a significant influence on the failure mode and ultimate shear strength of a reinforced beam. Addition of fibres improved the beam stiffness and ductility as well as transformed the mode of failure into a more ductile one. Inclusion of steel fibres also reduced the beam deformations substantially at all load levels, controlled dowel bar, delay crack formation, shear cracking by controlling the crack width and length in propagation. Hence, the deflection of the beam was increased experimentally as steel fibre had increased the bendability of concrete structure.

The addition of steel fibres in concrete provides an effective crack arresting mechanism and bridging effect to serve as energy dissipation and stress transfer. Overall, the ultimate shear strength increased with the increment of steel fibre content in concrete. However, NWRC-W/S beam still possessed the highest ultimate shear strength among the other beams. Moreover, the actual behaviour of shear failure can be determined through inclined cracks such as flexural-shear cracks and web-shear cracks which fallen in diagonal failure modes.

CHAPTER 6

CONCLUSIONS AND RECOMMENDATIONS

6.1 Conclusions

This research project presents a comprehensive experimental program for studying the shear behaviour of 0.6 % and 0.7 % steel fibre reinforced concrete beams without stirrups. The main objectives of this study are to study the hardened properties of SFRC-0.6 and SFRC-0.7 on compressive strength, splitting tensile strength and water absorption; to investigate experimentally the shear behaviour of SFRC-0.6 and SFRC-0.7 beams without stirrups; and to study the shear behaviour of SFRC-0.6 and SFRC-0.7 beams as compared to conventional normal weight reinforced concrete beams.

As a result of this experimental study on the characteristics of SFRC beam, it has been observed that the compressive strength of concrete specimens with the inclusion of 0.6 % and 0.7 % were 32.01 MPa (increment of 6.93 %) and 33 MPa (increment of 10.23 %) respectively as compared to plain concrete with 29.94 MPa in compressive strength. Increase in compressive strength can be explained when introducing of fibres can reduce the shear stress in concrete against this shear plane. Besides, concrete with inclusion of steel fibre is likely to be confined and slightly take more load. Besides that, the splitting tensile of concrete specimens SFRC-0.6 and SFRC-0.7 were 3.18 MPa (increment of 13.98 %) and 3.29 MPa (increment of 17.92 %) respectively as compared to normal concrete with 2.79 MPa tensile strength. This strength enhancement is due to the fibre-bridging mechanism possessed by fibres with the concrete matrix and act as a multi-dimensional reinforcement. It absorbs energy and transfers the energy from applied load to other parts of concrete. Moreover, the SFRC showed improved durability as compared to normal concrete as it was found that there was a reduction of 2.82 % and 6.50 % in water absorption of SFRC-0.6 and SFRC-0.7 respectively. Steel fibre concrete has lower water absorption and lower permeability than plain concrete as steel fibre in concrete resist movements, therefore affecting permeability to decrease.

Furthermore, the ultimate shear strength of 0.6 % and 0.7 % SFRC beams had increased 31.82 % and 36.36 % respectively as compared to the NWRC beam without stirrups, whereas NWRC beam with stirrup increased 43.18 % in ultimate shear strength which possessed better performance in ductility. From the four-point bending

shear test on the concrete beams, the results showed that concrete with hooked steel fibre provided higher post-cracking stiffness, an increase in the shear capacity and energy absorption than plain concrete. Inclusion of steel fibres also reduced the beam deformations substantially at all load levels, controlled dowel bar, delay crack formation, shear cracking by controlling the crack width and length in propagation. Hence, the deflection of the beam was increased experimentally as steel fibre had increased the bendability of concrete structure. However, NWRC-W/S beam still possessed the highest ultimate shear strength among the other beams due to its higher energy absorption capacity and higher ductility. Moreover, the actual behaviour of shear failure can be determined through inclined cracks such as flexural-shear cracks and web-shear cracks which fallen in diagonal failure modes. All of the tested beams possessed an arch action in a shear-transfer mechanism where the shear was transmitted directly to the support through a compression strut that would develop between two adjacent web-shear cracks formed in a member. Besides, it can be noticed that reinforced concrete beams with steel fibres possessed more cracks, but they were smaller than in plain concrete with narrower crack spacing.

Overall, the steel fibres that intersected in the cracking plane absorb the residual strength improving the post-crack compressive behaviour. Hence, steel fibres can improve durability and the behaviour at serviceability limit state as they are able to permit effective stress transfer using bridging mechanism and reduce crack width and crack spacing.

6.1 Recommendations for Future Work

Even though this research has proven that steel fibre can improve the mechanical properties in concrete as well as shear strength in structural members, but the introduction of steel fibres in 0.6 % and 0.7 % by volume fraction is found to be less effective to replace the conventional shear stirrup reinforcement. Hence, the scope of the research can be expanded further based on the findings obtained from this research. Further investigations can be done on the composite effect of stirrups and steel fibres on shear behaviour of beams where steel fibres are used to replace stirrups partially.

Moreover, the results of the experiment indicated that the existing design is conservative and undervalue the contribution of concrete and shear reinforcement to the capacity of total shear. Hence, recommendations with less conservative should be validated by more experimental work findings. Besides, there is less precision

assessment of the shear strength as sectional methods used in provisions of current design such as ACI and Eurocode 2 in evaluating shear strength are empirical or semi-empirical. Rational analysis model such as lattice theory, finite element, shear friction model, crack sliding model, compression field-based model and so on can be applied to assess the shear strength of concrete beams to yield accurate and consistent results.

The study of shear in the beam has a versatile complex behaviour and it possesses brittle failure mode when exceeding the tensile strength value. Once brittle failure is initiated, concrete can losses its loading capacity completely and disintegrate. Hence, the improvement related to fibre reinforced concrete should be proposed for the current formulations in the Design Codes. Another recommendation is to further investigate other significant parameters especially the fibre efficiency factor in orientation, length factor in critical fibre length, space factor in critical fibre spacing, distribution, configuration and aspect ratio of steel fibre in determining their effect on the structural performance. As stated in Ferrara, Ozyurt and Di Prisco (2011), the structural beam can be improved effectively in mechanical performance if the orientation of the fibres can be counterpart with the principle tensile stress direction in the greatest degree possible.

Besides, a push-off test should be introduced in fibre reinforced concrete research to study the shear transfer mechanisms in the elements of fibre reinforced concrete. The test is carried out subjected to direct shear loads with better crack width control to enhance the test response in evaluating interlocking of aggregate in various concrete matrixes, at a distinct level of compressive strength and various type of steel fibres.

Moreover, the structural performance of the beam can be stimulated using a numerical method as well as generating analysis by using the finite element method. Structural performance such as strength, mode of failure and ultimate deflection under the stimulated loading can be generated and compare with the results obtained from experimental beam testing practically. Abbas, et al. (2014) had performed the NLFEA strategy using Abaqus as it used to take in the tensile constitutive models conveniently for SFRC. The modelling also offers some material models for non-linear analysis with the correlated cracking process of plain concrete.

Lastly, the study can be further explored using other loading schemes which are substantially different from monotonic concentrated loading, such as uniform

loading, cyclic loading, dynamic loading or reversed loading to further analyse the behaviour is reinforced beam under loading condition.

REFERENCES

Abbas, A. A., Syed Mohsin, S. M., Cotsovos, D. M. and Ruiz-Teran, A.M., 2014. Shear behaviour of steel-fibre-reinforced concrete simply supported beams. *Proceedings of the Institution of Civil Engineers-Structures and Buildings*, 167(9), pp.544-558.

Abbass, W., Khan, M. I. and Mourad, S., 2018. Evaluation of mechanical properties of steel fiber reinforced concrete with different strengths of concrete. *Construction and Building Materials*, 168, pp.556-569.

ACI Committee 544, 1999. *Design considerations for steel fiber reinforced concrete*. ACI544.4R-88 Manual of Concrete Practice.

Afroughsabet, V. and Ozbakkaloglu, T., 2015. Mechanical and durability properties of high-strength concrete containing steel and polypropylene fibers. *Construction and building materials*, 94, pp.73-82.

Amit Rai and Joshi, Y. P., 2014. Applications and properties of fibre reinforced concrete. *International Journal of Engineering Research and Applications*, 4(5), pp. 123-131.

Altaan, S. and Anay, R., 2015. Prediction of the shear strength of steel fibre reinforced concrete beams. In: Altaan, S., *Eighth International Conference on Fibre Concrete FC2015*. Czech Technical University, 10-9 September 2015. Prague, Czech Republic: Fibre Concrete 2015.

Altun, F., Haktanir, T. and Ari, K., 2007. Effects of steel fiber addition on mechanical properties of concrete and RC beams. *Construction and Building Materials*, 21(3), pp.654-661.

Anyfantis, K. N. and Tsouvalis, N. G., 2010. Characterization of fiber bridging in mode II fracture growth of laminated composite materials. *Applied Mechanics and Materials*, 24-25(2010), pp. 245-250.

Association Society for Testing and Materials, 2002. D6272 – 02 *Standard test method for flexural properties of unreinforced and reinforced plastics and electrical insulating materials by four-point bending*. United States: ASTM.

Association Society for Testing and Materials, 2003. C511 – 03 *Standard specification for mixing rooms, moist cabinets, moist rooms, and water storage tanks used in the testing of hydraulic cements and concretes*. United States: ASTM.

Association Society for Testing and Materials, 2004. C496 – 04 *Standard test method for splitting tensile strength of cylindrical concrete specimens*. United States: ASTM.

Association Society for Testing and Materials, 2005. C143 – 08 *Standard method of test for slump of hydraulic cement concrete*. United States: ASTM.

Association Society for Testing and Materials, 2006. C1602-06 *Standard specification for mixing water used in the production of hydraulic cement concrete*. United States: ASTM.

Association Society for Testing and Materials, 2006. C192-06 *Standard specification for making and curing concrete test specimens in the laboratory*. United States: ASTM.

Association Society for Testing and Materials, 2006. C33-06 *Standard specification for concrete aggregates*. United States: ASTM.

Association Society for Testing and Materials, 2006. C642 – 06 *Standard test method for density, absorption, and voids in hardened concrete*. United States: ASTM.

Association Society for Testing and Materials, 2007. C150-07 *Standard specification for portland cement*. United States: ASTM.

Association Society for Testing and Materials, 2013. E8/E8M-13a *Standard Test Methods for Tension Testing of Metallic Materials.* United States: ASTM.

Association Society for Testing and Materials, 2015. C470/C470M-15 *Standard test methods for molds for forming concrete test cylinders vertically*. United States: ASTM.

Babar, V. T., Joshi, P. K. and Shinde, D. N., 2015. Shear strength of steel fiber reinforced concrete beam without stirrups. *International Journal of Advanced Engineering Technology*, 15, p.18.

Balendran, R.V., Zhou, F. P., Nadeem, A. and Leung, A. Y. T., 2002. Influence of steel fibres on strength and ductility of normal and lightweight high strength concrete. *Building and environment*, 37(12), pp.1361-1367.

Balouch, S. U., Forth, J. P.and Granju, J. L, 2010. Surface corrosion of steel fibre reinforced concrete. *Cement and Concrete Research*, 40(3), pp. 410-414.

Banthia, N. and Sappakittipakorn, M., 2007. Toughness enhancement in steel fiber reinforced concrete through fiber hybridization. *Cement and Concrete Research*, 37(9), pp.1366-1372.

Barros, J. and Figueiras, A., 1992. Flexural behavior of SFRC, testing and modeling. *Journal of Materials in Civil Engineering*, 11(4).

Batson, G. B., 1977. *Strength of steel fiber concrete in adverse environments*. Illinois: Defence Technical Information Center.

Behbahani, H. P., Nematollahi, B. and Farasatpour, M., 2011. *Steel fiber reinforced concrete: A review*. Kandy-SriLanka: ICSECM.

Bernard, E. S., 2004. Durability of cracked fibre reinforced shotcrete. *Shotcrete: More Engineering Developments.* Sydney, Australia: Balkema Publishers, pp. 59-66.

Birgisson, S. R., 2011. *Shear resistance of reinforced concrete beams without stirrups* PhD dissertation. Reykjavik University.

Boulekbache, B., Hamrat, M., Chemrouk, M. and Amziane, S., 2012. Influence of Yield Stress and Compressive Strength on Direct Shear Behaviour of Steel Fibre-reinforced Concrete. *Construction and Building Materials*, 27(1), pp.6-14.

British Standards Institution, 2009. BS 12390-03:2009 *Testing hardened concrete – Part 1: Shape, dimensions and other requirements for specimens and moulds*. London: BSI.

British Standards Institution, 2013. BS EN 206:2013 *Concrete – Specification, performance, production and conformity.* London: BSI Standards Publication.

Byung Hwan, O., 1992. Flexural analysis of reinforced concrete beams containing steel Fibers. *Journal of Structural Engineering, ASCE*, 118(10).

Choi, K. K., Hong-Gun, P. and Wight, J. K., 2007. Shear strength of steel fiber-reinforced concrete beams without web reinforcement. *ACI Structural Journal*, 104(1), pp.12-21.

Cladera, A. and Mari, A. R., 2005. Experimental study on high-strength concrete beams failing in shear. *Engineering Structures*, 27(10), pp. 1519-1527.

Cladera, A. and Mari, A. R., 2004. Shear design procedure for reinforced normal and high-strength concrete beams using artificial neural networks. Part I: Beams without stirrups. *Engineering Structures*, 26(7), pp. 917-926.

Cladera, A. and Mari, A. R., 2004. Shear design procedure for reinforced normal and high-strength concrete beams using artificial neural networks. Part II: Beams with stirrups. *Engineering Structures*, 26(7), pp. 927-936.

Cladera Bohigas, A., 2003. *Shear design of reinforced high-strength concrete beams*. PhD Theses. Universitat Politècnica de Catalunya.

Clifford, A. O. O., David, W. B., Stephanie, J. B. and Nikos, N., 2016. *Pull-out response of discrete innovative hooked-end steel fibre shape and geometry embedded in self compacting concrete.* United Kingdom: University of Portsmouth.

Cristina, F., Aires, C., Joaquim, B. and Delfina, G., 2015. Durability of steel fiber reinforced self-compacting concrete. *Construction and Building Materials*, 80, pp. 155-166.

Cuenca, E., 2014. *On shear behavior of structural elements made of steel fiber reinforced concrete*. Springer.

Dahake, A. G. and Charkha, K. S., 2016. Effect of steel fibers on strength of concrete. *Journal of Engineering, Science & Management Education*, 9(1), pp. 45-51.

Duggal, S. K., 2008. *Building materials*. 3rd ed. New Delhi: New Age International (P) Ltd, Publishers

Eleonora, M., 2011. *Shear capacity of steel fibre reinforced concrete beams without conventional shear reinforcement*. Master. Royal Institute of Technology.

El-Ariss, B., 2006. Shear mechanism of cracked concrete. *International Journal of Applied Mathematics and Mechanics*, 2(3), pp. 24-31.

European Committee for Standardization, 2004. *BS EN 1992-1-1 Eurocode 2: Design of concrete structures, Part 1-1: General rules and rules for buildings*. Brussels: CEN.

Faisal, F. W., 1990. *Properties and applications of fiber reinforced concrete*. JKAU: Eng. Sci., 2, pp. 49-63.

Ferrara, L., Ozyurt, N. and Di Prisco, M., 2011. High mechanical performance of fibre reinforced cementitious composites: the role of "casting-flow induced" fibre orientation. *Materials and Structures*, 44(1), pp.109-128.

Gambhir, M. L., 2013. *Concrete Technology: Theory and practice*. 5th ed. New Delhi: McGraw Hill Education.

Guray, A., Riza Secer, O. K. and Semih, U., 2017. An experimental study on the shear strength of SFRC beams without stirrups. *Journal of Theoretical and Applied Mechanics*, 55(4), pp. 1206-1217.

Hai, H. D., 2009. *Shear behaviour of steel fiber reinforced concrete beams without stirrup reinforcement*. PhD. University of Michigan.

Harvinder, S., 2017. *Steel fiber reinfroced concrete: Behavior, modelling and design*. Singapore: Springer Transaction in Civil and Environmental Engineering.

Hassanpour, M., Shafigh, P. and Mahmud, H. B., 2012. Lightweight aggregate concrete fiber reinforcement–a review. *Construction and Building Materials*, 37, pp.452-461.

Holschemacher, K., Müller, T. and Fischer, A., 2006. Effect of fibre type on properties of steel fibre reinforced concrete. In: *Proceedings of The Tenth East Asia-Pacific Conference on Structural Engineering & Construction*. Bangkok, Thailand, pp. 383-388.

Hoseini, M., Bindiganavile, V., and Banthia, N., 2009. The effect of mechanical stress on permeability of concrete: A review. *Cement and Concrete Composites*, 31, pp. 213-220.

Jean-Francois, T. and Nemkumar, B., 1994. Concrete reinforced with deformed steel fibers, Part 1: Bond-slip mechanisms. *ACI Materials Journal*, 91(5), pp. 435-446.
Jean-Francois, T. and Nemkumar, B., 1994. Toughness characterization of steel-fiber reinforced concrete. *Journal Master Civil Engineering*, 6(2), pp. 264-289.

Jin-Ha, H., Deuk Hang, L., Hyunjin, J., Kang Su, K., Soo-Yeon, S. and Joo-Won, K., 2013. Shear behavior models of steel fiber reinforced concrete beams modifying softened truss model approaches. *Materials*, 6, pp. 4847-4867.

Jothi, D., 2008. Application of fiber reinforcement concrete technique in civil constructions. *African Research Review*, 2(4).

Karim, M. A., Abas, N. F. and Mydin, M. O., 2014. Investigating the mechanical properties of high performance concrete with a steel fibre admixture. In: *MATEC Web of Conferences*. Vol. 17, p. 01007. EDP Sciences.

Katzer, J., 2006. Steel fibers and steel fiber reinforced concrete in civil engineering. *Pacific Journal of Science and Technology*. 7(1), pp. 53-58.

Khaloo, A., Raisi, E. M., Hosseini, P. and Tahsiri, H., 2014. Mechanical performance of self-compacting concrete reinforced with steel fibers. *Construction and Building Materials*, 51, pp.179-186.

Khuntia, M., Bozidar, S., and Goel, S, C., 1999. Shear strength of normal and high strength fiber reinforced concrete beams without stirrups. *ACI Structural Journal*, 96(2), pp. 282-290.

Kumutha, R. and Vijai, K., 2009. Effect of steel fibers on the properties of concrete. *Journal of Reinforced Plastics and Composites*, 29(4), pp. 531-538.

Kwak, Y. K., Eberhard, M. O., Kim, W. S. and Kim, J., 2002. Shear strength of steel fiber-reinforced concrete beams without stirrups. *ACI Structural Journal*, 99(4), pp. 530-538.

Liaojun, Y., Yi, S., Licheng, G., Xiuqi, L., Meiying, Z., Liyong, Jia., Alderliesten, R. C. and Benedictus, R., 2017. Mode I fatigue delamination growth with fibre bridging in multidirectional composite laminates. *Engineering Fracture Mechanics*, 189(2018), pp. 221-231.

Mangat., P. S. and Gurusamy, K., 1987. Chloride diffusion in steel fibre reinforced marine concrete. *Cement and Concrete Research*, 17(3), pp. 385-396.

Marí, A., Cladera, A., Bairán, J., Oller, E. and Ribas, C., 2014. Shear-flexural strength mechanical model for the design and assessment of reinforced concrete beams subjected to point or distributed loads. *Special Column on Shear Failure Test and Analysis of Concrete Structures*, 8(4), pp. 337-353.

Mello, E., Ribellato, C. and Mohamedelhassan, E., 2014. Improving concrete properties with fibers addition. *International Journal of Civil, Environmental, Structural, Construction and Architectural Engineering*, 8(3), pp. 249-254.

Mihashi, H. and Leite, J. P. D. B., 2004. State of the art report on control of cracking in early age concrete. *Journal of Advanced Concrete Technology*, 2(2), pp. 141-154.

Miloud, B., 2005. Permeability and porosity characteristics of steel fiber reinforced concrete. *Asian Journal of Civil Engineering*, 6, pp. 317-330. Mosley, W. H., Hulse, R. and Bungey, J. H., 2012. *Reinforced concrete design: to Eurocode 2*. 7th ed. Macmillan International Higher Education.

Mudgal, D. N., 2012. *An experimental investigation of the characteristics properties and structural behavior of silica fume concrete produced with hybrid fibers*. Kolhapur: Shivaji University.

Naaman, Antoine, E. and Shah Surendra, P., 1976. Pull-out mechanisms in steel fiber reinforced concrete. *Journal of the Structural Division, ASCE*, pp. 1537-1548.

Neil, M. H., Daniel, A. K. and Robert, F. M., 2005. *Simplified shear design of structural concrete members*. NCHRP.

Neville, A.M., 2011. *Properties of concrete*. 5th ed. Harlow, England: Pearson Education Limited.

Nguyen Duc, T. and Nguyen Viet, T., 2018. Shear resistance of steel fiber-reinforced concrete beams without conventional shear reinforcement on the basis of the critical shear band concept. *Engineering Structures*, 168(2018), pp. 698-707.

Nyiutsa, S. A. and Aondowase, J. S., 2013. Effect of water-cement ratio on the compressive strength of gravel-crushed over burnt bricks concrete. *Civil and Environmental Research*., 3(4), pp. 74-82.

O'Neil, E. F. and Devlin, J. T., 1999. *Durability of fiber-reinforced concrete under flexural stress in a severe marine environment*. Vicksburg: Defense Technical Information Center.

Pant, A. S. and Parekar, S. R., 2009. Steel fiber reinforced concrete beams under bending, shear and torsion without web reinforcement. *International Journal of Recent Trends in Engineering*, 1(6), pp. 2009.

Prudencio, L., Austin, S., Jones, P., Armelin, H. and Robins, P., 2006. Prediction of steel fibre reinforced concrete under flexure from an inferred fibre pull-out response. *Materials and Structures*, 39(6), pp.601-610.

Punmia, B. C., Jain, A. K., Jain, A. K., Jain, A. K. and Jain, A. K., 2007. *Limit state design of reinforced concrete*. Firewall Media.

Rahmani, T., Kiani, B., Sami, F., Fard, B. N., Farnam, Y. and Shekarchizadeh, M., 2011. Durability of glass, polypropylene and steel fiber reinforced concrete. In: *Proceedings of the International Conference on Durability of Building Materials and Components*. Porto, Portugal, 12 April 2011. pp. 12-15.

Raj, J. L. and Rao, G. A., 2015. Shear strength of RC deep beam panels–A review. *International Journal of Research in Engineering and Technology*, 3(16), pp.89-103.

Raju, 2014. Review on shear behaviour of reinforced concrete beam without transverse reinforcement. *International Journal of Engineering Research and Applications*, 4(8), pp. 116-121.

Ranjan Sahoo, D. and Abhumanyu, S., 2014. Effect of steel fiber content on behaviour of concrete beams with and without Stirrups. ACI Structural Journal, 111(5), pp. 1157-1166.

Remigijus, S. and Gediminas, M., 2007. The influence of shear span ratio on load capacity of fibre reinforced concrete elements with various steel fibre volumes. *Journal of Civil Engineering and Management*, 13(3), pp. 209-215.

Remigijus, S. and Gediminas, M., 2010. Influence of fibre shape on the strength of steel fibre reinforced concrete. In: The 10th International Conference. *Modern Building Materials, Structures and Techniques*, pp. 763-767. Vilnius, Lithuania, 19-21 May 2010.

Selvi, M. T. and Thandavamoorthy, T. S., 2013. Studies on the properties of steel and polypropylene fibre reinforced concrete without any admixture. *International Journal of Engineering and Innovative Technology (IJEIT)*, 3(1), pp.411-416.

Shah Surendra and Rangan, 1994. Effect of fiber addition on concrete strength. *Indian Concrete Journal.*

Shibata, T. and Goto, Y., 1996. Shear failure of reinforced concrete beams subjected to diagonal tension. *Eleventh World Conference on Earthquake Engineering.* [online] Available at: < http://www.iitk.ac.in/nicee/wcee/article/11_1195.PDF> [Accessed 29 July 2018].

Shraddhu, S., 2017. *Special types of concrete*. Building Materials.

Siva Kishore, I. and Mallika Chowdary, Ch., 2016. Influence of steel fibers as admix in normal concrete mix. *International Journal of Civil Engineering and Technology (IJCIET)*, 7(1), pp. 93-103.

Spearing, S. M. and Evans, A. G., 1992. The role of fiber bridging in the delamination resistance of fiber-reinforced composites. *Acta Metallurgica et Materialia*, 40(9), pp. 2191-2199.

Tantary, M. A., Upadhyay, A. and Prasad, J., 2012. Influence of steel fibers on the shear strength of concrete. *Journal of Engineering, Computers & Applied Sciences*, 1(10), pp.88-92.

Taylor, R. E., 1998. CINDAS data series on materials properties. *Thermal Expansion of Solids.* United States: ASM International.

Thomas, J., and Ramaswamy, A., 2007. Mechanical properties of steel fiber reinforced concrete. *ASCE Journal of Materials in Civil Engineering*, 19(5), pp. 385-392.

Vasudev, R. and Vishnuram, B. G., 2013. Studies on steel fibre reinforced concrete– A sustainable approach. *International Journal of Scientific & Engineering Research*, 4(5), pp.1941-1944.

Vegera, P., Khmil, R. and Blikharskyy, Z., 2014. *The shear capacity of reinfroced concrete beams with different shear span to effective depth ratio*. Budownictwo.

Velayutham, G. and Cheah, C. B., 2014. The effects of steel fibre on the mechanical strength and durability of steel fibre reinforced high strength concrete (SFRHSC) subjected to normal and hygrothermal curing. In: *MATEC Web of Conferences*, 10, p. 2004. EDP Sciences.

Victor, M., Alexander, M., Anders, S. and Gregor, F., 2018. Corrosion resistance of steel fibre reinforced concrete – A literature review. *Cement and Concrete Research*, 103 (2018), pp. 1-20.

Wight, J. K. and MacGregor, J. G., 2008. *Reinforced concrete: Mechanics and design*. 5th ed. Upper Saddle River: Pearson Prentice Hall, pp. 247-248.

Xia, J., Xiao, Y., Mackie, K. R., Al-Ramahee, M. and Mirmiran, A., 2015. Dowel action and shear strength contribution of high strength rebar embedded in ultra-high performance fiber reinforced concrete. *Engineering Structures*, 83, pp.223-232.

Yang, Y., Walraven, J. and Uijl, J. D., 2016. Shear behavior of reinforced concrete beams without transverse reinforcement based on critical shear displacement. *Journal of Structural Engineering*, 143(1), p.04016146.

Yehia, S., Douba, A., Abdullahi, O. and Farrag, S., 2016. Mechanical and durability evaluation of fiber-reinforced self-compacting concrete. *Construction and Building Materials*, 121, pp.120-133.

Yoo, D.Y., Kim, S., Kim, J. J. and Chun, B., 2019. An experimental study on pullout and tensile behavior of ultra-high-performance concrete reinforced with various steel fibers. *Construction and Building Materials*, 206, pp.46-61.

You, Z., Ding, Y. and Niederegger, C., 2010. Replacing stirrups of self-compacting concrete beams with steel fibers. *Transactions of Tianjin University*, 16(6), pp.411-416.

Yuji, I. and Hideki, K., 1996. Experimental study on seismic behavior of R/C diagonally reinforced short beam. *Eleventh World Conference on Earthquake Engineering.* [online] Available at: < http://www.iitk.ac.in/nicee/wcee/article/11_1386.PDF> [Accessed 29 July 2018].

Zagon, R., Popa, M., Bindea, M. and Kiss, Z., 2013. Replacement of conventional shear reinforcement in a steel fibre reinforced-ultra high performance cement beam. *Buletinul Institutului Politehnic din lasi. Sectia Constructii, Arhitectura*, 59(5), p.27.

Zhongjin, L., 2011. *Advanced concrete technology*. New Jersey: John Wiley & Sons.

APPENDICES

APPENDIX A: Detailed Beam Design

Parameters:

Width of beam, b = 125 mm

Depth of beam, h = 200 mm

Length of beam, L= 800 mm

Nominal cover, C_{nom} = 25 mm

Length from support = 50 mm

Top compression bar = R8

Bottom tension bar = H8

Shear link = R8

Shear-to-span ratio:

Shear-to-span ratio, $\frac{a_v}{d} < 3$ (shear strength)

Effective depth of beam, d= 200-25-8-(8/2) = 163 mm

Shear span, $a_v < 3(163)$

$a_v < 489$ mm, 2(50) + 2(489) + 300 = 1378 mm (l)

By using a_v = 200 mm,

$2(a_v)$ + 300 +100 = beam length (800 mm)

Checking,

$\frac{a_v}{d} = \frac{200}{163} = 1.227 < 3$ (Acceptable)

Moment capacity of beam:

Compression reinforcement at top = 2R8 (A_s = 101 mm^2)

Tension Reinforcement at bottom = 2H8 ($A_{s'}$ = 101 mm^2)

F_{ck} = 25 N/mm^2

f_{yk} for H8 = 500 N/mm^2

f_{yk} for R8 = 250 N/mm^2

Depth of compression reinforcement, d'= 25 + 8 + (8/2) = 37 mm

$z_2 = d - d'$ = 163 – 37 = 126 mm

$z_1 = d - s/2$ = 163 – 12.4/2 = 156.8 mm > 0.95 *d* (154.85 mm)

$F_{st} = F_{sc} + F_{cc}$

$(0.87)(f_{yk})(A_s) = (0.87)(f_{yk})(A_s') + (0.567)(f_{ck})(b)(s)$

$0.87(500)(101) = 0.87(250)(101) + 0.567(25)(125)s$

s = 12.40 mm

$s = 0.8\,x$

x = 15.5 < 0.617 *d* (100.57 mm)

∴Tension bar has yielded as assumed

$\frac{d'}{x} = \frac{37}{15.5}$ = 2.39 (> 0.38)

∴ Compression bar has not yielded, decrease *d*' or increase *x* by increase the width of beam.

For F_{yk} less than 500 N/mm² for adequate safe check:

$\frac{d'}{d} = \frac{37}{163}$ = 0.23 (> 0.171)

$M = (F_{sc})(z_2) + (F_{cc})(z_1)$

= (21967.5)(126) + (21971.25)(156.8)

= 6.21 kNm

<u>Shear link selection:</u>

Minimum spacing of H8, $\frac{A_{sw,min}}{s} = \frac{(0.08)(f_{ck})^{0.5}(b)}{f_{yk}}$

$= \frac{(0.08)(25)^{0.5}(125)}{500}$

$= 0.1$

$\frac{101}{s} = 0.1$

s = 1010 mm > 0.75 d (122.25 mm)

Minimum spacing of R8, $\frac{A_{sw,min}}{s} = \frac{(0.08)(f_{ck})^{0.5}(b)}{f_{yk}}$

$= \frac{(0.08)(25)^{0.5}(125)}{250}$

$= 0.2$

$\frac{101}{s} = 0.2$

s = 505 mm > 0.75 d (122.25)

Max spacing, S_{max} = 0.75 d

= (0.75)(163)

= 122.25 mm

∴ Shear link with 100 mm (R8-100) c/c was selected.

Anchorage Bond:

Tension:

$l_{bd} = (\propto_1)(\propto_2)(\propto_3)(\propto_4)(\propto_5)(\ l_{b,\ rqd})(\frac{A_{s,req}}{A_{s,prov}})$

$= (\propto_1)(\propto_2)(\propto_3)(\propto_4)(\propto_5)(\frac{f_{yk}}{4.6\ f_{bd}})\ \emptyset$

$= (0.7)(1)(\frac{500}{4.6(3)})(8)$

= 202.9 mm

Take conservatively $\propto_3$ - $\propto_5$ = 1

Good bond condition, f_{bd} = 3 N/mm^2

$\propto_1$ = 0.7 (tension)

$\propto_2$ = 1 - 0.15 (C_d - 3∅)/∅ (other than straight)

= 1 – 0.15 (25 – 24)/8

= 0.98 ($0.7 \leq \propto_2 \leq 1.0$) ∴Acceptable

Concrete cover coefficient, C_d = 25

Compression:

$l_{bd} = (\propto_1)(\propto_2)(\propto_3)(\propto_4)(\ l_{b,\ rqd})(\frac{A_{s,req}}{A_{s,prov}})$

$= (\propto_1)(\propto_2)(\propto_3)(\propto_4)\frac{f_{yk}}{4.6\ f_{bd}})\ \emptyset$

$= (0.7)(1)(\frac{250}{4.6(3)})(8)$

$= 101.45$ mm

∴ Provided minimum anchorage length of 12∅ = 96 mm.

APPENDIX B: Design of Trial Mix Proportion

Concrete mix design form

Job title .....

Stage	Item		Reference or calculation	Values
1	1.1	Characteristic strength	Specified	30 N/mm² at 28 days Proportion defective ..... %
	1.2	Standard deviation	Fig 3	..... N/mm² or no data ..... N/mm²
	1.3	Margin	C1 or Specified	(k = ...) ..... × ..... = ... N/mm² ..... N/mm²
	1.4	Target mean strength	C2	30 + ... = 30 N/mm²
	1.5	Cement strength class	Specified	~~42.5~~/52.5
	1.6	Aggregate type: coarse Aggregate type: fine		Crushed/~~uncrushed~~ ~~Crushed~~/uncrushed
	1.7	Free-water/cement ratio	Table 2, Fig 4	0.6
	1.8	*Maximum free-water/ cement ratio*	*Specified*	..... Use the lower value: 0.6
2	2.1	Slump or Vebe time	Specified	Slump 60 - 180 mm or Vebe time ..... s
	2.2	Maximum aggregate size	Specified	20 mm
	2.3	Free-water content	Table 3	205 kg/m³
3	3.1	Cement content	C3	205 ÷ 0.6 = 341.67 kg/m³
	3.2	*Maximum cement content*	*Specified*	..... kg/m³
	3.3	*Minimum cement content*	*Specified*	..... kg/m³
				use 3.1 if ≤ 3.2 use 3.3 if > 3.1 341.67 kg/m³
	3.4	Modified free-water/cement ratio		.....
4	4.1	Relative density of aggregate (SSD)		2.65 ~~known~~/assumed
	4.2	Concrete density	Fig 5	2372.22 kg/m³
	4.3	Total aggregate content	C4	2372.22 − 205 − 341.67 = 1825.53 kg/m³

5	5.1 Grading of fine aggregate	Percentage passing 600 µm sieve	56.24	%
	5.2 Proportion of fine aggregate	Fig 6	41	%
	5.3 Fine aggregate content	C5	1825.53 × 0.41 = 748.47 kg/m³	
	5.4 Coarse aggregate content		1825.53 − 748.47 = 1077.06 kg/m²	

Quantities	Cement (kg)	Water (kg or litres)	Fine aggregate (kg)	Coarse aggregate (kg) 10 mm	20 mm	40 mm
per m³ (to nearest 5 kg)	341.67	205	748.47	359.02	718.04	
per trial mix of ..... m³						

Items in italics are optional limiting values that may be specified (see Section 7).

Concrete strength is expressed in the units N/mm². 1 N/mm² = 1 MN/ m² = 1 MPa. (N = newton; Pa = pascal.)

The internationally known term 'relative density' used here is synonymous with 'specific gravity' and is the ratio of the mass of a given volume of substance to the mass of an equal volume of water.

SSD = based on the saturated surface-dry condition.

APPENDIX C: Results of Steel Tensile Test of H8

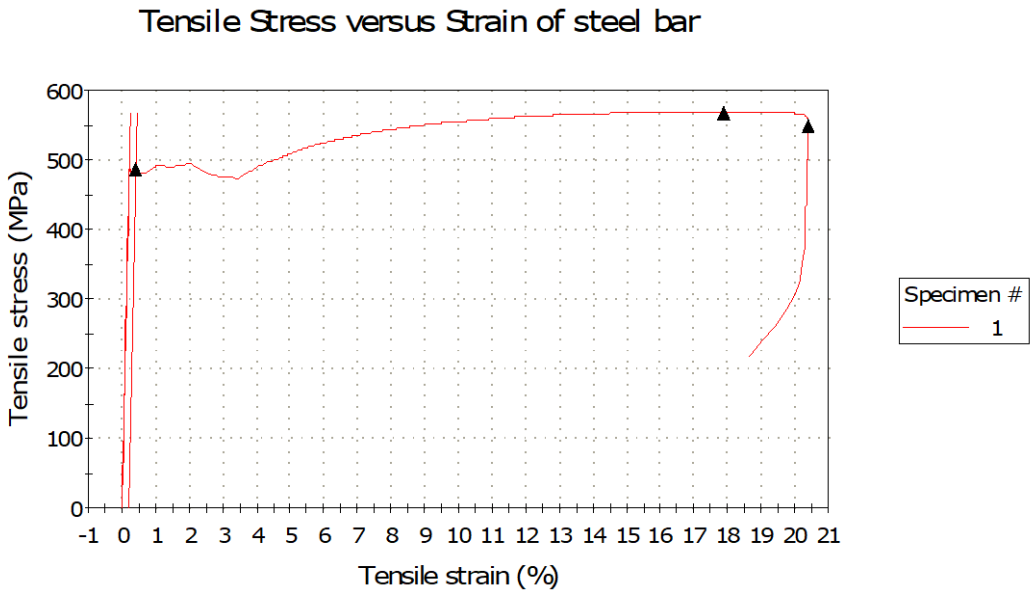

	Length (mm)	Diameter (mm)	Area (mm^2)
1	200.67000	7.94000	49.51433
Median	200.67000	7.94000	49.51433
Mean	200.67000	7.94000	49.51433

	Load at Maximum Tensile stress (N)	Maximum Tensile stress (MPa)	Load at Yield (Offset 0.2 %) (N)
1	28136.44707	568.24860	24030.93108
Median	28136.44707	568.24860	24030.93108
Mean	28136.44707	568.24860	24030.93108

	Extension at Maximum Tensile stress (mm)	Initial Area at Area Reduction (mm^2)	Modulus (E-modulus) (MPa)
1	30.68696	49.51433	214980.29785
Median	30.68696	49.51433	214980.29785
Mean	30.68696	49.51433	214980.29785

Table C1: Physical Measurement of H8 Steel Bar Specimen

Reading / Dimension (mm)	Measurement 1 (top)	Measurement 2 (middle)	Measurement 3 (end)	Average
Initial diameter, d_0	7.94	7.86	8.03	7.94
Final diameter, d_f	8	4.63	8.04	-
Initial length, L_0	201	200	201	200.67
Final length, L_f	233	234	233	233.33

APPENDIX D: Results of Steel Tensile Test of R8

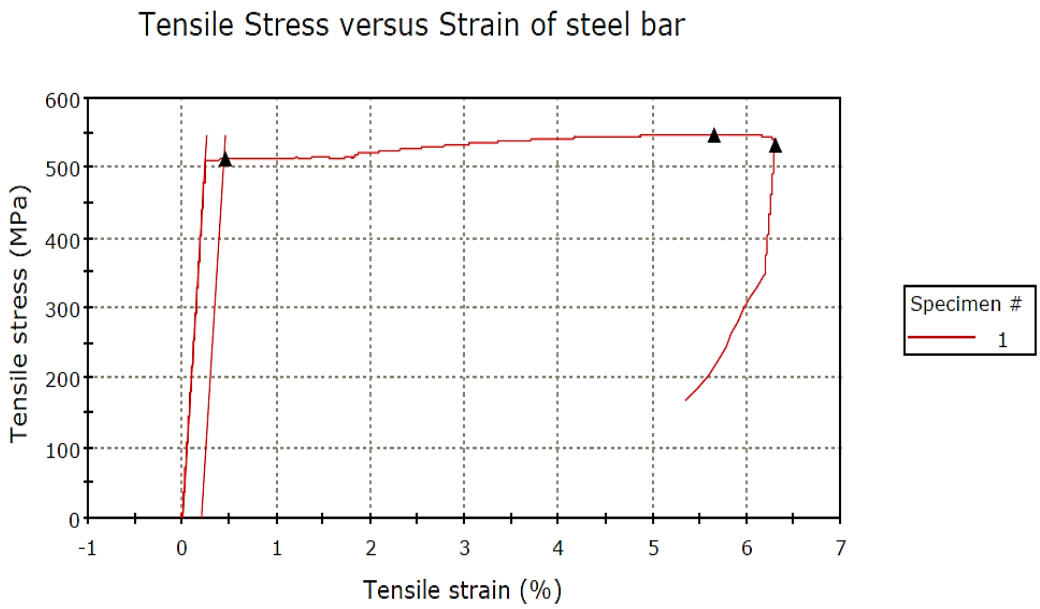

	Diameter (mm)	Load at Maximum Tensile stress (N)	Area (mm^2)
1	7.89000	26701.16425	48.89268
Median	7.89000	26701.16425	48.89268
Mean	7.89000	26701.16425	48.89268

	Maximum Tensile stress (MPa)	Modulus (E-modulus) (MPa)	Load at Yield (Offset 0.2 %) (N)
1	546.11778	203231.73828	24992.18379
Median	546.11778	203231.73828	24992.18379
Mean	546.11778	203231.73828	24992.18379

	Extension at Maximum Tensile stress (mm)	Length (mm)	Initial Area at Area Reduction (mm^2)
1	13.14179	200.00000	48.89268
Median	13.14179	200.00000	48.89268
Mean	13.14179	200.00000	48.89268

Table D1: Physical Measurement of R8 Steel Bar Specimen

Reading / Dimension (mm)	Measurement 1 (top)	Measurement 2 (middle)	Measurement 3 (end)	Average
Initial diameter, d_0	7.84	7.97	7.85	7.89
Final diameter, d_f	7.84	4.73	7.8	-
Initial length, L_0	241	240	240	240.33
Final length, L_f	256	257	256	256.33

APPENDIX E: Physical Measurement and Compression Peak Load of Concrete Cube Specimens

Curing Period	Mix Details	Specimen	Dimension (mm)			Mass (g)			Compression Peak Load (kN)
			Length	Width	Depth	Hardened	SSD	Oven-dried	
7 Days	NWRC	1	151.5	149.0	148.0	7845.5	7922.0	7653.0	547.2
		2	151.0	151.0	152.0	7903.0	7974.0	7742.0	589.3
		3	151.0	150.0	151.5	7850.0	7907.0	7649.5	561.9
	Average		151.2	150.0	150.5	7866.2	7934.3	7681.5	566.1
	SFRC-0.6	1	152.5	152.0	152.0	8121.5	8171.5	7920.0	574.8
		2	151.0	151.0	150.0	7942.0	7993.5	7726.0	586.5
		3	152.0	152.5	151.0	8154.0	8202.0	7967.0	568.7
	Average		151.8	151.8	151.0	8072.5	8122.3	7871.0	576.7
	SFRC-0.7	1	151.0	150.5	151.5	8007.0	8054.0	7822.0	579.5
		2	150.0	151.5	153.0	8206.0	8253.0	8021.5	565.0
		3	151.0	150.0	150.0	7829.0	7867.0	7611.5	572.9
	Average		150.7	150.7	151.5	8014.0	8058.0	7818.3	572.5
28 Days	NWRC	1	150.0	150.0	150.3	7942.5	8040.0	7767.0	620.5
		2	148.0	151.0	152.0	8032.0	8012.5	7721.0	703.9
		3	151.5	151.0	148.0	7925.0	8008.5	7722.0	703.0
	Average		149.8	150.7	150.1	7966.5	8020.3	7736.7	675.8
	SFRC-0.6	1	152.0	152.0	150.0	8122.5	8200.5	7927.0	729.8
		2	151.0	150.5	148.0	8037.0	8104.5	7813.0	740.4
		3	151.0	152.5	149.0	7977.0	8049.0	7775.5	733.6
	Average		151.3	151.7	149.0	8045.5	8118.0	7838.5	734.6
	SFRC-0.7	1	149.0	152.0	149.0	8010.0	8090.5	7849.5	745.1
		2	151.0	151.0	150.0	8152.0	8240.0	7941.0	760.0
		3	151.0	152.0	150.0	7976.0	8071.0	7802.5	752.0
	Average		150.3	151.7	149.7	8046.0	8133.8	7864.3	752.4

APPENDIX F: Physical Measurement and Compression Peak Load of Concrete Cylinder Specimens

Curing Period	Mix Details	Specimen	Dimension (mm)		Mass (g)	Compression Peak Load (kN)
			Length	Diameter		
7 Days	NWRC	1	200.0	100.0	3681.0	71.4
		2	200.5	100.0	3654.5	72.6
		3	200.0	100.0	3628.0	78.2
	Average		200.2	100.0	3654.5	74.1
	SFRC-0.6	1	200.0	100.0	3768.0	81.7
		2	199.5	100.0	3703.0	80.5
		3	200.5	100.0	3699.0	79.5
	Average		200.0	100.0	3723.3	80.6
	SFRC-0.7	1	200.0	100.0	3778.0	82.6
		2	200.0	100.0	3739.0	80.2
		3	199.5	100.0	3682.5	81.7
	Average		199.8	100.0	3733.2	81.5
28 Days	NWRC	1	199.5	100.0	3622.0	95.3
		2	200.0	100.0	3663.0	76.2
		3	200.0	100.0	3627.0	91.9
	Average		199.8	100.0	3637.3	87.8
	SFRC-0.6	1	200.0	100.0	3719.5	98.8
		2	200.5	100.0	3674.0	99.1
		3	200.0	100.0	3692.0	101.6
	Average		200.2	100.0	3695.2	99.8
	SFRC-0.7	1	200.0	100.0	3714.0	104.2
		2	199.5	100.0	3687.5	100.3
		3	200.5	100.0	3721.0	105.9
	Average		200.0	100.0	3707.5	103.5

APPENDIX G: Experimental Strain Results of Four-point Bending Test

For NWRC W/OS Beam

Load applied	LVDT 1 (left)	LVDT 2 (middle)	LVDT 3 (right)	Steel Strain Gauge
kN	mm	mm	mm	με
0	0	0	0	0
10	0.780	1.010	0.875	72
20	1.650	1.730	1.672	164
30	2.545	2.600	2.640	258
40	3.280	3.480	3.320	421
50	4.720	4.980	4.812	825
60	5.760	6.142	5.904	1125
70	6.975	7.480	7.145	1522
80	7.960	8.430	8.270	1887
88	8.920	9.230	9.040	2185
Fail				
60	9.450	9.940	9.640	2297

For NWRC W/S Beam

Load applied	LVDT 1 (left)	LVDT 2 (middle)	LVDT 3 (right)	Steel Strain Gauge
kN	mm	mm	mm	με
0	0	0	0	0
10	0.870	1.074	1.010	92
20	1.560	1.740	1.690	209
30	2.235	2.354	2.325	328
40	2.930	3.050	2.952	492
50	3.500	3.910	3.630	651
60	4.961	5.130	5.010	1031
70	5.830	6.012	5.980	1276
80	6.735	6.860	6.738	1473
90	7.650	7.970	7.720	1630
100	8.450	8.800	8.560	1825
110	9.320	9.670	9.480	2039
120	10.455	10.642	10.540	2196
126	11.360	11.645	11.470	2352
Fail				
100	12.010	12.420	12.130	2458

For SFRC-0.6 Beam

Load applied	LVDT 1 (left)	LVDT 2 (middle)	LVDT 3 (right)	Steel Strain Gauge
kN	mm	mm	mm	με
0	0	0	0	0
10	0.860	1.020	0.910	69
20	1.440	1.616	1.553	134
30	1.980	2.180	2.100	213
40	2.440	2.610	2.500	307
50	2.870	3.020	2.930	418
60	4.350	4.640	4.510	713
70	5.560	5.870	5.632	986
80	6.470	6.710	6.680	1283
90	7.550	7.720	7.630	1578
100	8.800	9.010	8.970	1801
110	9.720	10.010	9.830	2007
116	10.620	10.910	10.740	2297
Fail				
90	11.300	11.620	11.420	2397

For SFRC-0.7 Beam

Load applied	LVDT 1 (left)	LVDT 2 (middle)	LVDT 3 (right)	Steel Strain Gauge
kN	mm	mm	mm	με
0	0	0	0	0
10	0.930	1.045	0.980	54
20	1.605	1.680	1.624	119
30	2.300	2.410	2.382	193
40	2.980	3.105	3.010	263
50	3.430	3.620	3.480	393
60	4.650	4.900	4.830	723
70	5.570	5.820	5.720	1053
80	6.640	6.900	6.840	1274
90	7.670	7.920	7.860	1470
100	8.720	9.050	8.960	1714
110	9.690	10.080	9.935	1991
120	10.920	10.980	10.900	2304
Fail				
90	11.580	11.900	11.670	2415

APPENDIX H: Shear Strength Calculation

Shear Design Complied to Eurocode 2:

1) Concrete sections that do not require design shear reinforcement:

Shear capacity of concrete, $V_{Rd,c}$

= [0.12 k (100 ρ_1 f_{ck})$^{1/3}$] $b_w d$

= [0.12 (2) ((100)($\frac{101}{(125)(163)}$)(24.95))$^{1/3}$] (125)(163)

= 11.31 kN

with a minimum value of

$V_{Rd,c}$ = [0.035 k$^{3/2}$ $f_{ck}{}^{1/2}$] b_wd

= [0.035 (2)$^{3/2}$ (24.95)$^{1/2}$] (125)(163)

= 10.08 kN

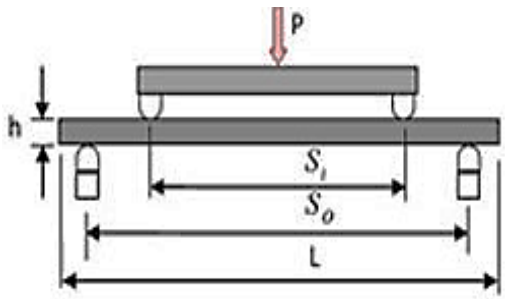

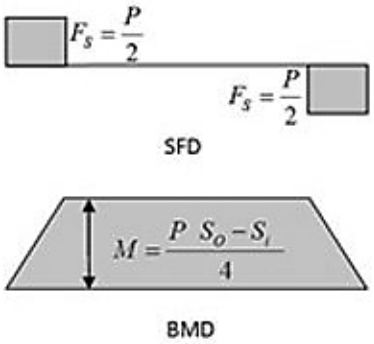

V_{Ed} = 4 M / (700 – 300)

= [4 × 6.21 × 10^6 / (700 – 300)]

= 62.1 kN

---

2) The variable strut inclination method for sections that do not require shear reinforcement:

a) The diagonal compressive strut:

$$V_{Rd,max} = \frac{0.36\, b_w\, d\, (1 - f_{ck}/250)\, f_{ck}}{(\cot\theta + \tan\theta)}$$

$$= \frac{[(0.36)(125)(163)(1 - \frac{24.95}{250})\,(24.95)]}{(\cot 45^o + \tan 45^o)}$$

= 82.37 kN

b) Vertical shear reinforcement:

V_{wd} = 0.87 $\frac{A_{sw}}{s}$ 0.9d f_{yk} cot θ

= (0.87)($\frac{101}{100}$)(0.9)(163)(511.16)(cot 45^o)

= 65.89 kN (> V_{Ed})

c) Additional longitudinal tensile force in the tension steel:

ΔF_{td} = 0.5 V_{Ed}cot θ

= (0.5)(62.1)(cot 45^o)

= 31.05 kN